A Common Currency of Motivation: How Curiosity and Reward Shape the Brain's Memory Systems

Kevin Reniers

Faculty of Social Science, Donders Institute, Radboud University

SOW-DGCN05: Practical Training and Thesis

Prof. Dr. Harold Bekkering & Dr. Lieke L. F. van Lieshout

August 21, 2025

Acknowledgements

I want to give an immense thank you to prof. dr. Harold Bekkering and dr. Lieke van Lieshout for giving me the opportunity to work with such amazing people such as themselves, Isabelle Stikker and Claire Zhang on such an amazing project. Without Harold's vision and trust this whole project would have never happened. Without Lieke's realism and experience this project would have never gotten shape. Without Isabelle's determination and help this project would never have been finished. And without Claire's kindness and statistical prowess this project would have been a very fancy behavioural experiment with sealed fMRI data stored in a drawer somewhere.

Additionally, I am grateful for prof. dr. Roshan Cools's extensive feedback and giving us the opportunity to collaborate on this fMRI project together. I also want to thank dr. Olympia Colizoli for her useful help with the fMRI statistical design. Also a warm thanks to prof. dr. Floris de Lange and dr. Nils Kohn for their helpful input and time and prof. dr. Christian Beckmann for his advice on functional connectivity (even though in this thesis we haven't gotten to that). And lastly, I am grateful for the help dr. Jose Marques gave us in setting up the MRI system and for dr. Bern Figner's advice on the use of mixed-effects models.

Abstract

Curiosity and reward incentives, respectively representing intrinsic and extrinsic motivations, have both been found to be effective motivators of memory formation, but previous findings on a potential interaction effect between the two have not agreed. It is also still not clear how the two motivators are similarly or dissimilarly represented in the brain in support of memory formation, with the inferior parietal lobule (IPL) as a contestant of curiosity processing and the vmPFC and anterior hippocampus as regions in support of value-based, motivated memory. Therefore, we used an adapted version of the trivia paradigm to understand the main effects of curiosity and reward incentives and their interaction on immediate same-day and delayed 7-day later recall performance whilst we recorded participants' BOLD activity in the MRI scanner. We found that curiosity robustly predicted increased recall likelihood whilst reward incentives improved recall only for the lowest and highest reward levels, and conversely, the interaction effect between curiosity and reward on recall likelihood was found to be significant for medium-high rewards only. Further exploratory analysis showed as the trials progressed, a decreasing and eventually detrimental effect of reward on recall that was ameliorated as curiosity went up. Neurally, we found both positive and negative modulation in the inferior parietal cortex (IPL) and only negative activity in the ventral medial prefrontal cortex (vmPFC) in support of both curiosity- and reward-motivated memory. Anterior hippocampal (aHPC) activity during encoding was not found to correlate with motivated memory formation whilst it did positively predict remembered trials over forgotten trials without considering either motivator. Further research should look into more specific IPL hypotheses of motivated memory formation and should focus on anticipatory hippocampal activity, instead of activity during encoding, in support of motivated memory formation. Additionally future work should look at the neural correlates of time-dependent motivated memory effects. Our findings can inform both educational researchers and educators to look out for temporally-dynamic negative effects of extrinsic rewards on memory formation – and the potential benefit of high curiosity-fostering study material in reducing their effect.

Contents

A Common Currency of Motivation: How Curiosity and Reward Shape the Brain's Memory Systems

Try to remember the last time you picked up a textbook in order to study for a test during your studies, middle or high school period. You were probably quite curious for some information, and not at all for other subjects, chapters or passages – happy to continue reading to learn some, but not others. In order to remember the information better, you might have treated yourself with a cookie after reading a chapter, you might have been incentivized by the potential for a high grade on the test or the 10-euro 'report card money' you always got from your grandma. These factors could all have influenced your chances of encoding and consolidating your study material into memory.

These situations could be described in two ways. You either read some passages because of an intrinsic drive for information, leading you to read onwards for the sake of knowledge itself; An

information incentive, or as many call it, *curiosity*. Or, when the thought of sweets or grandma's pocket change drove you to study, you were driven by extrinsic motivators; *Reward* incentives[1].

The first of the two, curiosity, has many faces – one of which is epistemic curiosity; the intrinsic drive to gain knowledge (Berlyne, 1954). Loewenstein (1994) added on to Berlyne and proposed that curiosity is driven by a perception of a gap in one's knowledge, which can lead to specific curiosity: a search for information that will close the gap. More recent work has looked at curiosity as an intrinsic motivator that is capable of driving behaviour and influencing memory (e.g. Gruber et al., 2014). The second motivator of behaviour we discuss, reward incentives, has also been found to improve memory (Adcock et al., 2006): the anticipation of reward can be a strong reinforcer – or extrinsic motivator – that boosts memory to perform well.

The neural correlates of reward- and curiosity-enhanced memory have been investigated and a plethora of neural systems have been associated with the many aspects of either curiosity (Gruber et al., 2014; Kang et al., 2009; Murphy et al., 2021; Van Lieshout, Vandenbroucke, Müller, Cools, & De Lange, 2018) or reward (Adcock et al., 2006; Loh, Kumaran, et al., 2016; Wittmann et al., 2008). In real-world learning contexts like educational settings, curiosity as an intrinsic motivator and reward incentives as a more extrinsic motivator often exist and effect behaviour at the same time (Ryan & Deci, 2020). Hence, to understand their effects on learning and memory, it is of importance to look at both in a combined context. An emerging field is doing exactly this (Duan et al., 2020; Meliss et al., 2024; Meliss & Murayama, 2022). However, there is still no agreement on the similarities and differences between curiosity and reward processing, with different studies reporting partly diverging and non-overlapping results (Duan et al., 2020; Meliss et al., 2024; Meliss & Murayama, 2022; Murayama & Kuhbandner, 2011; Swirsky et al., 2021). Two questions remain; Why do curiosity and reward sometimes seem to work independently from each other in promoting memory, whilst on other occasions they interact with each other? And secondly, are these two motivational processes expressed in the brain similarly, or do they differentiate somewhere? Therefore, in this thesis project, we will aim to describe the behavioural effects of curiosity and reward on memory and understand the neural systems underlying both curiosity-enhanced and reward-enhanced memory formation to see where they share neural correlates and where they disassociate.

---

[1] For brevity, we will sometimes shorten 'reward incentives' and speak of just 'reward'.

To do this, we have created a version of the trivia paradigm which closely resembles, but improves on, the design from Duan et al. (2020). We present participants with 244 trivia questions from a large database from Fastrich et al. (2018) and ask them to rate how curious they are to obtain the answer. Additionally, we pry their prior knowledge by asking them how confident they are that they know the answer. Then, we choose the 144 most and least curious questions on an individual basis and present them again, but now in the MRI scanner. This time, we also satisfy participants' curiosity by presenting the answer to the trivia questions. During the MRI session we show half of the questions in a rewarded condition, in which participants are incentivised by three levels of reward: 0, 1 and 3 euro. Since we believe that behaviour in a 0-euro trial can be very different from behaviour in a completely non-rewarded context – even though the utilitarian reward value is the same – shown for instance by research into the undermining effect (Murayama & Kuhbandner, 2011), we present the other half of the questions in a completely non-rewarded block. This second, non-rewarded block is an addition to the study from Duan et al. (2020), that we feel is important to understand if curiosity's effect on memory changes in rewarded contexts compared to non-rewarded contexts – and to bridge research that operationalises reward either in a blocked or a trial-based manner. Lastly, we test participants' memory of the answers to the trivia questions by asking them to make an immediate recall test after they get out of the scanner, as well as a delayed recall test one week later.

Curiosity has a marked positive effect on improving memory formation. Murayama & Kuhbandner (2011) showed that interesting questions show higher recall rates in a 7-day delayed incidental recall test compared to uninteresting questions – i.e., even though participants were not told they would be tested, there was still a dissociable, positive effect. Gruber et al. (2014) replicated these findings with individual-specific curiosity ratings and later research also found the effect using an intentional recall test by explicitly telling participants they would be tested, instead of giving them a surprise, incidental test (Duan et al., 2020). Therefore, we predict that curiosity will have a positive effect on recall performance within our experiment.

Gruber et al. (2014) found that in the right hippocampus, there was an interaction between curiosity and memory. In memory research, brain activity related to remembered items, compared to forgotten items has been dubbed the subsequent-memory effect (Kim, 2011). Hippocampal activity and connectivity, for instance, is robustly implicated in the subsequent-memory effect (Kim, 2011; Palacio & Cardenas, 2019). When a motivator like curiosity (or reward) supports memory formation,

we can then speak of a curiosity-motivated (or reward-motivated) subsequent-memory effect. For instance, hippocampal and reward circuitry co-activation has been associated with curiosity-motivated subsequent-memory (Murphy et al., 2021; Poh et al., 2022a). Therefore, we predict that curiosity-motivated subsequent-memory will be associated with hippocampal activity during the relief stage (when the answer is presented) – i.e. hippocampal activity will be greater for high curiosity questions whose answers were later remembered compared to low curiosity questions whose answers were later remembered.

Curiosity has also been associated with uncertainty processing (Poli et al., 2024; Van Lieshout, De Lange, et al., 2021; Van Lieshout, Traast, et al., 2021) where curiosity is defined as the drive to reduce uncertainty. Neurally, there is evidence that uncertainty is associated with inferior parietal lobule processing (Huettel et al., 2005; Vickery & Jiang, 2009) and that this activity relates to curiosity (Van Lieshout, Vandenbroucke, Müller, Cools, & De Lange, 2018). Looking solely at curiosity effects in the brain, the inferior parietal lobule has indeed been reported before during curiosity induction (Duan et al., 2020; Meliss et al., 2024). Hence, we predict that the inferior parietal lobule is positively associated with curiosity induction (during question presentation) and the curiosity-motivated subsequent-memory effect during curiosity relief.

Just like intrinsic curiosity, extrinsic reward incentives have also been found to predict recall (Adcock et al., 2006; Loh, Kumaran, et al., 2016; Wittmann et al., 2008). Knowlton & Castel (2022) discuss how value can have a positive impact on memory via different processes. An automatic system is thought to encompass dopaminergic signals to the hippocampus, whilst a more strategic process helps memory through frontal areas like the inferior frontal gyrus. Therefore, we predict that reward incentives will have a positive effect on recall – i.e., recall will be higher in the rewarded condition compared to the non-rewarded condition. Additionally, recall will be higher for each increment of the reward magnitude (i.e. recall: 3 euro > 1 euro > 0 euro).

The human reward circuit has been argued to encompass the substantia nigra and ventral tegmental area – parts of the midbrain – the ventral striatum, as well as cortical structures like the orbitofrontal cortex (OFC) and the anterior cingulate cortex (ACC) (Haber & Knutson, 2010). Different components of this circuit have been found to functionally connect with the hippocampus to promote memory formation (Adcock et al., 2006). Adcock et al. (2006) were early pioneers in showing that functional correlations between the ventral tegmental area (VTA) and the hippocampus preceding a

to-be-remembered stimulus predicted later memory of said stimulus. Additionally, these authors found that VTA, nucleus accumbens (NAcc) and hippocampal activation during high-reward cues correlated with later remembered but not forgotten scenes. Results that have since been corroborated more often (e.g. Elliott et al., 2022; Frank et al., 2019; Wittmann et al., 2005, 2008). Given these findings, we predict that hippocampal activity during the presentation of the answer (i.e. during curiosity relief) will positively relate to the reward-motivated subsequent-memory effect – i.e., hippocampal activity will be higher for remembered items in the rewarded condition compared to the non-rewarded condition. Additionally, the hippocampus will be positively parametrically modulated by the reward magnitude for remembered items when we compare 0-, 1- and 3-euro trials during curiosity relief (parametric reward-motivated subsequent-memory effect).

Apart from subcortical constituents of the reward system, Haber & Knutson (2010)'s review discusses how the OFC activates in the presence of rewards; the medial prefrontal cortex (mPFC) – and specifically the ventromedial prefrontal cortex (vmPFC) – might respond to outcomes that are rewarding. Frank et al. (2019), additionally to hippocampal-striatal functional connectivity, found functional connectivity between the hippocampus and the medial prefrontal cortex (mPFC) and orbitofrontal cortex (OFC) to be predictive of reward sensitivity for memory formation. Miendlarzewska et al. (2016) discuss the vmPFC to play a part in consolidating new memories into new networks of pre-existing knowledge and to be guiding decisions based on value comparison. Interestingly, the vmPFC is also thought to integrate orthogonal reward values that are represented in the OFC (Blanchard et al., 2015) and combines them into one subjective value (D. V. Smith et al., 2014). This subjective value does not only represent reward, but also the value of prior information (Blanchard et al., 2015), i.e. a valued curiosity signal. This subjective value may then be recruited for memory formation (Rolls, 2022). Hence, we predict that curiosity will be positively represented within the vmPFC during the induction of curiosity (i.e. the question presentation) and reward will be positively represented in the vmPFC during answer presentation. Additionally, the vmPFC will be positively associated with both the curiosity-motivated and reward-motivated subsequent memory effects during the answer presentation – i.e., higher activation is associated with high curiosity questions (compared to low curiosity questions) and questions in the rewarded condition (versus the non-rewarded condition) that were later remembered instead of forgotten. Moreso, we also predict that within the rewarded condition, the reward magnitude for remembered questions is positively parametrically

modulated by the vmPFC (parametric reward-motivated subsequent-memory effect). Note that we predict both the curiosity- and reward-motivated subsequent-memory effects to positively predict hippocampal and vmPFC activity, whilst we predict that the IPL is specific to the curiosity-motivated subsequent-memory effect.

Some studies find that curiosity and reward incentives both improve memory formation additively (Duan et al., 2020; Meliss et al., 2024), meaning that both curiosity and reward independently increase memory performance. Other studies, however, find an interaction between the two. Murayama & Kuhbandner (2011) found reward incentives to only affect memory for answers to trivia questions on trials that were rated as being less interesting. High curiosity questions were not influenced by rewards anymore. I.e., there was a negative interaction between reward and curiosity. In a similar light did Swirsky et al. (2021) find that only for low curiosity questions, rewards were helpful in improving memory – i.e. a negative interaction. Using a somewhat different paradigm to the trivia one, Meliss & Murayama (2022) used magic tricks to induce curiosity in participants. They found that the curiosity-driven memory benefit was significantly higher in the group that did not receive any incentives, whose benefit was positive, versus the group that did receive incentives, whose benefit was negative – meaning that more lower curiosity trials were encoded into memory than higher curiosity trials. Cerasoli et al. (2014) investigated 40 years of intrinsic motivation research as a whole (so not just curiosity) and found that intrinsic motivation was stronger, the less salient rewards were. However, most surprising of all and in contrast with the more curiosity specific studies, they found a positive interaction effect of reward and intrinsic motivation. However, this effect did reduce when reward incentives were distant and non-salient compared to salient and direct reward incentives. Given these findings we predict that there will be a negative interaction between curiosity and reward incentives: the higher one's curiosity level, the less effect the reward condition will have on later recall.

Giving a preview of our results, we found that curiosity is indeed a positive predictor of recall. Rewards show a more complex pattern; there was no difference in recall between the reward conditions, but when viewed separately, 0- and 3-euro trials – but not 1-euro trials – positively predicted recall when compared to the no reward condition. Furthermore, only for 1-euro trials (compared to the no-reward condition) there was a significant, positive interaction effect between curiosity and reward incentives. Further investigation showed that these effects changed when considering trial number: The further on in the experiment, the less effect rewards had on recall

compared to the no-reward condition. Additionally, curiosity seemed to ameliorate this deterioration in the reward effect. Neurally, we found that the right inferior parietal lobule activity negatively associated with both motivated subsequent-memory effects, counter to our hypotheses. The hippocampus was implicated with unmotivated but neither motivated subsequent memory, also unexpectedly given our hypotheses. Whole brain analysis showed widespread activation that represented curiosity and reward incentives, and their respective motivated subsequent-memory effects that were very similar and overlapping. Further investigation of the fMRI BOLD dataset should investigate the temporal changes in the reward effect and the curiosity and reward interaction effect we found behaviourally.

Method

Participants

In total, 47 participants with a mean age of 23.89 (SD=3.04, range: 19-35) participated in the experiment. Of these, 34 were cisgender females and 13 were cisgender males. The mode of handedness was right handedness (N=41), followed by left handedness (N=5) and ambidextrousness (N=1).

One participant was excluded a-priori (without looking at the data) for excessive movement (visible during scanning session) and not being able to keep their eyes open for multiple blocks. Three participants were excluded because we had to stop the experiment prematurely just before or during the MRI scan. Thus, the sample size for the main behavioural analyses is 43. Two participants had to be removed from the fMRI analyses due to an incorrect registration of the *headscout* during scanning, causing issues in the preprocessing stage. This leaves us with 41 participants that were included in the fMRI analyses.

All participants gave written informed consent according to the Declaration of Helsinki prior to participation. The experiment was approved by the local ethics committee (CMO Arnhem-Nijmegen, The Netherlands) under a general ethics approval protocol ("Imaging Human Cognition", CMO 2014/288) and was conducted in compliance with these guidelines.

Sampling procedure

For this project, participants had to be MRI compatible, hence the standard Donders Institute exclusion criteria for fMRI research were used. Additionally, a maximal age limit of 40 years was set to limit any age effects related to memory. Participants were recruited using the Radboud SONA

Research Participation System, through which participants can volunteer themselves for the experiment.

Payment for this study has been organised according to the standard rules set by the Donders Institute. Participants will receive €15,- per hour whilst participating, and an additional maximum of €10,- in incentives for giving the correct answer to randomly chosen questions during the testing phase, equal to the corresponding amount of money shown to them during the incentive presentation in the MRI phase (0, 1 or 3 euros). We expected each participant to come in for 4 hours, earning them €60,- excluding incentives. Including the incentives, this will total in between €60,- and €70,- per participant.

Sample size justification

For the behavioural hypotheses, a preregistered power analysis was done before the start of the experiment to estimate the power we would obtain given our specified models and reported effect sizes from the literature (Reniers et al., 2025). Because mixed effects models are complex, it is not possible to analytically determine power, or the required sample size given a desired power. Therefore, we resort to simulation-based calculations of power in R (R Core Team, 2023) using the guide from Kumle et al. (2021). R packages used were the 'simr' package (Green & MacLeod, 2016; Version 1.0.7) and the 'mixedpower' package (Kumle et al., 2020; Version 0.1.0).

We use a combination of rerunning analyses on an already existing dataset (Fastrich et al., 2018) and of effect sizes reported in the literature (Swirsky et al., 2021). We aim for 80% power with an alpha level of 5%. For technical details on how we performed the power analysis, please see Appendix B: Power Analysis. The results from this power analysis are shown in Figure 23 from the appendix. We conclude that 40 participants and 144 trials are enough to detect the required effect sizes (reward condition, curiosity and their interaction) reported in the literature with more than 80% power. The sample size for the MRI part of the experiment was determined based on how much people we were able to scan within the provided budget for the study. This was the main constraint on our total sample size.

Materials and Procedure
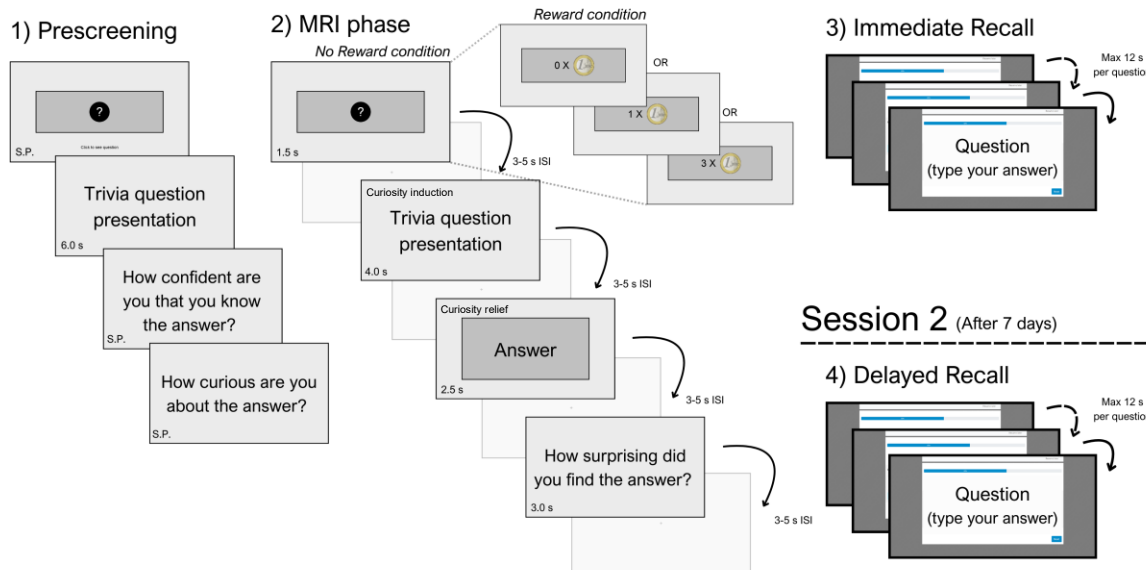
Experimental design

The study consists of four parts (see **Figure *1***). Part one is a prescreening phase. Part two is the MRI phase. Part three and four are the testing phases, split over session 1 (immediate recall) and session 2 (delayed recall).

Figure 1
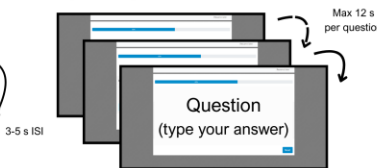
Experimental task design

Note: For ease of presentation, the surveys that were administered as described below are not depicted in this schema. S.P. = Self-Paced. The confidence question is on a 10-point Likert scale with verbal anchor points (ranging from "Not confident at all", and "Somewhat confident" (in the middle) to "Extremely confident"). The curiosity question is also on a 10-point Likert scale with verbal anchor points (ranging from "Not curious at all", and "Somewhat curious" (in the middle) to "Extremely curious"). The surprise ratings are not analysed within this thesis.

In part one, participants are sat in a behavioural lab / cubicle behind a computer. Before starting phase 1, they complete the four-item perceived competence scale (PCS) (used for exploratory analyses not further described in this thesis). Afterwards, they get to see 244 trivia questions that were obtained from an online database from Fastrich et al. (2018). First a question mark is presented to them, asking them to click if they are ready to see the question. Then, the question is presented for 6 seconds. After each question, the timing being self-paced, they are asked how confident they are that they know the answer and how curious they are to get the answer to the question – both measured using a Likert scale with a range from one to ten. Participants click on the position they deem most fitting and then click on a continue button to confirm their answer. Participants will not get the answer to the trivia questions during this phase. From these 244 questions, 144 questions will be selected for the main phase after we have removed questions with a

confidence rating of 9 and 10. If a participant ends up with less than 144 questions with a lower than 9 confidence rating, they will not be able to take part in the main phase and be sent home with the appropriate payment. We select the questions with the highest and lowest curiosity rating and split them into a high and low curiosity category based on the median to ensure enough variability in the curiosity ratings. If one of the categories is not completely filled by questions that are above or below the median, we randomly select items with a median value to fill up the categories. After the prescreening, the participants fill in the PCS a second time.

In part two, participants will lie down in the MRI scanner. Participants must complete two blocks each consisting of 3 smaller subblocks, where each block corresponds to one of two conditions: a Reward (R) or Non-Reward (NR) condition. In the reward condition, participants receive a random reward incentive corresponding to a chance to win either 0, 1 or 3 euros later in the (immediate and delayed recall) testing phase. Each subblock contains an equal amount of 0-, 1- and 3-euro trials. In the non-rewarded condition, they are presented with a question mark in a circle, to visually mimic the euro stimuli in the reward condition. Note that the 0X 1 euro manipulation is different from the no-reward condition. Participants will be randomly assigned to start with either the reward or the non-rewarded condition (Latin-square design). Thus, all participants get to partake in both conditions. Each subblock contains as much high as low curiosity questions.

Within one trial, participants will first see the reward incentive or the question mark (for 1.5 seconds). Then, they will be presented with one of the trivia questions that they have already seen during the prescreening phase (for 4 seconds). Hereafter, the answer is presented on the screen whilst the question is displayed in a smaller font (for 2.5 seconds). Lastly, participants are presented with a sliding scale asking them to rate how surprising they found the answer to the trivia question to be (eleven options/ticks to choose from) for which they have 3 seconds to answer using an MRI-safe button box. This variable will be used for exploratory analyses outside of the scope of this thesis.

Between all screens a fixation cross is presented according to a random jitter of 3 to 5 seconds with a uniform distribution. Each of the two blocks consists of three subblocks of 24 trials with resting periods in between during which the scanner will be turned off and on again. One block is therefore 72 trials long. In total, 144 trials will be shown to each participant. In between subblock 3 and 4 (i.e. when the condition switches) an anatomical scan will be made that last approximately five

minutes. Both the prescreening and the main MRI phase programs were made by altering the code from Hankel (2023) to suit our experimental design.

In part three and four, participants are tested on their memory for the answers to the 144 trivia questions that were selected for them after the prescreening and shown during the MRI scan. Participants were explicitly told at the beginning of study session 1 (and in the online study advertisement) that there would be two recall tests – thus, we measure intentional encoding into memory for the recall variable. Part three is an immediate test that will be administered after participants come out of the MRI. Part four is a delayed test that will be administered after 7 days (on-site, in the same behavioural labs as during the immediate recall test). In order to make scheduling easier in the light of weekends or off-days, we allow the delayed recall test to be administered after 6 or 8 days if scheduling is not possible otherwise. The online survey software LimeSurvey (Limesurvey GmbH, n.d.) will be used to administer the recall tests. During the tests, participants will get to read a trivia question and answer it by typing it in a textbox. They have a maximum of 12 seconds to answer the question before the next one is shown. Before starting the immediate recall test, the participants fill in the PCS for a third time. Lastly, after the immediate recall test they fill out the HEXACO personality test (which will be used for exploratory analyses outside the scope of this thesis). In addition, after the delayed recall test participants fill out a last survey which includes a trait curiosity survey and engagement questions to gain insight into how much the participant engaged with the material at home (used for exploratory analysis, also not described in this thesis).

Behavioural analysis

To estimate the effects of curiosity and reward on recall, we will use Bayesian mixed-effects models using the 'brms' package (Bürkner, 2017) based on STAN (Carpenter et al., 2017) in R (R Core Team, 2023; Version 4.3.3). We use the 'batchtools' package (Lang et al., 2023) to utilise the computational power of the Donders Institute's HPC cluster in performing model estimation. We planned and preregistered (Reniers et al., 2025) that we would use the 'lme4' package (Bates et al., 2015) to perform the mixed-effects analysis, but due to estimation problems that we could not solve, we switched to the use of Bayesian estimation.

Within models 1, 2 and 3, the dependent variable is *recall*, dummy coded with a 1 for remembered answers and a 0 for forgotten answers. Because we have two measurements for recall, the immediate and the delayed recall tests, we introduce the covariate *test type* that represents either

the immediate or delayed recall test, which is included in model 1, 2 and 3. The dataset will be transformed to long format so that recall for immediate and delayed tests can be accounted for within the models.

In model 1, 2 and 3, further independent variables are *curiosity* for the answer to a trivia question and the covariate *confidence* in knowing the answer, both ranging from 1-10 but centred before inclusion in the models.

In model 1, the independent variable reward *condition* is used as a measure of reward, dummy coded with 1 for the rewarded condition (R) and 0 for the non-rewarded condition (NR). In model 2 and 3, the independent variable *reward* is introduced as a more specific measure of reward. This is a categorical predictor with 4 levels: NR (for non-rewarded condition trials) and 0, 1 and 3 (i.e. the reward magnitudes in the rewarded condition). NR is the reference level.

In model 3, the independent variable *trial* number is introduced – which represents the trial number in the MRI phase of the experiment, ranging from trial 1 to 144. The trial variable is centred before inclusion in the model.

For estimation of the parameters in the Bayesian mixed-effects models, the Bernoulli family with the logit link will be used together with 4 chains, each with 10,000 iterations. We use the default 'brms' prior distributions for logistic regression: a uniform prior for the fixed effects coefficients and a student t-test distribution for the random intercepts and standard deviations of the random slopes, characterised by $t(df = 3, \mu = 0, \sigma = 2.5)$. Coefficient estimates will be deemed statistically significant when their 95% Credible Interval excludes 0. Specific model regression formulas are described below each model results table in Appendix C: Behavioural results.

To check for potential issues regarding the estimation, we look whether the ESS values for each parameter is 100 times larger than the number of chains times 4, i.e. whether ESS > 400. Additionally we check whether $\hat{R} > 1.01$, which would indicate a problem. Lastly, to see if the chains converge properly, we will look at the density plots of parameters estimates to see if the distributions of the chains overlap and whether the trace plots show randomness without any discernible pattern. If any of these checks do not hold, we increase the number of iterations in the model and rerun it.

Mixed effects models are powerful statistical tools that greatly reduce the possibility of Type 1 errors (Barr et al., 2013). However, some authors note that maximal models are not optimal, suggesting that more parsimonious models might be preferred (Bates et al., 2018). Hence, for models

1 and 2, we compare three different sub models in their explanatory power of the data; one maximal model with all theoretically justifiable random intercept, slopes and correlations included (sub model a); one model were we leave out the random correlations with respect to model a (sub model b); and lastly, one model were we leave out the random structure for the question items with respect to model a (sub model c). Using the *loo* function (Vehtari et al., 2017) from the *brms* package (Bürkner, 2017; Version 2.22.0) we compare these three models with leave-one-out cross-validation. If any of the more parsimonious models don't statistically significantly differ from the maximal model, we use the most parsimonious model in the reporting of our results. If $|\triangle ELPD/SE| > 2$, we deem a model to be significantly worse than the best performing model, and consequently we will choose the better performing model.

Additional R packages that were used were, in alphabetical order: the *dplyr* package (Wickham et al., 2023), the *emmeans* package (Lenth, 2024), the *ggplot2* package (Wickham, 2016), the *gridExtra* package (Auguie, 2017), the *jtools* package (Long, 2022), the *lattice* package (Sarkar, 2008) and the *psych* package (Revelle, 2025).

fMRI pre-processing

Preprocessing was done using fMRIprep, version 24.1.1 for all participants except five subjects who due to technical issues with the fieldmap co-registration required the updated fMRIprep version 25.1.2. Registration from $2.5mm^3$ native bold space to $2mm^3$ MNI-152 standard space (MNI152NLin6Asym) was done by antsRegistration. All further analyses described hereafter were done in $2mm^3$ MNI-152 standard space (MNI152NLin6Asym).

fMRIprep requests all users to include an unedited and standardised 'boilerplate' into research papers with complete information on the preprocessing programs and versions used. You can find these boilerplates in Appendix G: fMRIprep boilerplates.

We manually checked all visual reports made by fMRIprep to look for any artifacts in the fieldmap, BOLD and anatomical coregistrations. Based on the estimated FD motion parameter we excluded a subblock if its mean FD > 0.3 mm or the maximum FD > 3.0 mm.

fMRI analysis

For all our fMRI models, we used FSL's Feat (Smith et al., 2004; Version 6.00). To estimate group-level effects, the modelling exists out of three levels with explicitly different FEAT runs. In the first level (event-based) we added our main effects and their temporal derivatives as regressors, as

well as motion confounds estimated by fMRIprep. These were convolved with the Double-Gamma HRF. Prewhitening was done by FEAT. Spatial smoothing with a FWHM of 6mm was used to strike a balance between sensitivity for presumed larger activation clusters in the cortex without missing out on specificity in smaller subcortical regions (using recommendations from Mikl et al. (2008)).

First-level contrasts to estimate the different effects are described below. In the second-level, fixed effects were used to combine subjects' runs into one. In the third level, group level activation was estimated using FLAME1+2. Statistical inference was based on cluster-extend based thresholding using a primary z-threshold of $z>3.1$ and a family-wise error (FWE) correction cluster p-value of $p<0.05$. The primary threshold was preregistered on Open Science Framework (Reniers et al., 2025) to be $z>2.3$, but later consideration showed a more conservative threshold to be more fitting following recommendations from Woo et al. (2014).

We created two fMRI models to investigate difference in brain activity related to two different reward operationalisations. In fMRI model 1 (*Condition Model*), we looked at between block effects related to the R and NR reward conditions, similar to behavioural model 1. In model 2 (*Reward Only Model*), we further investigated the effect of the three different levels of reward (0, 1 and 3 euros) using linear parametric modulation utilising only the reward condition blocks. This model is not entirely equivalent to behavioural model 2 because NR trials were excluded from this analysis.

In fMRI model 1 and 2, to investigate brain regions that were responsive to differences in curiosity levels during curiosity induction, we created an explanatory variable (EV) that consisted of a boxcar function for the duration of the question presentation screen (4 s) for questions that had a high curiosity value (calculated by individual median values) and one EV for low curiosity questions. Two contrasts were created to determine brain regions with higher activation for high versus low curiosity questions (High curiosity > Low curiosity) and vice versa (Low curiosity > High curiosity).

In fMRI model 1 and 2, the curiosity-motivated subsequent-memory effect was operationalised using an EV that consisted of a boxcar function for the duration of the answer presentation screen (2.5 s) for questions that had a high curiosity value and were remembered in the delayed recall test (excluding all forgotten questions) and one EV for low curiosity questions that were remembered in the delayed recall test. Two contrasts were made to determine brain regions that showed a positive curiosity-motivated subsequent-memory effect (High curiosity for remembered

items > Low curiosity for remembered items) and a negative curiosity-motivated subsequent-memory effect (Low curiosity for remembered items > High curiosity for remembered items).

In fMRI model 1 and 2, the subsequent memory effect (SME) was operationalised using an EV that consisted of a boxcar function for the duration of the answer presentation screen (2.5 s) for answers that were remembered during the delayed recall test and an additional EV for items that were forgotten during the delayed recall test. Two contrasts were made to determine brain regions that showed a positive subsequent-memory effect (Remembered delayed recall items > Forgotten delayed recall items) and a negative subsequent-memory effect (Forgotten delayed recall items > Remembered delayed recall items).

In fMRI model 1, the reward effect was operationalised by created two EV's in the 2nd-level (i.e. the first higher level analysis) in FEAT. Per subject, a *NR* EV combined their three non-rewarded blocks. A second *R* EV combined their three rewarded blocks[2]. These were combined in three 2nd-level contrasts per subject: a mean contrast (NR + R), a positive reward (R > NR) and negative reward (NR > R) contrast, using fixed effects. This resulted in all 1st level contrasts for curiosity and the subsequent-memory effects, being split into three: a mean version to obtain their main effect, and two modulated by the negative and positive reward effect. The main reward effect was based on the average activity for all questions during the answer presentation screen (1.5 s) by combining all forgotten en remembered items into a 1st level 'average answer presentation contrast' and at the group inference level (3rd level) looking at the positive and negative 2nd level reward modulation contrasts.

In fMRI model 1, the reward-motivated subsequent-memory effect was operationalised as the combination of the first level positive subsequent-memory effect contrast (Remembered > Forgotten) and the 2nd-level reward modulation contrasts for the positive reward-motivated subsequent memory effect (R>NR) and the negative reward-motivated subsequent-memory effect (NR>R).

In fMRI model 2, the reward effect was operationalised by creating one EV with a boxcar function during the answer screen presentation (2.5 s) that was parametrically modulated by centred values of 0, 1 and 3 representing the trial-level reward incentives. Two contrasts, a positive and a negative reward effect, were made from this parametric reward EV.

---

[2] Of course, we adjusted the design matrix for any missing or excluded blocks.

In fMRI model 2, the interaction between the curiosity- and reward-motivated subsequent-memory effects were made by using the Interaction option in the 1st-level Feat design, creating two EV's: One positive curiosity-motivated SME interacted with the positive parametric reward EV (High curiosity for remembered items > Low curiosity for remembered items X positive parametrically modulated reward) and one negative curiosity-motivated SME interacted with the positive parametric reward EV (Low curiosity for remembered items > High curiosity for remembered items X positive parametrically modulated reward).

In both fMRI models, we modelled the randomly jittered ISI crosshairs as well as the incentive presentation and surprise rating screen as boxcars of their respective durations to account for activation related to these "irrelevant" stimuli. Additionally, the confound regressors estimated by fMRIprep that we added to the design matrix to account for movement in the scanner were: global_signal, a_comp_cor_00, a_comp_cor_01, a_comp_cor_02, a_comp_cor_03, a_comp_cor_04, trans_x, trans_y, trans_z, rot_x, rot_y, rot_z, cosine00, cosine01, cosine02, cosine03, cosine04, cosine05, cosine06, cosine07, cosine08.

Region Of Interest analysis

We conducted ROI analysis using pre-defined anatomical regions as preregistered on Open Science Framework (OSF) (Reniers et al., 2025). We extracted the average z-value within each ROI per subject using the 2nd-level contrasts from FSL. These were analysed in R (R Core Team, 2023) using a one-sample two-sided t-test. Statistical significance was determined by an alpha level of p<.01 as a consequence of a Bonferroni correction for comparing five ROI's.

To create the ROI masks, we used the cortical and subcortical Harvard Oxford atlases pre-installed in FSLeyes (S. M. Smith et al., 2004). The vmPFC ROI was defined as a combination of the subcallosal, frontal medial cortex, anterior cingulate gyrus and paracingulate gyrus cut at $MNI\ z - value = 4\ mm$ and thresholded at $.10$. The left and right inferior parietal lobule were created by combining all supramarginal and angular gyrus subdivisions and thresholded at .10. The left and right anterior hippocampus were created using the hippocampus masks cut at $MNI\ y - value = -22\ mm$ (Zeidman & Maguire, 2016) and thresholded at $.10$.

MRI set-up[3]

---

[3] We follow the guidelines from Poldrack et al. (2008) in reporting our MRI methods.

Images were acquired on a Siemens Prisma 3.0T Scanner (model: MAGNETOM 3.0T XR Numaris/X VA60A-0CT2). Each participant came in for one MRI session, which consisted of 6 subblocks (for each of which we had a separate sequence run). Each subblock had a slightly different amount of volumes due to the randomly jittered ISI after each screen but contained around 1300 volumes. Volumes were obtained using the *epfid* (Echo-Planner Imaging) sequence using GRAPPA acceleration with an acceleration factor of 2. The field of view was set to 210mm, with a 2.5mm slice thickness and an 84 x 84 x 51 matrix size. The acquisition orientation was transversal, and the coverage of the z-axis was 51 slices x 2.5mm = 127.5mm. We imaged the whole brain, excluding the full cerebellum. Acquisition was done using an interleaved order, a TR of 380.0ms, TE 1 of 13.40ms, TE 2 of 34.80ms, TE 3 of 56.20ms and a flip angle of 75°.

Results

Behavioural results

Model 1: Condition Model

Using our first model we investigated our three behavioural hypotheses; If curiosity was successful in positively predicting recall; Whether there was a difference in recall probability between the reward and non-rewarded conditions; And if curiosity and reward negatively interacted in predicting recall.

Firstly, we compared three sub models of Model 1 to see if adding question items into the random effects structure or including random correlations improved model predictive capabilities (**Table 1**). We found that Model 1c, which excluded a random structure for the question items, performed significantly worse than the maximal model 1a in predicting the data ($|\triangle ELPD/SE|$ = 2.91 > 2). Model 1b, which excluded the random correlations within the random effects structure, also performed significantly worse than the maximal model 1a ($|\triangle ELPD/SE|$ = 32.87 > 2). Thus, for Model 1, we will report the results from the maximal model 1a.

Table 1

Model comparison between three different Bayesian Condition models (Model 1)

| Model	ELPD	$\triangle$ELPD	*SE*	$\triangle$ELPD/SE	*p_loo*
Model 1c: MM without random structure for question items	**-6740.5**	**-1748.6**	**53.20**	**-32.87**	**122.4**
Model 1b: MM without random correlations	**-5008.5**	**-16.6**	**5.70**	**-2.91**	**604.4**
Model 1a: Maximal model (MM)	-4991.9				632.9
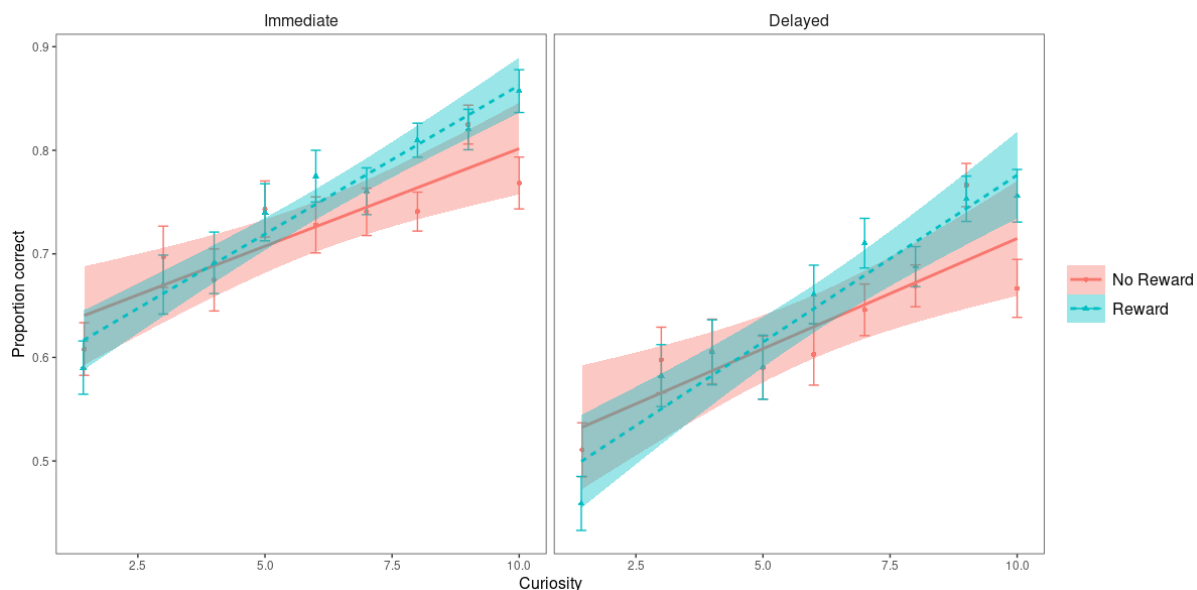
Note: Bold font indicates a significant effect, where $|\triangle ELPD/SE| > 2$ indicated a significant difference between models. The maximum model was defined as: is_correct ~ 1 + curiosity * condition * test_type + confidence + (1 + curiosity * condition *

test_type + confidence | participant_ID) + (1 + curiosity * condition * test_type + confidence | question_ID). *Underscored is the random structure for question items that was not present in model 1 with respect to the maximal model. The random correlations in model 2 were removed from the maximal model.*

Results (see **Figure 2**) indicate that curiosity is positively associated with recall likelihood (β=0.08, *Error*=0.03, 95% CI [0.03, 0.14]), in line with our hypothesis. The Reward Condition was not associated with significant changes in the likelihood of recall compared to the No Reward condition (β=0.06, *Error*=0.11, 95% CI [-0.15, 0.26]), contrary to our hypothesis. The interaction between the Reward Condition and curiosity was not associated with recall likelihood either (β=0.02, *Error*=0.03, 95% CI [-0.04, 0.09]), which was again not in line with our expectations.

Figure 2

Recall as a function of curiosity, reward condition and test time point

Note: *Results show that curiosity is positively associated with recall likelihood. We found no statistical difference in recall likelihood between the no-reward and reward condition nor an interaction effect between curiosity and condition. Results show that curiosity is positively associated with recall likelihood. We found no statistical difference in recall likelihood between the no-reward and reward condition. The legend refers to the two different reward conditions. Confidence bands are 95% confidence intervals.*

As for the covariates, the Immediate Test had a higher recall likelihood than the Delayed Test (β=0.81, *Error*=0.10, 95% CI [0.62, 1.02]). Additionally, confidence was positively associated with recall likelihood (β=0.13, *Error*=0.02, 95% CI [0.08, 0.18]).

Furthermore, test type did not significantly interact with either the curiosity effect (β=0.00, *Error*=0.03, 95% CI [-0.06, 0.06]), the condition effect (β=0.10, *Error*=0.12, 95% CI [-0.13, 0.33]) or the interaction between curiosity and condition (β=0.01, *Error*=0.04, 95% CI [-0.07, 0.09]). For a complete overview of the results, please refer to **Table 4** of Appendix C: Behavioural results.

Model 2: Reward Levels Model

To better understand the effect of the different reward levels within the reward condition on recall – compared to the no reward condition – we exploratorily created a new model that splits the reward condition variable by its three levels: 0, 1 and 3 euro. The effects of each of these rewards are compared to the reference, NR condition.

Firstly, we compare three sub models of model 2 to see which random effects structure is optimal (**Table 2**). We find that model 2c, which excludes the random structure for question items, performs significantly worse (|$\triangle ELPD/SE$| = 33.18 > 2) than the maximal model (model 2a) in predicting the data. Model 2b, which excludes the random correlations with respect to the maximal model, does not significantly perform worse than the maximal model (|$\triangle ELPD/SE$| = 1.75 < 2). Hence, for Model 2, we will report the more parsimonious model without random correlations (model 2b).

Table 2

Model comparison between three different Bayesian Reward Level models (model 2)

Model	ELPD	$\triangle$ELPD	*SE*	$\triangle$ELPD/SE	*p_loo*
Model 2c: MM without random structure for question items	**-6713.7**	**-1801.7**	**54.3**	**-33.18**	**211.9**
Model 2b: MM without random correlations	-4921.1	-9.1	5.20	-1.75	912.3
Model 2a: Maximal model	-4912.0				920.5

*Note: Bold font indicates a significant effect, where |$\triangle ELPD/SE$| > 2 indicated a significant difference between models. The maximum model was defined as: is_correct ~ 1 + curiosity * reward * test_type + confidence + (1 + curiosity * reward * test_type + confidence | participant_ID) + (1 + curiosity * reward * test_type + confidence | question_ID). Underscored is the random structure for question items that was not present in model 1 with respect to the maximal model. The random correlations in model 2 were removed from the maximal model.*

The estimated model indicates that curiosity is positively associated with recall likelihood (*β*=0.07, *Error*=0.03, 95% CI [0.01, 0.13]), in line with the result from model 1 and with our hypothesis. The effects of reward levels (in the Reward condition) were compared against the No Reward (NR) condition trials. Of these three, the difference between NR and 0-euro trials were positively associated with recall likelihood (*β*=0.31, *Error*=0.16, 95% CI [0.01, 0.62]). The difference between NR and 3-euro trials were also positively associated with recall likelihood (*β*=0.52, *Error*=0.17, 95% CI [0.19, 0.88]). For 1-euro trials, the difference with NR trials was not associated with recall likelihood (*β*=0.27, *Error*=0.17, 95% CI [-0.05, 0.60]). These combined results (**Figure 3**) are seemingly in contrast with our first model (model 1) in which we found no significant effect of reward condition on recall likelihood. However, they are partly in line with our hypothesis in which we predicted that reward

would have a positive effect on recall. However, we did not predict specifically that this reward-effect would not be present for 1-euro trials.

When looking at the 1-euro reward level, there was a positive interaction between curiosity and reward on recall likelihood (β=0.12, *Error*=0.06, 95% CI [0.01, 0.23]). Thus, there is a stronger effect of curiosity on recall likelihood in 1-euro trials compared to no-reward condition trials. However, when looking at the 0-euro (β=0.05, *Error*=0.06, 95% CI [-0.06, 0.16]) and 3-euro (β=0.02, *Error*=0.06, 95% CI [-0.09, 0.13]) reward levels, the interaction between the reward effect and curiosity was not associated with recall likelihood. I.e., there was no difference in the strength of the curiosity effect in NR trials compared to 0- and 3-euro trials. These results are not in line with the results from model 1, where we found no interaction between reward condition and curiosity on recall likelihood. We did predict that curiosity and reward would interact, only we expected a negative and not a positive interaction. Additionally, we did not predict that the interaction between curiosity and reward on recall likelihood would only exist for 1-euro trials but not the other trials.

Figure 3

Recall as a function of curiosity, reward level and test time point

Note: Results showed that there was a significantly positive effect of curiosity on recall likelihood. Compared to the baseline No-Reward condition, 0- and 3-euro trials positively predicted recall likelihood, whilst 1-euro trials did not. Additionally, we found a positive interaction between curiosity and 1-euro trials (compared to the No-Reward condition), but no interaction was found for 0- and 3-euro trials. The legend refers the four different reward levels. Error bars are the mean plus and minus the standard error of the mean.

Additionally, we found that the covariates test type and confidence both had credible intervals not including zero and were hence found to be associated with recall likelihood. Specifically, there was

a lower recall likelihood in the Delayed test compared to the Immediate test (*β*=-0.74, *Error*=0.09, 95% CI [-0.93, -0.55]), and the higher ones confidence in knowing the answer, the higher the recall likelihood (*β*=0.15, *Error*=0.02, 95% CI [0.10, 0.20]). This agrees with the findings from the first model, model 1.

Additionally, we found that test type (delayed recall compared to the reference immediate recall) did not statistically significantly interact with the curiosity effect (*β*=0.00, *Error*=0.03, 95% CI [-0.05, 0.06]), the 0-euro (*β*=-0.21, *Error*=0.16, 95% CI [-0.53, 0.11]), 1-euro (*β*=-0.22, *Error*=0.17, 95% CI [-0.54, 0.11]) or 3-euro (*β*=-0.08, *Error*=0.17, 95% CI [-0.41, 0.25]) reward effect or the interaction between curiosity and the 0-euro (*β*=0.04, *Error*=0.06, 95% CI [-0.08, 0.17]), 1-euro (*β*=-0.05, *Error*=0.06, 95% CI [-0.17, 0.07]) or 3-euro (*β*=-0.01, *Error*=0.06, 95% CI [-0.13, 0.12]) reward effect in predicting recall likelihood. For a complete overview, please refer to **Table 5** in Appendix C: Behavioural results.

Model 3: Trial Model

The interaction effects in model 1 and 2 were counter to our predictions, so we looked into explanations of the effect. Previous research has shown that variability in cognition plays an important factor in behaviour (Judd et al., 2024) so we wondered how the interaction effect changed over time, as a proxy for variability within the sample. Thus, we created a third (exploratory) model in which we investigate the temporal progressions of the reward and curiosity effects (see **Figure 4**). We did this by including the trial number as a variable in the model and modelled the interactions between trial number and both curiosity and reward separately (2-way interactions) and together (3-way interaction). In order to reduce model complexity, and the fact that none of its interactions in the models described above were significant, we removed the interactions of *test type* with curiosity and reward and included it only as a main variable.

The main effect of curiosity on recall likelihood was found to be significantly positive (*β*=0.0764, *Error*=0.0277, 95% CI [0.0217, 0.1304]), consistent with our hypothesis and the results from model 1 and model 2. For the reward effect, only the 3-euro reward shows a significant increase in recall likelihood compared to NR trials in this model (*β*=0.6899, *Error*=0.2071, 95% CI [0.3021, 1.1169]). Conversely, 0-euro trials (*β*=0.2279, *Error*=0.1611, 95% CI [-0.0867, 0.5535]) and 1-euro trials (*β*=0.2735, *Error*=0.1897, 95% CI [-0.0852, 0.6676]) did not show to be statistically significantly predictive of recall likelihood. The fact that the 0-euro effect now has the lowest effect size from the

three reward levels and is not significant anymore is different from model 2. However, the 3-euro

effect consistently significantly improves recall likelihood in both model 2 and this model. The

hypothesis that reward improves recall likelihood is thus still partly corroborated when correcting for

the effect of trial number.

We found that the main effect of trial was not statistically different from 0 (β=0.0021,

Error=0.0019, 95% CI [-0.0017, 0.0059]), however, trial number did negatively interact with the 3-euro

reward incentive (compared to NR) (β=-0.0114, *Error*=0.0050, 95% CI [-0.0212, -0.0017]) – i.e. the

further on in the experiment, the less effective the 3-euro reward incentive was.

The interaction effects of curiosity with the 0-euro (β=0.0754, *Error*=0.0592, 95% CI [-0.0399,

0.1913]) , 1-euro (β=0.0793, *Error*=0.0598, 95% CI [-0.0391, 0.1957]) and 3-euro (β=-0.0022,

Error=0.0613, 95% CI [-0.1256, 0.1171]) reward levels (compared to NR) all included zero, meaning

there was no statistically significant effect. Thus, compared to model 2, the 1-euro interaction with

curiosity on recall likelihood is now not statistically significant anymore whilst the interactions between

the 0- and 3-euro rewards with curiosity on recall likelihood remain insignificant compared to model 2.
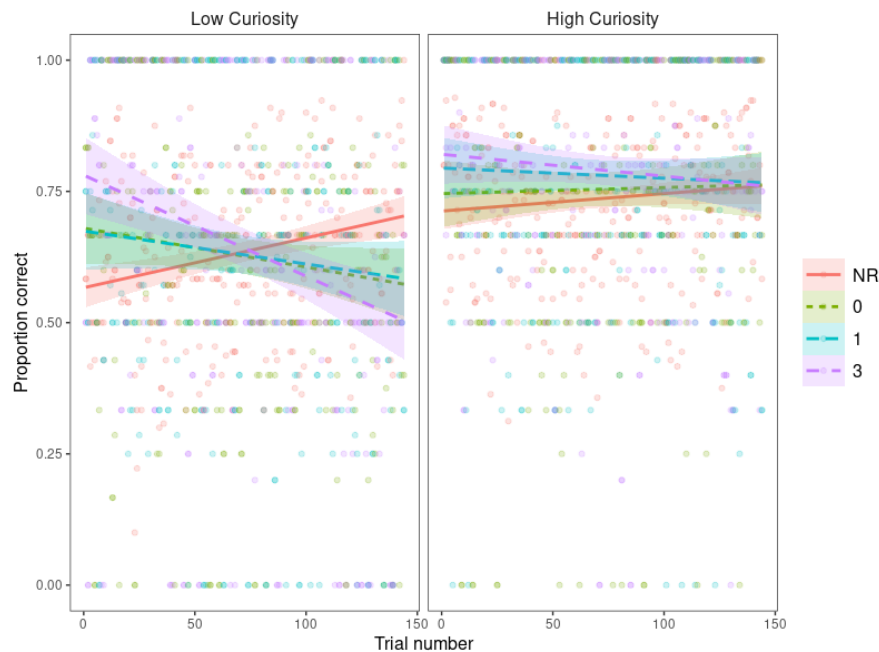
Interestingly, we found that the interaction between trial and all reward levels was positively

modulated by curiosity. The three-way interaction of trial, curiosity and the 3-euro reward (β=0.0039,

Error=0.0017, 95% CI [0.0007, 0.0073]) excluded zero and was thus found to be statistically

significant. Additionally, the 1-euro reward (β=0.0031 *Error*=0.0015, 95% CI [0.0000, 0.0061]) and the

0-euro reward (β=0.0031, *Error*=0.0013, 95% CI [0.0005, 0.0057]) were also positive and statistically

significant. This means that the decreasing effectiveness of the 3-, 1- and 0-euro rewards in improving

recall as the trials progressed, became less strong the more a participant was curious for a question.

In other words, curiosity seemed to ameliorate the detrimental effect of trial progression on the reward

effects.

For illustration, in odds ratio terms, this means that at trial 1, the model estimates that the

interaction between curiosity and 0-euro (*OR*=0.87), 1-euro (*OR*=0.87) and the 3-euro (*OR*=0.76)

rewards (with respect to NR) are lower than 1 – i.e. the effect of the respective rewards goes down as

curiosity goes up. Whilst at trial 144, the model estimates that the interaction between curiosity and 0-

euro (*OR*=1.34), 1-euro (*OR*=1.35) and the 3-euro (*OR*=1.32) rewards (with respect to NR) are higher

than 1 – i.e. the effectiveness of the respective rewards goes up as curiosity goes up. Thus, this

means that the negative interaction effect between curiosity and reward is there – like we predicted –

but only so in earlier trials – a novel finding we did not predict at all.

Figure 4

Effect of trial on recall per reward level and split between low and high curiosity

Note: The results from model 3 showed that curiosity was found to positively predict recall likelihood. Only 3-euro trials, and not 0- and 1-euro trials, showed to have a significantly higher recall likelihood compared to the No-Reward condition. The main effect of trial number was not significant, but we found a significantly negative interaction effect between trial number and 3-euro trials (compared to NR trials). Lastly, we found that the 3-way interactions between trial, curiosity and all three reward levels was positive. In other words, we found that in early trials there was a negative interaction effect between curiosity and the three reward levels compared to baseline (NR), and in later terms there is a positive interaction between curiosity and the three reward levels – which expressed itself as curiosity reducing the negative effect of all rewards on recall.
The legend refers to the four different reward levels. Plots are split based on the by-participant median curiosity. The mixed-effect regression model included curiosity as a numerical predictor ranging from 1-10, not a categorical split variable. The confidence bands are 95%-confidence intervals based on the mean proportions correct at each combination of reward level and curiosity level.

The effect of the covariate test type was significantly different from zero – where recall in the delayed recall test was lower than in the immediate recall test (β=-0.9309, *Error*=0.0943, 95% CI [-1.1196, -0.7488]. Confidence was again positively predictive of recall (β=0.1627, *Error*=0.0295, 95% CI [0.1060, 0.2208]). Both findings are consistent with the results from model 1 and model 2. For a complete description of the model results, please refer to **Table 6** in Appendix C: Behavioural results.

Neuroimaging results

In order to better understand the neural correlates of curiosity and reward and their effects on memory, we investigate both whole brain activation patterns and BOLD activity for specific regions of interest (ROI). We investigate our results in two ways. The first, the *Condition Model* (fMRI model 1), considers reward as a between-block variable. In this model we compare non-rewarded trials with

rewarded trials to obtain the reward effect, regardless of the magnitude of the reward in the rewarded trials. Additionally, we delve deeper in the effect of the different magnitude of reward on brain activity in a model that only considers the rewarded trials – directly replicating Duan et al. (2020) – the *Reward Only Model* (fMRI model 2).

Curiosity induction

Firstly, we investigated neural activity during the induction of curiosity, which takes place when participants get to see the question (for the second time, after having seen it during the prescreening out of the scanner), without getting an answer to the question yet. We hypothesised that high curiosity questions would elicit higher activity in the bilateral IPL and the vmPFC than for low curiosity questions.

Firstly, we look at regions that show higher BOLD activity during the presentation of high curiosity questions, compared to low curiosity questions – i.e. activity related to curiosity induction during the question presentation screen. Due to some estimation problems in the Condition Model (fMRI model 1), we will only use the results from the Reward Only Model (fMRI model 2) to look into neural activity related to curiosity induction[4].

We see a large cluster with peak activity (see table fMRI model 2: Reward Levels Only Model) in the left paracingulate gyrus, as well as clusters in the bilateral precuneous, bilateral frontal pole, the left superior parietal lobule – with overlap of the angular gyrus, a main structure of the inferior parietal lobule. More clusters were found in the left middle frontal gyrus, left insular cortex, right frontal orbital cortex, the posterior middle temporal gyrus and lastly in the inferior frontal gyrus pars opercularis (**Figure 5**, yellow shade).

When we look at regions where BOLD activity is higher for low curiosity questions compared to high curiosity questions, we see clusters with peak activity in the bilateral postcentral gyrus and the right posterior supramarginal gyrus, all overlapping the inferior parietal lobule. Additionally, clusters were found in the bilateral inferior lateral occipital cortex, the right superior lateral occipital cortex, right precentral gyrus, right posterior cingulate gyrus, right insular cortex, right frontal pole, one cluster

---

[4] The variation COPE (varcope) for the High Curiosity variable in the first level of the model could not be estimated properly by FSL FEAT, causing an incapability of the model to compute t-values for the group level estimates for the variables High, High > Low and Low > High Curiosity during the question (curiosity induction) presentation.
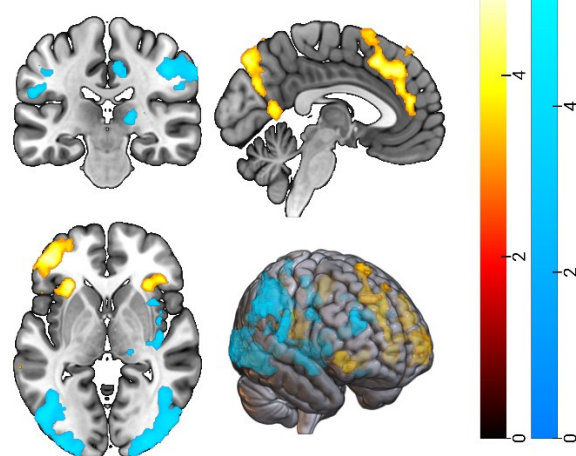
in the right thalamus and lastly a cluster with overlap (not peak activity[5]) in the left anterior hippocampus and amygdala (**Figure 5**, blue shade).

To determine more specifically, based on our hypotheses, if our regions of interest are implicated in curiosity induction, we conducted an ROI analysis. Activity in the right inferior parietal lobule was significantly lower for high curiosity questions compared to low curiosity questions, $M=-0.38$, $SE=0.07$, $t_{(40)}=-5.33$, $p<.001$ (**Figure 6**), partly confirming our hypothesis that the inferior parietal lobule is implicated in curiosity induction – but against our prediction that activity would be higher for high curiosity questions, not low curiosity. Contrary to our expectation, BOLD activity in the vmPFC did not significantly differ between high and low curiosity questions ($M=-0.02$, $SE=0.08$, $t_{(40)}=-0.24$, $p=.88$). Neither did BOLD activity in the left IPL ($M=-0.11$, $SE=0.07$, $t_{(40)}=-1.49$, $p=.144$). Even though we made no hypotheses about activity in the hippocampal formation during curiosity induction, activity in the right aHPC ($M=-0.19$, $SE=0.11$, $t_{(40)}=-1.72$, $p=.093$) and left aHPC ($M=-0.17$, $SE=0.11$, $t_{(40)}=-1.52$, $p=.137$) was not associated with curiosity.

---

[5] Peak 'activity' was in white matter, but the cluster extended into the hippocampus and amygdala.

Figure 5
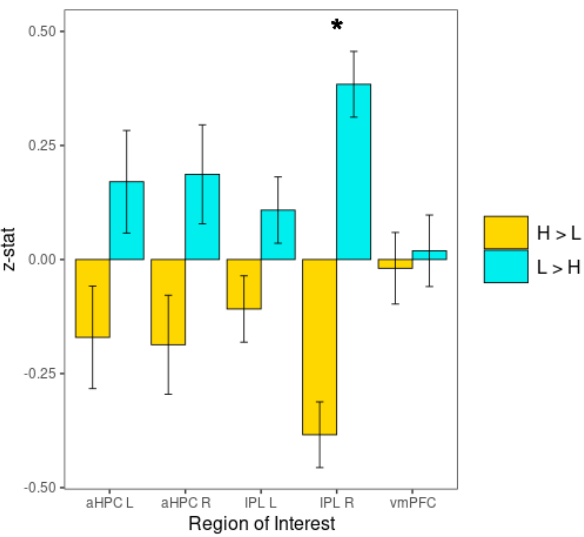
Curiosity induction, whole brain analysis (fMRI model 2)

Note: Values in this map are group-level z-value. The yellow shade represents the High > Low Curiosity effect and the blue shade the Low > High Curiosity effect for the curiosity ratings during the question presentation screen. Images are with a Left-Right orientation (neurological convention). MNI152-coordinates (-4, -25, -1).

Figure 6

Curiosity induction, ROI analysis (fMRI model 2)

*Note: The yellow bars represent the mean z-value in the specific ROI for the High > Low Curiosity during the question screen contrast, from the Reward Only model. The blue contrast represents the Low > High Curiosity during the question screen contrast. Both contrasts are redundantly displayed for clarity but note the symmetry. Error bars represent the mean plus and minus the standard error of the mean.*
* Indicates that the z-value is significantly different from 0 after Bonferroni correction to p<.01 for the five-fold comparison.

Curiosity-motivated subsequent-memory effect

We have seen where curiosity induction is associated with BOLD activity in the brain. We are also interested in how curiosity supports learning and memory. Therefore, we look at the curiosity-motivated subsequent-memory effect (SME). We do this by comparing activity for remembered answers only (in the delayed recall) during curiosity relief, i.e. the answer presentation screen. Of these remembered answers, we compare activity during the answer screen for high curiosity questions compared to low curiosity questions. We predicted that the bilateral IPL, bilateral aHPC and vmPFC would show higher activity for high curiosity and remembered questions compared to low curiosity and remembered questions.

Firstly, within fMRI model 1 (see table fMRI model 1: Condition Model), we look at cluster activity in the whole brain by investigating where high curiosity questions whose answers were remembered show higher BOLD activity than low curiosity questions whose answers were remembered (**Figure 7**, yellow shade). We find peak activity in clusters in the bilateral superior lateral occipital cortex with overlap of the bilateral IPL. Additionally a cluster showed peak activity in the left

anterior paracingulate gyrus with overlap of the vmPFC. We found more clusters in the right superior frontal gyrus, bilateral frontal pole with an additional cluster in the left frontal pole, bilateral frontal orbital cortex, the left posterior middle temporal gyrus, and right cerebellum.
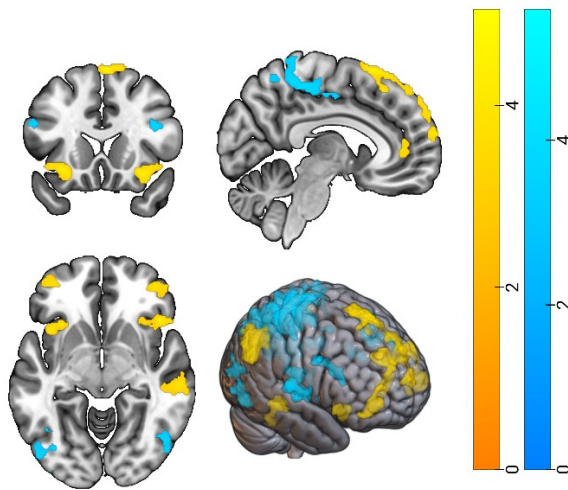
Regions where BOLD activity was higher for low curiosity questions whose answers were remembered than high curiosity questions whose answers were remembered (**Figure 7**, blue shade) had peak activity in clusters in the bilateral superior lateral occipital cortex and the left occipital pole – all with a very small overlap of the IPL in their respective hemispheres. Additional clusters were found in the right inferior lateral occipital cortex, the right precentral gyrus, the left inferior frontal gyrus pars opercularis, the right central opercular cortex and lastly the left posterior superior temporal gyrus.

We compare this with the Reward Only Model (see table fMRI model 2: Reward Levels Only Model) for completeness. Clusters where activity was greater for high curiosity questions whose answers were remembered than for low curiosity questions (**Figure 8**, yellow shade) had peak activity in the left superior lateral occipital cortex, with overlap of the left IPL, as well as the right occipital pole, left inferior frontal gyrus pars opercularis and left frontal pole.

The opposite contrast, where low curiosity questions show greater activity than high curiosity questions whose answers are remembered (**Figure 8**, blue shade) showed clusters with peak activity in the right postcentral gyrus but extending down into the right IPL. Two clusters in the bilateral planum temporale, one in the right temporooccipital middle temporal gyrus, one in the right parietal operculum cortex and one in the left inferior lateral occipital cortex also extended up into the IPL within their respective hemispheres. A cluster in the right medial frontal pole showed a large overlap with the right and to a smaller degree the left vmPFC. Additionally, a cluster was found in the left insular cortex and lastly a cluster overlapping (but not with a peak in) the right thalamus.

Figure 7
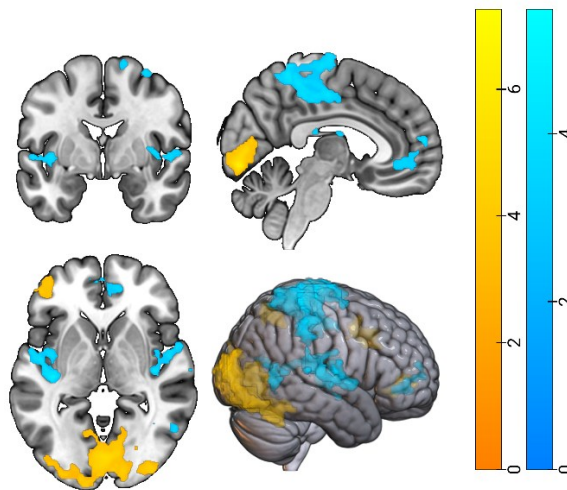
Curiosity-motivated subsequent-memory effect during curiosity relief, whole brain analysis of the Condition Model (fMRI model 1)

Figure 8

Curiosity-motivated subsequent-memory effect during curiosity relief, whole brain analysis of the Reward Only Model (fMRI model 2)

*Note: Values in this map are group-level z-value. The yellow shade represents the High Curiosity > Low Curiosity for Remembered items during the answer presentation screen contrast. The blue shade represents the Low Curiosity > High Curiosity for Remembered items during the answer presentation screen contrast.*
Images are with a Left-Right orientation (neurological convention). MNI152-coordinates (6, 18, -7).

Note: Values in this map are group-level z-value. The yellow shade represents the High Curiosity > Low Curiosity for Remembered items during the answer presentation screen contrast. The blue shade represents the Low Curiosity > High Curiosity for Remembered items during the answer presentation screen contrast.
Images are with a Left-Right orientation (neurological convention). MNI152-coordinates (5, -2, -1).

ROI analysis within the condition model (fMRI model 1) showed that BOLD activity in none of the ROIs was significantly modulated by the curiosity-motivated SME: left aHPC (M=0.00, SE=0.03, $t_{(40)}$=0.13, p=.90), right aHPC (M=-0.02, SE=0.02, $t_{(40)}$=-0.65, p=.52), left IPL (M=0.00, SE=0.05, $t_{(40)}$=0.08, p=.94), right IPL (M=0.04, SE=0.06, $t_{(40)}$=0.72, p=.48) nor the vmPFC (M=0.10, SE=0.07, $t_{(40)}$=1.37, p=.177) – against our expectation that activity in the IPL, aHPC and vmPFC would have been. Comparing this with the results from the Reward Only Model (fMRI model 2), we see one interesting difference. Namely, BOLD activity in the right IPL does seem to be modulated by the curiosity-motivated SME (M=-0.18, SE=0.06, $t_{(40)}$=-3.00, p=.005); i.e. activity in the right IPL is lower for high curiosity questions whose answers were remembered compared to low curiosity questions. This is again partly in line with our hypothesis in the sense that activity in the IPL is associated with the curiosity-motivated SME. However, it is again our expectation that this effect is negative and not positive. Activity in the other regions was not significantly modulated by the curiosity-motivated SME: left aHPC (M=0.09, SE=0.10, $t_{(40)}$=0.88, p=.38), right aHPC (M=0.07, SE=0.10, $t_{(40)}$=0.66, p=.51), left

IPL (M=-0.00, SE=0.06, $t_{(40)}$=-0.05, p=.96) and vmPFC (M=-0.09, SE=0.08, $t_{(40)}$=-1.13, p=.26) – again, against our expectations.

Figure 9
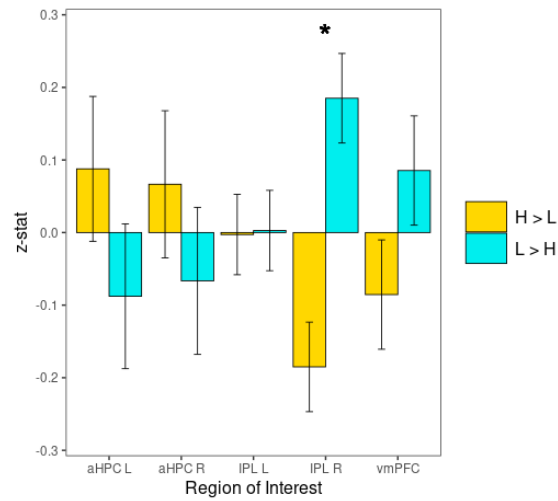
Curiosity-motivated subsequent-memory effect, ROI analysis of the Condition Model (fMRI model 1)

Note: The yellow bars represent the mean z-value in the respective ROI for the High > Low Curiosity for Remembered answers only during the answer screen presentation contrast, from the Condition Model. The blue contrast represents the Low > High Curiosity for Remembered items during the answer screen presentation contrast. Both contrasts are redundantly displayed for clarity but note the symmetry. Error bars represent the mean plus and minus the standard error of the mean.

Figure 10

Curiosity-motivated subsequent-memory effect, ROI analysis of the Reward Only Model (fMRI model 2)

Note: The yellow bars represent the mean z-value in the respective ROI for the High > Low Curiosity for Remembered answers only during the answer screen presentation contrast, from the Reward Only Model. The blue contrast represents the Low > High Curiosity for Remembered items during the answer screen presentation contrast. Both contrasts are redundantly displayed for clarity but note the symmetry. Error bars represent the mean plus and minus the standard error of the mean.
* Indicates that the z-value is significantly different from 0 after Bonferroni correction to p<.01 for the five-fold comparison

Reward incentive

We are also interested in the effect of reward incentives on BOLD activity. During the presentation of the reward incentive at the beginning of the trial, different BOLD activity can be the cause of dissimilar stimuli being presented (a euro coin versus a circle with a question mark). Therefore, we look into the effect of reward during the remembering stage of the trial – i.e. during the answer screen presentation. We predicted that the vmPFC would show higher activity within the reward compared to the no reward condition and that the vmPFC would show higher activity as the reward magnitude goes up.

A whole brain analysis of the Condition Model (see table fMRI model 1: Condition Model) results in two significant clusters where BOLD activity is higher in the Rewarded blocks compared to the No Reward blocks. The first cluster had peak activity in the left occipital pole and the second
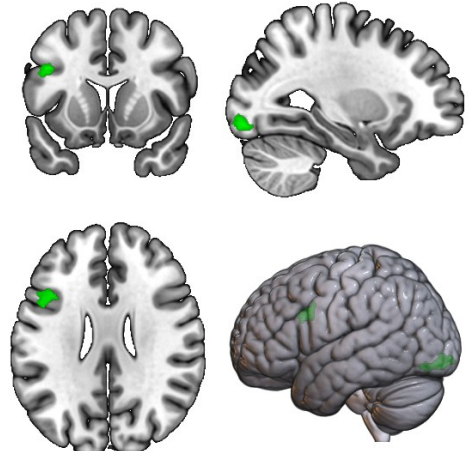
cluster did so in the middle frontal gyrus (**Figure *11***). There were no significant clusters that showed greater activity for the No Reward condition compared to the Reward condition.

When we parametrically modulated the reward level (0, 1 or 3 euro) for only those trials in the rewarded blocks, we find more widespread activity across the brain (see table fMRI model 2: Reward Levels Only Model). For the positive parametric modulation of reward magnitude (**Figure *12***, green shade), we found clusters with peak activity in the left occipital pole, left precentral gyrus, left inferior frontal gyrus pars triangularis, left posterior middle temporal gyrus and left amygdala but overlapping the anterior hippocampus. This means that within these regions, a linear increase in reward incentive was associated with higher BOLD activity. The two clusters from the Condition Model (fMRI model 1) described above also fall within two of these Reward Only Model (fMRI model 2) clusters.

Clusters where the reward magnitude negatively parametrically modulated BOLD activity (**Figure *12***, blue shade) had peak activity in the bilateral anterior supramarginal gyrus, both falling mostly within the IPL. A cluster in with its peak in the left superior lateral occipital cortex touched and very slightly overlapped the posterior part of the IPL. Another cluster in the right paracingulate gyrus and one with peak activity in the right subcallosal cortex were partially contained within the vmPFC. Additionally, two separate clusters in the right precuneous cortex, the left superior parietal lobule, the right precentral gyrus, right superior frontal gyrus and the right frontal pole were found.

Figure 11
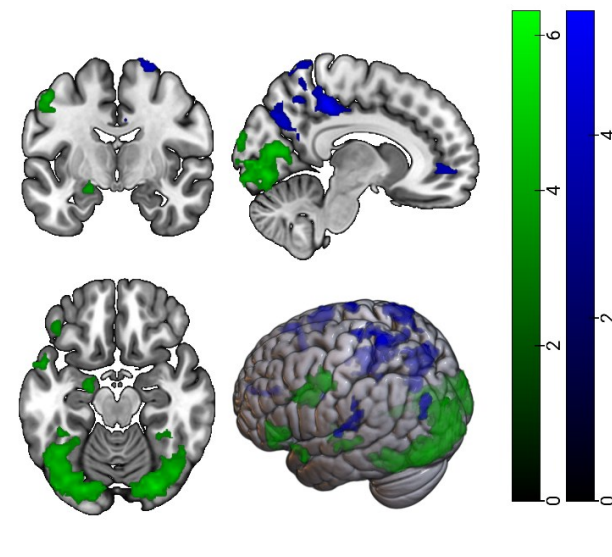
Reward incentive effect during curiosity relief, whole brain analysis of the Condition Model (fMRI model 1)

Figure 12

Parametric modulation of reward incentive during curiosity relief, whole brain analysis of the Reward Only Model (fMRI model 2)

Note: Values in this map are group-level z-value. The green shade represents the Reward > No Reward during the answer screen presentation contrast. Images are with a Left-Right orientation (neurological convention). MNI152-coordinates (-27, 12, 26).

Note: Values in this map are group-level z-value. The green shade represents the positive modulation of reward during the answer screen presentation, for rewarded blocks only. The blue shade represents the negative modulation of reward. Images are with a Left-Right orientation (neurological convention). MNI152-coordinates (9, -8, -17).
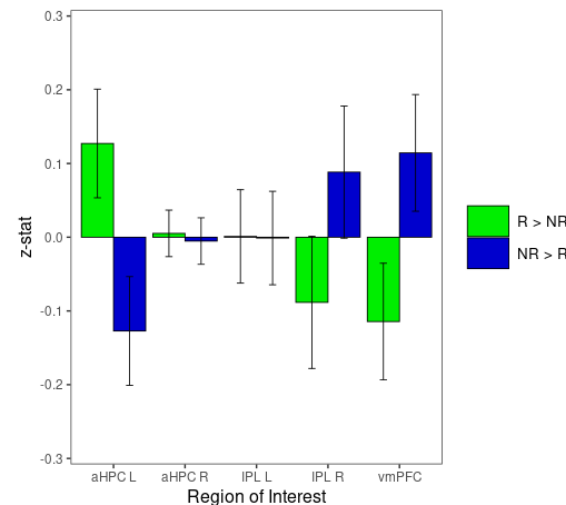
ROI analysis within the Condition Model (fMRI model 1), showed that none of the ROIs were significantly modulated by the reward condition (**Figure *13***): left aHPC (M=0.13, SE=0.07, $t_{(40)}$=1.72, p=.092), right aHPC (M=0.01, SE=0.03, $t_{(40)}$=0.17, p=.87), left IPL (M=0.00, SE=0.06, $t_{(40)}$=0.02, p=.99), right IPL (M=-0.09, SE=0.09, $t_{(40)}$=-0.99, p=.33), vmPFC (M=-0.11, SE=0.08, $t_{(40)}$=-1.45, p=.156). We did not expect to not find any effect in the vmPFC.

Within the Reward Only Model (fMRI model 2) only the right inferior parietal lobule was significantly modulated by reward incentive magnitude, M=-0.19, SE=0.06, $t_{(40)}$=-3.09, p=.004. I.e. the right inferior parietal lobule showed less BOLD activity as the reward incentive went up in value (**Figure *14***) . We did not predict this in our a-priori hypotheses as we described the IPL solely to curiosity-related processing. This finding suggests a more general motivational role of the right IPL. The left aHPC did not survive Bonferroni correction (M=0.20, SE=0.09, $t_{(40)}$=2.08, p=.044), and the right aHPC (M=0.19, SE=0.10, $t_{(40)}$=2.01, p=.051) and the left IPL (M=-0.06, SE=0.05, $t_{(40)}$=-1.28, p=.21) were also not statistically significantly modulated by reward magnitude during curiosity relief.

Counter to our expectations, activity in the vmPFC was not related to reward processing either (M=0.02, SE=0.07, $t_{(40)}$=0.24, p=.81).

Figure 13
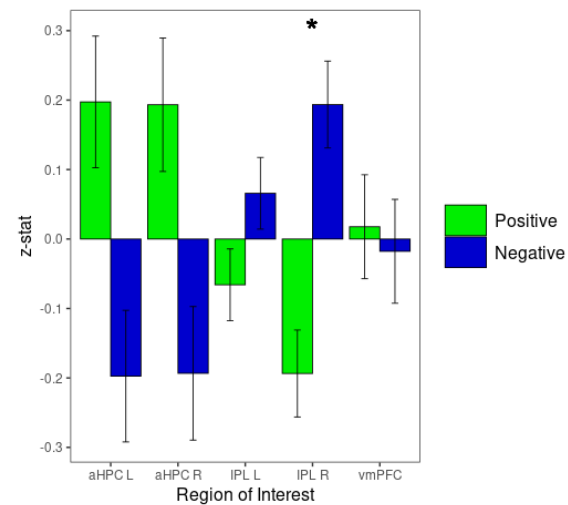
Reward effect during curiosity relief, ROI analysis for the Condition Model (fMRI model 1)

Note: The green bars represent the mean z-value of the respective ROIs for the Reward > No Reward contrast during curiosity relief, i.e. the answer presentation screen from the Reward Only Model. The blue bars represent the No Reward > Reward. Both contrasts are redundantly displayed for clarity but note the symmetry. Error bars represent the mean plus and minus the standard error of the mean.

Figure 14

Parametric modulation of reward incentive during curiosity relief, ROI analysis for the Reward Only Model (fMRI model 2)

Note: The green bars represent the mean z-value of the respective ROIs for the positive parametric modulation of reward during curiosity relief, i.e. the answer presentation screen from the Reward Only Model. The blue bars represent the negative parametric modulation. Both contrasts are redundantly displayed for clarity but note the symmetry. Error bars represent the mean plus and minus the standard error of the mean.
* Indicates that the z-value is significantly different from 0 after Bonferroni correction to p<.01 for the five-fold comparison.

Reward-motivated subsequent-memory effect

Now that we know which brain regions are associated with reward, estimated using both the condition model (fMRI model 1) and the reward only model (fMRI model 2), we are also interested in how reward supports memory for trivia question answers, i.e. the reward-motivated subsequent-memory effect. We hypothesised that activity in the vmPFC and the bilateral aHPC would be higher for remembered compared to forgotten questions in the rewarded versus the non-reward condition. We also predicted these regions to increase their activity for the subsequent-memory effect when rewards increased in magnitude.

Within the Condition Model (see table fMRI model 1: Condition Model), we find that there is one significant cluster where we find increased activity for the no reward condition compared to the
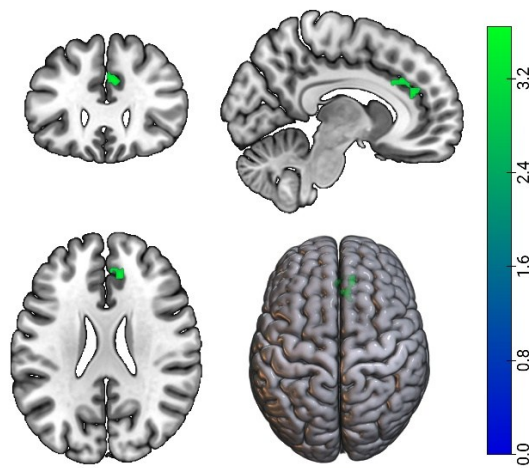
rewarded condition in relation to the subsequent memory effect: in the right paracingulate gyrus (**Figure 15**). So, BOLD activity here is greater when answers are remembered (compared to forgotten) and the trial is in a non-rewarded (compared to a rewarded) block. Another way of saying this is that there is deactivation in the rewarded context in support of the subsequent-memory effect.

More significant clusters were found in the Reward Only Model (see table fMRI model 2: Reward Levels Only Model). We found clusters whose subsequent-memory effect (activity for remembered items that is greater than for forgotten items) is positively parametrically modulated by reward (**Figure 16**, orange shade) to have peak activity in the left occipital pole, left precentral gyrus, right inferior frontal gyrus pars triangularis, right posterior temporal fusiform cortex and right superior lateral occipital cortex – the last of which showed overlap with the right IPL.

For regions where reward negatively modulates activity for the subsequent-memory effect (**Figure 16**, green shade), we find peak cluster activity in the right planum temporale and left parietal operculum cortex, both clusters mostly contained by the IPL. A cluster in the right frontal medial cortex was fully part of our vmPFC defined volume. Other clusters were found in the left postcentral gyrus, right frontal pole and right superior lateral occipital cortex, slightly overlapping the posterior part of the IPL. In other words, when one is rewarded, these regions show a deactivation pattern in support of the subsequent-memory effect.

Figure 15
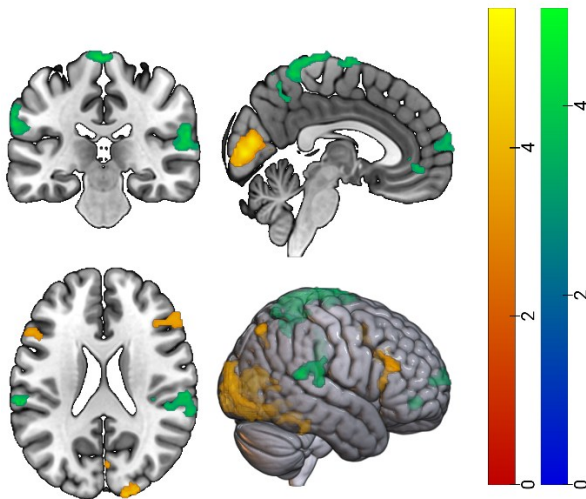
Reward-motivated subsequent-memory effect, whole brain analysis of the Condition Model (fMRI model 1)

Figure 16

Reward-motivated subsequent-memory effect, whole brain analysis of the Reward Only Model (fMRI model 2)

Note: Values in this map are group-level z-values. The green shade represents the combination of the No Reward > Reward and Remembered > Forgotten during the answer screen presentation contrast. Images are with a Left-Right orientation (neurological convention). MNI152-coordinates (8, 27, 24).
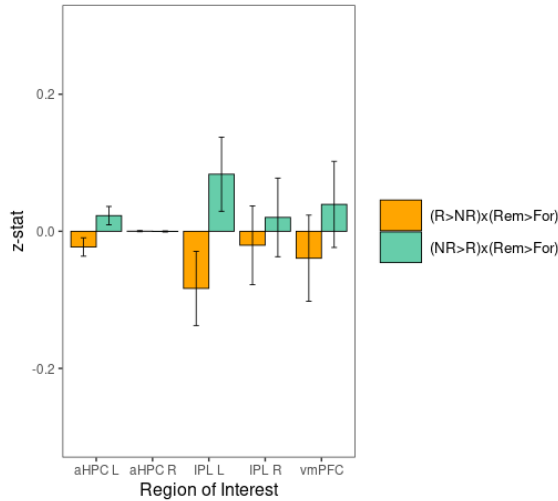
Note: Values in this map are group-level z-values. The orange shade represents the interaction of reward with the Remembered > Forgotten during the answer screen presentation contrast, for rewarded blocks only. The green shade represents the interaction of negative reward with the Remembered > Forgotten during the answer screen presentation contrast, for rewarded blocks only. Images are with a Left-Right orientation (neurological convention). MNI152-coordinates (3, -27, 22).

ROI analysis of the Reward Only Model (fMRI model 2) showed that none were modulated by the reward-motivated subsequent-memory effect. The effect in the right aHPC did not survive Bonferroni correction (M=0.18, SE=0.09, $t_{(40)}$=2.04, p=.048). Additionally, activity in the left aHPC (M=0.13, SE=0.09, $t_{(40)}$=1.52, p=.137) and vmPFC (M=-0.07, SE=0.08, $t_{(40)}$=-0.86, p=.0.39) was also not significantly modulated by the reward-motivated subsequent-memory effect – all counter to our hypotheses. Activity in the left IPL (M=-0.03, SE=0.06, $t_{(40)}$=-0.56, p=.58) and right IPL (M=-0.12, SE=0.07, $t_{(40)}$=-1.78, p=.082) was also not modulated by reward magnitude.

Figure 18
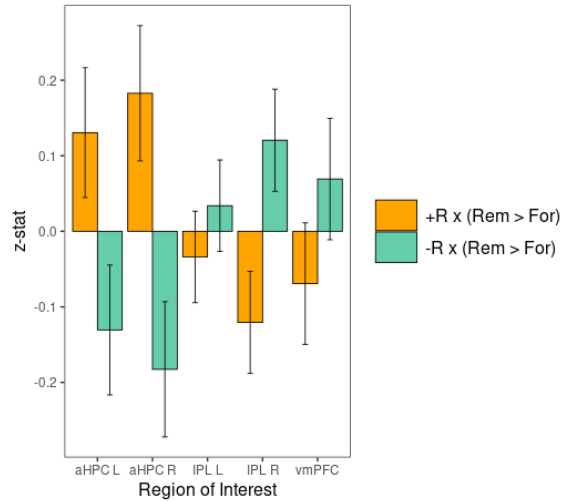
Reward-motivated subsequent-memory effect, ROI

analysis, for the Reward Only Model (fMRI model 2)

Note: The orange bars represent the mean z-value of the respective ROIs for the Remembered > Forgotten during curiosity relief (i.e. the answer presentation screen) contrast combined with the Reward > No Reward contrast, from the Reward Only Model. The aquamarine-coloured bars represent the No Reward > Reward contrast in combination with the subsequent-memory effect (Remembered > Forgotten). Both contrasts are redundantly displayed for clarity but note the symmetry. Error bars represent the mean plus and minus the standard error of the mean.

Note: The orange bars represent the mean z-value of the respective ROIs for the interaction of the positive parametric modulation of reward during curiosity relief (i.e. the answer presentation screen) with the Remembered > Forgotten contrast, from the Reward Only Model. The aquamarine-coloured bars represent the interaction of the negative parametric modulation of reward during curiosity relief (i.e. the answer presentation screen) with the Remembered > Forgotten contrast. Both contrasts are redundantly displayed for clarity but note the symmetry. Error bars represent the mean plus and minus the standard error of the mean.

Overlap in the curiosity- and reward-motivated subsequent-memory effects

We have seen how curiosity and reward separately support memory formation. Comparing the effects from the Reward Only Model (fMRI model 2) directly (see **Figure *19***), we see overlapping activation and a few distinct hubs. We now visually describe these regions – i.e. no statistical method like conjunction analysis was used for this thesis to determine similarity in activation patterns.
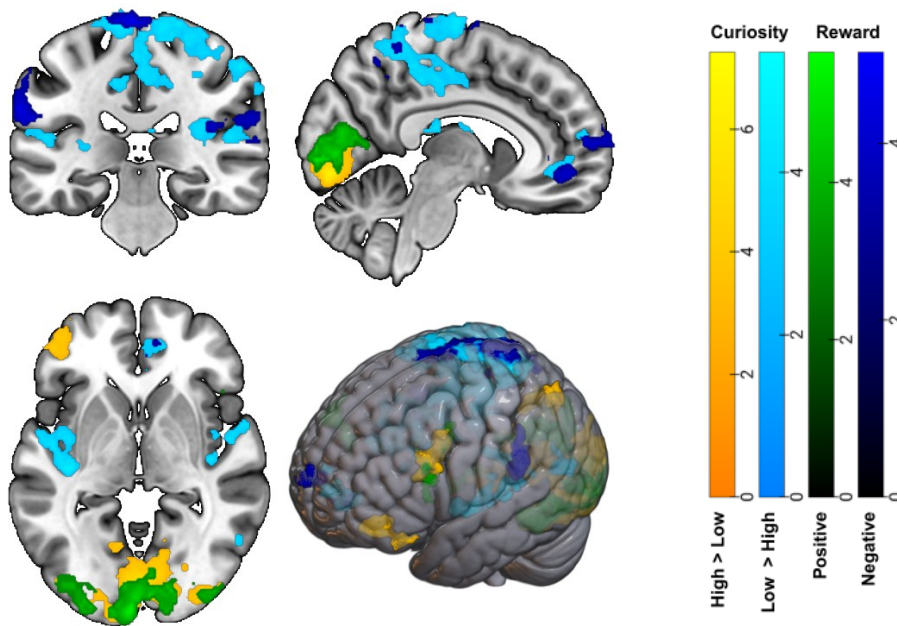
The large occipital pole clusters that stretch bilaterally for both the curiosity- and reward-motivated SME's overlapped almost entirely. The curiosity cluster in the inferior frontal gyrus overlapped partly with that of the reward-cluster that peaked in the precentral gyrus, but the reward-cluster reached more posteriorly and the curiosity-cluster more anteriorly. The reward-motivated inferior frontal pole cluster and the curiosity-motivated SME cluster in the frontal pole also overlapped partly and showed the same posterior-anterior patterns as the former two clusters.

For the negative effects, i.e. higher activity for low curiosity (or deactivation for high curiosity) and decreased activity for higher reward magnitude, we again find multiple overlapping clusters.

Activity in the posterior precuneous is only expressed for the negative reward effect but more anteriorly in the precuneous both effects are represented. Both show overlap across the post- and precentral gyrus, the bilateral posterior cingulate gyrus as well as the bilateral superior parietal lobule. Activity in the right IPL is seen for both effects, but in the left IPL, there is a tiny cluster for the reward effect only. vmPFC activity is represented by two overlapping clusters for both the curiosity- and reward-motivated SMEs stretching the paracingulate gyrus and frontal pole. Subcallosal activity is specific to the negative reward-motivated SME effect and a thalamic cluster for the negative curiosity-motivated SME. Bilateral posterior insular clusters that extended into the planum temporal were also only found for the curiosity-motivated subsequent-memory effect.

Figure 19

Comparison between the curiosity- and reward-motivated subsequent memory effects, whole brain analysis of the Reward Only Model

Note: Values in this map are group-level z-values. The effects represent the curiosity- and reward-motivated subsequent-memory effects during the answer presentation screen, i.e. during curiosity relief, for the Reward Only Model. The different overlays are copies from, in order, **Figure 8** *and* **Figure 16** *(note that the colours for the reward-motivated subsequent-memory effect had to be changed from those used in figure 18 to make the overlay more contrasting with the curiosity-motivated SME). MNI-coordinates (7, -30, -2).*

Reward x Curiosity-motivated subsequent-memory effect

Having seen the commonalities and differences between the curiosity- and reward-motivated subsequent-memory effects, we are also interested in whether they interact. I.e., does the effect of curiosity differ when we present rewards compared to no reward or when we modulate the magnitude of the reward. We exploratorily looked at this effect, since we have made no a-priori hypothesis. We
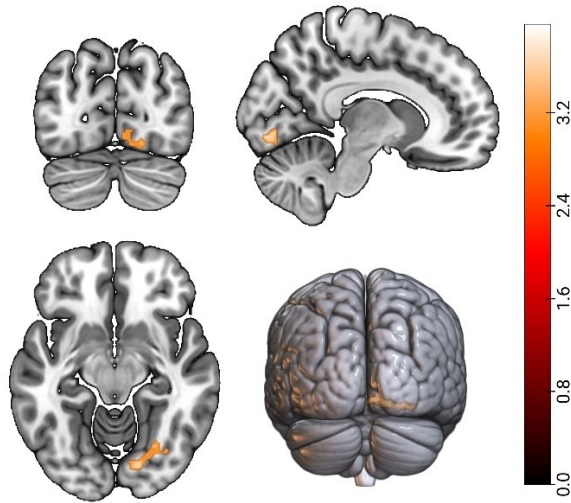
found no significant clusters for the former effect. Thus, we found no regions where the effect of the curiosity-motivated subsequent-memory effect changed between the rewarded and non-rewarded blocks (fMRI model 1).

We found one cluster in the Reward Only model (see table fMRI model 2: Reward Levels Only Model), namely in the lingual gyrus (**Figure 20**). Thus, when the reward magnitude linearly increased, the lingual gyrus showed an increasing greater activity for high curiosity questions whose answers were later remembered compared to low curiosity questions.

ROI analysis of the Reward Only model (fMRI model 2) showed that none of the ROIs were significantly modulated by the interaction between the reward- and curiosity-motivated subsequent-memory effects (**Figure 21**). The vmPFC showed marginal significance for the uncorrected alpha level, M=-0.13, SE=0.06, $t_{(40)}$=-2.01, p=.051 – but would nonetheless not survive Bonferroni correction. The effect in the left aHPC (M=-0.02, SE=0.09, $t_{(40)}$=-0.26, p=.80), right aHPC (M=0.03, SE=0.08, $t_{(40)}$=0.32, p=.75), left IPL (M=0.00, SE=0.05, $t_{(40)}$=0.08, p=.93) and right IPL (M=0.02, SE=0.06, $t_{(40)}$=0.27, p=.79) were also not statistically significant.

Figure 20
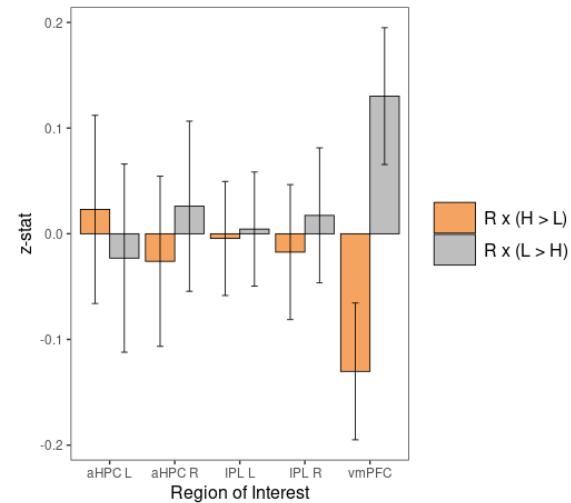
Interaction between the reward and curiosity-motivated subsequent-memory effect, whole brain analysis of the Reward Only Model (fMRI model 2)

Figure 21

Interaction between the reward and curiosity-motivated subsequent-memory effect, ROI analysis of the Reward Only Model (fMRI model 2)

Note: Values in this map are group-level z-values. The orange shade represents the interaction of the positive parametric modulation of reward with the High > Low Curiosity for Remembered items contrast, during the answer presentation screen. Images are with a Left-Right orientation (neurological convention). MNI152-coordinates (10, -78, -11).

Note: The orange bars represent the mean z-value of the respective ROIs for the interaction of the positive parametric modulation of reward during curiosity relief (i.e. the answer presentation screen) with the High > Low Curiosity for Remembered items contrast, from the Reward Only Model. The grey bars represent the mean z-stat of the respective ROIs for the interaction with the Low > High Curiosity for Remembered items contrast. Both contrasts are redundantly displayed for clarity but note the symmetry. Error bars represent the mean plus and minus the standard error of the mean.

Subsequent-memory effect
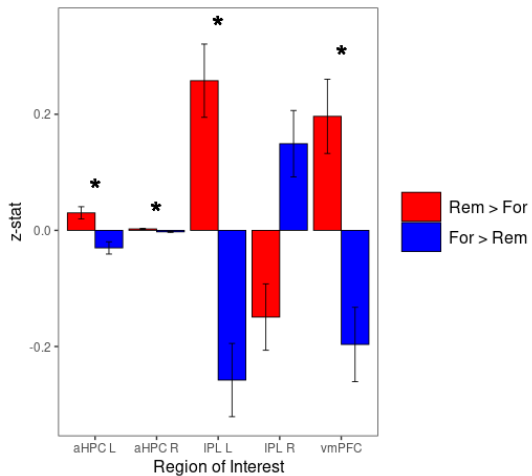
We have seen how curiosity and reward are expressed functionally in the brain, and how they might support learning by looking at their respective motivated subsequent-memory effects. In order to put these results into perspective, we will also exploratorily – i.e. we made no a-priori hypotheses – look into the unmotivated subsequent memory effect and see how our chosen ROIs behave during encoding using fMRI model 1 (Condition Model).

During the encoding phase, i.e., the answer presentation screen. We found that both the left aHPC (M=0.030, SE=0.011, $t_{(40)}$=2.85, p=.007) and the right aHPC (M=0.0025, SE=0.0009, $t_{(40)}$=2.91, p=.006) showed significantly higher BOLD activity for later remembered trivia answers compared to forgotten answers. The left IPL also showed significantly higher BOLD activity for remembered items (M=0.26, SE=0.06, $t_{(40)}$=4.08, p<.001). The right IPL showed a trend where BOLD activity decreased for remembered items, compared to forgotten items, but this did not survive Bonferroni correction

(M=-0.15, SE=0.06, $t_{(40)}$=-2.61, p=.013). The vmPFC did show statistically significantly higher BOLD activity in the remembered over forgotten trials (M=0.20, SE=0.06, $t_{(40)}$=3.07, p=.003).

Figure 22

Subsequent-memory effect, ROI analysis (fMRI model 1)

Note: The red bars represent the mean z-value of the respective ROIs for the Remembered > Forgotten contrast during the curiosity relief screen, i.e. answer presentation screen, from the Condition Model. The blue bars represent Forgotten > Remembered contrast. Both contrasts are redundantly displayed for clarity but note the symmetry. Error bars represent the mean plus and minus the standard error of the mean.
* Indicates that the z-value is significantly different from 0 after Bonferroni correction to p<.01 for the five-fold comparison.

Discussion

In this thesis we aimed to understand the effects of curiosity and reward incentives on memory formation by looking at both behavioural and neural patterns related to motivated learning. We found that curiosity is a positive predictor of recall, in accordance with our hypothesis. Rewards show a more complex pattern; there was no difference in recall likelihood between the reward conditions (model 1), but when viewed separately, 0- and 3-euro trials – but not 1-euro trials – positively predicted recall likelihood when compared to the no reward condition (model 2). Furthermore, within this model only for 1-euro trials (compared to the no-reward condition) there was a significant, positive interaction effect between curiosity and reward incentives, again counter to our hypothesis that there would a negative interaction between curiosity and condition. Further investigation showed that these effects changed when considering trial number (model 3). I.e., the further on in the experiment, the less effect rewards had on recall compared to the no-reward condition. Additionally, curiosity seemed to ameliorate this time-dependent deterioration of the reward effect. Thus, early on in the experiment there was a negative interaction effect – an effect we had

predicted to span the entire experiment – but later trials showed an opposite positive interaction in which curiosity decreased the late-onset negative effects that reward had on recall likelihood.

Neurally, we found both positive and negative IPL activity in support of the curiosity- and reward-motivated SME's – counter to our ideas that there would only be positive activity for the curiosity-motivated SME. The hippocampus was implicated with unmotivated but neither motivated subsequent memory. Within the ROI analyses, the vmPFC was not implicated in either motivated subsequent-memory effect, however whole brain analysis did show a downregulation of the vmPFC in support of curiosity and reward-motivated subsequent-memory. Further investigation of the fMRI BOLD dataset should investigate the temporal changes in the reward effect and the curiosity and reward interaction effect we found behaviourally to understand how changes in brain states are associated with changes in motivation and motivated memory.

Curiosity predicts memory formation, supported by diverse IPL neural processing

In all three behavioural models we found that curiosity improves recall, whether it is immediate (same day) or delayed (a week later). This is in line with previous findings showing that curiosity can be a strong motivator for memory formation in both immediate and delayed recall (Duan et al., 2020; Fastrich et al., 2018; Gruber et al., 2014; Kang et al., 2009; Meliss & Murayama, 2022). Within the nature of the trivia paradigm is the more subjective rating of curiosity we obtain, in contrast with more computational designs that manipulate for example the level of uncertainty (e.g. Jepma et al., 2012; Ten et al., 2021; Van Lieshout, Vandenbroucke, Müller, Cools, & de Lange, 2018) . Future research could combine stochastic relief of curiosity, implicit measures of curiosity like waiting time one is willing to pay for an answer (Van Lieshout, Vandenbroucke, Müller, Cools, & de Lange, 2018), choice of question instead of being given one per se (similar to the choice paradigm used by Ten et al. (2021) or the pseudo-choice of question used by Hankel (2023)); or the possibility to obtain more information after curiosity relief (Hankel, 2023) combined within the trivia paradigm to allow a deeper and less task-specific understanding of curiosity's effect on memory formation.

Neural activity during curiosity induction

In order to understand how curiosity motivates memory formation, we conducted both region of interest (ROI) and whole brain analyses. In the whole brain analysis, as predicted, we found left IPL activity that was higher for high curiosity questions during curiosity induction. Interestingly though, the left IPL was not modulated within the ROI analysis, perhaps owing to the fact that we used rather

large ROI's that were anatomically defined by the whole theoretical IPL, whereas specific activity associated with curiosity processing could be smaller in size, muddying potential statistical significance. We found a cluster that increased activity in the aHPC for low curiosity compared to high curiosity questions, counter to our prediction that aHPC activity would only positively show up for the curiosity-motivated SME. We also found, against our prediction, no cluster in the vmPFC. Previous research has implicated the left inferior parietal lobule in curiosity induction; Relating it to uncertainty that correlated with curiosity (Van Lieshout et al., 2018); to positive modulation of curiosity during question presentation in another trivia experiment (Duan et al., 2020); or to an increase in intersubject brain similarity within the adjacent supramarginal gyrus in response to high versus low curiosity (Meliss et al., 2024). Given the results from Van Lieshout, Vandenbroucke, Müller, Cools, & de Lange (2018) and the previous activity found in the IPL related to curiosity, the information-gap theory from Loewenstein (1994) is still a possible explanation of curiosity's antecedent: namely, that curiosity is a drive motivated by a need to reduce uncertainty.

Neural activity during curiosity relief: the curiosity-motivated subsequent-memory effect

Within the ROI analysis of the reward only model (fMRI model 2), we found the curiosity-motivated subsequent-memory effect (SME), measured during curiosity relief, to be modulated by significant downmodulation of the right IPL. Interestingly, during curiosity induction we also found significant downmodulation of the right IPL for high curiosity questions. Van Lieshout, Vandenbroucke, Müller, Cools, & De Lange (2018) found the right IPL to be associated with curiosity relief only, and not induction. Within our whole brain analyses, we found clusters including the bilateral IPL with both higher activity associated with the curiosity-motivated SME and decreased activity associated with the curiosity-motivated SME. We did not predict the negative activity in the IPL related to the curiosity-motivated SME – especially not that there would be both positive and negative modulation of curiosity-motivated SME within the IPL.

Numssen et al. (2021) found right IPL activity to be especially related to attentional processes. Uncapher & Wagner (2009) found that subsequent-memory related activity in the ventral posterior parietal lobule, i.e. the inferior parietal lobule, is mostly negative. Daselaar et al. (2004) also show that deactivation for remembered items is beneficial during cognitively demanding tasks. This allows us to interpret our deactivation clusters and ROI results in both curiosity-motivated models as beneficial downregulation of attentional processing for attributes that are not important for the task at hand.

The positive modulation of IPL subregions could on the other hand be associated with the actual processing of curiosity, like uncertainty (resolution). To disentangle these complex and nuanced results, it is of importance in future research to delve into the specific roles of different subregions within the IPL that are either associated with curiosity as a construct or with the motivated subsequent-memory effect and any related attentional processes.

Interestingly, t we did not find hippocampal activity for the curiosity-motivated SME, even though we did for the unmotivated subsequent-memory effect or for curiosity induction. Gruber et al. (2014) found hippocampal anticipatory activity during question presentation (curiosity induction) to predict subsequent memory whilst we measured the SME during the relief stage. Poh et al. (2022b) specify this by finding that ventral tegmental area (VTA) univariate activity modulated hippocampal pattern specificity (a measure a trial's similarity to a typical high curiosity state) which in turn is thought to influence the effect of curiosity on recall. So perhaps our theory that hippocampal activity during relief supports motivated memory should be sharpened to anticipatory activity in the hippocampus – i.e., there is a 'warming up' of the hippocampus during an unrelieved state of curiosity that predicts later recall whilst it is not hippocampal activity during encoding of the answer that supports motivated memory formation.

Additionally, within the reward-only model (fMRI model 2), for the curiosity-motivated SME we found a cluster that showed decreased vmPFC activity for high curiosity and remembered items, in contrast with our hypothesis. This is remarkable since the unmotivated subsequent-memory effect was positively associated with vmPFC activity, as vmPFC activity is usually associated with integrating information with preexisting knowledge (Miendlarzewska et al., 2016). Bialleck et al. (2011) found the vmPFC to preferentially activate when rewards were predictable, and when they were remembered whilst Ligneul et al. (2018) found vmPFC activity to correlate positively with surprise ratings of trivia answers and when they were remembered – i.e. the vmPFC can respond to predictable rewards or very surprising answers, assuming that answers are rewarding by relieving curiosity. Further analysis with the surprise and confidence ratings could elucidate the counterintuitive effect we found in the vmPFC.

Rewards can be helpful in memory formation, but the relationship is nuanced

We found that being in a reward-contingent condition did not result in larger recall benefits compared to being in a non-rewarded context when ignoring the reward magnitude (model 1).

However, when we included the magnitude of rewards in model 2, we did find that the potential to win 0 or 3 euros for a correct answer did improve memory later on, however receiving a 1-euro incentive did not – partly in line with previous research that found rewards to boost memory performance (Adcock et al., 2006; Wittmann et al., 2008, 2008) or recall within the trivia paradigm (Duan et al., 2020; Swirsky et al., 2021).

The comparison between trials in the non-rewarded condition and 0-euro incentivised trials in the rewarded condition showed that the rewarding context contributed to recall performance, even though the reward incentive itself was worth nothing, in line with previous research (Loh, Deacon, et al., 2016; Murayama & Kitagami, 2014).

A reason as to why we find these reward-level specific effects might be that the rewarding nature of the 3-euro (and perhaps 1-euro) incentives could have caused a tonic up-regulation of dopaminergic release in the SN/VTA that lasted longer than one trial, spilling over into 0-euro trials and causing 0-euro 'boosts' in memory performance (Loh, Kumaran, et al., 2016). Our additional behavioural analysis (see Appendix D: Additional Analyses, analysis 1) however showed no evidence for this hypothesis. Secondly, the reward effect might not have depended solely on reward magnitude but also on reward salience (Madan & Spetch (2012). As the two extremes, 0- and 3-euro trials would be the most salient. I.e., they earn you the least and the most; they are the most distant from the average reward; and attentionally the easiest to anchor to. Hence, as the most salient rewards they would subsequently have to most impact on recall likelihood.

Neural activity related to reward incentives and the reward-motivated subsequent-memory effect

Reward incentives and the reward-motivated subsequent-memory effect were associated with widespread clusters across the brain. Within the ROI analysis for the main parametric reward effect, we found activity in the right IPL to decrease as reward increases, similar to the pattern found for curiosity induction and relief. In the whole brain analysis, we found that next to the right IPL, the left IPL also contained a cluster with decreasing activity for higher rewards.

We did not find this effect in the ROI analysis of the reward-motivated subsequent-memory effect; however, in the whole brain analysis of the reward only model (fMRI model 2) we did find bilateral downmodulation of activity for the reward-motivated subsequent-memory effect in the IPL (i.e. when reward increases) – but also an increase in activity for the reward-motivated SME in a

cluster in a different subregion of the IPL. These complex results resemble those of the curiosity-motivated SME.

We did not hypothesise that the IPL would be modulated by the reward-motivated SME, but our results show a similar complex pattern as for the curiosity-motivated SME. Thus, we must adjust our idea that the IPL is a curiosity-specific region with regard to motivated subsequent-memory. Dubey et al. (2020) found the IPL to increase its activity in response to increased effort exertion during a social reward task. Thus, perhaps we found the positive IPL modulation in both curiosity- and reward-motivated memory because its processing is more related to increased effort: when the potential to earn more is higher, or when you are more curious, you exert more effort. On the other hand, the negative modulation of the IPL for reward-motivated SME could be related to decreasing attention for encoding-unrelated processes – similar to that of the curiosity-motivated SME.

Future research on the topic should focus on more fine-grained neural hypotheses to elucidate the inner workings of the IPL in motivated memory formation.

Additionally, we found no hippocampal and negative vmPFC activation, equivalent findings to those of the curiosity-motivated SME. Hippocampal activity could thus be more anticipatory, instead of during answer presentation. Deactivation of vmPFC activity for high rewards in combination with subsequent memory is still highly elusive and could be further investigated using surprisal and confidence ratings in tandem with reward effects.

The interaction between curiosity and reward incentives

Interestingly, we also found a behavioural interaction between reward and curiosity, but only for 1-euro trials compared to no-reward trials. I.e., for 1-euro trials the effect of curiosity on recall became stronger than it was in no-reward trials. Within 0- and 3-euro trials, there was no indication of an interaction effect, relative to the no-reward condition. These results are in stark contrast with the results from Swirsky et al. (2021), who found a negative interaction, or Duan et al. (2020), who found no significant interaction between reward and curiosity. Swirsky et al. (2021) hypothesise that experimental design differences like incidental versus intentional recall or a blocked versus a trial-based design might relate to the differences in results, however, we have shown that an interaction can exist in intentional recall and a trial-based reward operationalisation too. Perhaps our interaction effect is a result of our higher resolution or sensitivity – especially since we used 10 levels of curiosity

which has been shown to slightly improve sensitivity (Leung, 2011) – opposed to the seemingly three-bin curiosity scale from Duan et al. (2020).

The temporally dependent curiosity-reward interaction effect: a novel exploratory finding

Recent work has also established that there is considerable variability between people and trials within cognitive tasks (Judd et al., 2024). We wondered whether variability over time can explain any of the different findings regarding the interaction effect in the literature. We investigated whether including trial number – a proxy for how long someone has been doing the experiment – into the model changes anything in the effects we find.

The most important finding is that for low curiosity questions, there is a positive effect of reward on recall in early trials, but an undermining effect in later trials – i.e. when reward decreases performance. This positive effect of reward in early trials was there as well for high curiosity questions but decreased significantly in late trials – albeit not leading to an undermining effect as it did for low curiosity questions. This partly aligns our results with those of Swirsky et al. (2021) and Murayama & Kuhbandner (2011) – namely that at trial 1, we saw that the interaction between all reward conditions and curiosity is negative. However, as the trials progress, the interaction grows positively, eventually turning signs. Such that at trial 144 the model estimates that for rewarded trials the effect of curiosity is increased compared to non-rewarded trials, which does not agree with Swirsky et al. (2021) and Murayama & Kuhbandner (2011). However, this increase in the reward-curiosity interaction is characterised by counteracting the undermining effect of rewards on recall in later low-curiosity trials.

Previous research showed that food as a rewarding reinforcer can habituate in animals (Lloyd et al., 2014) or human children (Temple et al., 2008), where in the latter, novel foods cancelled this effect. Since there is evidence that food reinforcement behaves similar as reward incentive reinforcement (Lehner et al., 2017), this might explain the diminishing effectiveness of rewards as the trials progress. Interestingly, the effect of curiosity did not seem to decrease as time progressed. Showing there are potential differences in how curiosity versus reward incentives motivate memory formation.

These results shed light on the importance of the temporal dynamics of motivational effects and give researchers guidance to look further into the temporal dynamics of interacting motivational incentives. These temporal dynamics could be of great interest to educational researchers and educators, since in educational contexts, students are engaged for long periods of time with many

different intrinsic and extrinsic motivators influencing their behaviour. Understanding the short time-scale changes in effectiveness of reward reinforcers and the potential benefit of curiosity in ameliorating any reward-based undermining effects could be of major importance and gives way for more research into the topic.

Conclusion

We found that curiosity and reward incentives both support long-term semantic memory. Their combined behaviour is complex and depends on an interaction that changes over trial number, suggesting under-the-hood temporal dynamics that thus far have not been found and discussed. Whilst curiosity's beneficial effect on memory is robust and does not change over time, rewards do seem to deteriorate in their effectiveness on memory formation. The temporal nature of the interaction between curiosity and reward is highly relevant to educational contexts. These results highlight the importance of looking at (temporal) variability when investigating learning and motivation – something that educational researchers and educators should take note of.

Neurally, the curiosity- and reward-motivated learning effects show very similar activation patterns. We found complex inferior parietal lobule activations that show both increases and decreases in activity within different subregions in support of both curiosity- and reward-motivated subsequent memory. We also found counterintuitive downmodulation of the ventral medial prefrontal cortex in support of the motivated subsequent-memory effects. Hippocampal activity did not positively predict motivated subsequent memory during answer presentation, counter to our predictions – showing it might be more related to anticipatory processes in relation to motivated memory formation.

Overall, we have provided insight in how curiosity and reward are both linked to memory formation and have opened up new avenues for researchers to form more specific hypotheses on the similarities and differences between intrinsic and extrinsic motivators of memory formation.

References

Adcock, R. A., Thangavel, A., Whitfield-Gabrieli, S., Knutson, B., & Gabrieli, J. D. E. (2006). Reward-Motivated Learning: Mesolimbic Activation Precedes Memory Formation. *Neuron*, *50*(3), 507–517. https://doi.org/10.1016/j.neuron.2006.03.036

Auguie, B. (2017). *gridExtra: Miscellaneous Functions for 'Grid' Graphics*. https://CRAN.R-project.org/package=gridExtra

Badre, D., & Nee, D. E. (2018). Frontal Cortex and the Hierarchical Control of Behavior. *Trends in Cognitive Sciences*, *22*(2), 170–188. https://doi.org/10.1016/j.tics.2017.11.005

Ballard, I. C., Murty, V. P., Mckell Carter, R., Macinnes, J. J., Huettel, S. A., & Adcock, R. A. (2011). *Dorsolateral Prefrontal Cortex Drives Mesolimbic Dopaminergic Regions to Initiate Motivated Behavior*. https://doi.org/10.1523/JNEUROSCI.0895-11.2011

Barr, D. J., Levy, R., Scheepers, C., & Tily, H. J. (2013). Random effects structure for confirmatory hypothesis testing: Keep it maximal. *Journal of Memory and Language*, *68*(3), 10.1016/j.jml.2012.11.001. https://doi.org/10.1016/j.jml.2012.11.001

Bates, D., Kliegl, R., Vasishth, S., & Baayen, H. (2018). *Parsimonious Mixed Models* (No. arXiv:1506.04967). arXiv. https://doi.org/10.48550/arXiv.1506.04967

Bates, D., Mächler, M., Bolker, B., & Walker, S. (2015). Fitting Linear Mixed-Effects Models Using lme4. *Journal of Statistical Software*, *67*(1), 1–48. https://doi.org/10.18637/jss.v067.i01

Berlyne, D. E. (1954). A Theory of Human Curiosity. *British Journal of Psychology. General Section*, *45*(3), 180–191. https://doi.org/10.1111/j.2044-8295.1954.tb01243.x

Bialleck, K. A., Schaal, H.-P., Kranz, T. A., Fell, J., Elger, C. E., & Axmacher, N. (2011). Ventromedial Prefrontal Cortex Activation Is Associated with Memory Formation for Predictable Rewards. *PLoS ONE*, *6*(2), e16695. https://doi.org/10.1371/journal.pone.0016695

Blanchard, T. C., Hayden, B. Y., & Bromberg-Martin, E. S. (2015). Orbitofrontal Cortex Uses Distinct Codes for Different Choice Attributes in Decisions Motivated by Curiosity. *Neuron*, *85*(3), 602–614. https://doi.org/10.1016/j.neuron.2014.12.050

Bürkner, P.-C. (2017). brms: An R Package for Bayesian Multilevel Models Using Stan. *Journal of Statistical Software*, *80*(1), 1–28. https://doi.org/10.18637/jss.v080.i01

Carpenter, B., Gelman, A., Hoffman, M. D., Lee, D., Goodrich, B., Betancourt, M., Brubaker, M., Guo, J., Li, P., & Riddell, A. (2017). Stan: A Probabilistic Programming Language. *Journal of Statistical Software*, *76*(1). https://doi.org/10.18637/jss.v076.i01

Cerasoli, C. P., Nicklin, J. M., & Ford, M. T. (2014). Intrinsic motivation and extrinsic incentives jointly predict performance: A 40-year meta-analysis. *Psychological Bulletin*, *140*(4), 980–1008. https://doi.org/10.1037/a0035661

Cohanpour, M., Aly, M., & Gottlieb, J. (2024). Neural Representations of Sensory Uncertainty and Confidence Are Associated with Perceptual Curiosity. *The Journal of Neuroscience*, *44*(33), e0974232024. https://doi.org/10.1523/JNEUROSCI.0974-23.2024

Daselaar, S. M., Prince, S. E., & Cabeza, R. (2004). When less means more: Deactivations during encoding that predict subsequent memory. *NeuroImage*, *23*(3), 921–927. https://doi.org/10.1016/j.neuroimage.2004.07.031

Di Domenico, S. I., & Ryan, R. M. (2017). The Emerging Neuroscience of Intrinsic Motivation: A New Frontier in Self-Determination Research. *Frontiers in Human Neuroscience*, *11*. https://doi.org/10.3389/fnhum.2017.00145

Duan, H., Fernández, G., Van Dongen, E., & Kohn, N. (2020). The effect of intrinsic and extrinsic motivation on memory formation: Insight from behavioral and imaging study. *Brain Structure and Function*, *225*, 1561–1574. https://doi.org/10.1007/s00429-020-02074-x

Dubey, I., Georgescu, A. L., Hommelsen, M., Vogeley, K., Ropar, D., & Hamilton, A. F. D. C. (2020). Distinct neural correlates of social and object reward seeking motivation. *European Journal of Neuroscience*, *52*(9), 4214–4229. https://doi.org/10.1111/ejn.14888

Elliott, B. L., D'Ardenne, K., Murty, V. P., Brewer, G. A., & McClure, S. M. (2022). Midbrain–Hippocampus Structural Connectivity Selectively Predicts Motivated Memory Encoding. *Journal of Neuroscience*, *42*(50), 9426–9434. https://doi.org/10.1523/JNEUROSCI.0945-22.2022

Fastrich, G. M., Kerr, T., Castel, A. D., & Murayama, K. (2018). The role of interest in memory for trivia questions: An investigation with a large-scale database. *Motivation Science*, *4*(3), 227–250. https://doi.org/10.1037/mot0000087

Frank, L. E., Preston, A. R., & Zeithamova, D. (2019). Functional connectivity between memory and reward centers across task and rest track memory sensitivity to reward. *Cognitive, Affective, & Behavioral Neuroscience.* https://doi.org/10.3758/s13415-019-00700-8

Green, P., & MacLeod, C. J. (2016). simr: An R package for power analysis of generalised linear mixed models by simulation. *Methods in Ecology and Evolution*, *7*(4), 493–498. https://doi.org/10.1111/2041-210X.12504

Gruber, M. J., Gelman, B. D., & Ranganath, C. (2014). States of Curiosity Modulate Hippocampus-Dependent Learning via the Dopaminergic Circuit. *Neuron*, *84*(2), 486–496. https://doi.org/10.1016/j.neuron.2014.08.060

Gruber, M. J., & Ranganath, C. (2019). How Curiosity Enhances Hippocampus-Dependent Memory: The Prediction, Appraisal, Curiosity, and Exploration (PACE) Framework. *Trends in Cognitive Sciences*, *23*(12), 1014–1025. https://doi.org/10.1016/j.tics.2019.10.003

Haber, S. N., & Knutson, B. (2010). The Reward Circuit: Linking Primate Anatomy and Human Imaging. *Neuropsychopharmacology Reviews*, *35*, 4–26. https://doi.org/10.1038/npp.2009.129

Hankel, R. (2023). *Curiosity and learning in the face of extrinsic rewards: Do rewards disrupt or enhance depending on personal interests?*

Huettel, S. A., Song, A. W., & McCarthy, G. (2005). Decisions under Uncertainty: Probabilistic Context Influences Activation of Prefrontal and Parietal Cortices. *The Journal of Neuroscience*, *25*(13), 3304–3311. https://doi.org/10.1523/JNEUROSCI.5070-04.2005

Jepma, M., Verdonschot, R. G., van Steenbergen, H., Rombouts, S. A. R. B., & Nieuwenhuis, S. (2012). Neural mechanisms underlying the induction and relief of perceptual curiosity. *Frontiers in Behavioral Neuroscience*, *FEBRUARY 2012*. https://doi.org/10.3389/fnbeh.2012.00005

Judd, N., Aristodemou, M., Klingberg, T., & Kievit, R. (2024). Interindividual Differences in Cognitive Variability Are Ubiquitous and Distinct From Mean Performance in a Battery of Eleven Tasks. *Journal of Cognition*, *7*(1), 45. https://doi.org/10.5334/joc.371

Kang, M. J., Hsu, M., Krajbich, I. M., Loewenstein, G., McClure, S. M., Wang, J. T. Y., & Camerer, C. F. (2009). The wick in the candle of learning: Epistemic curiosity activates reward circuitry and

enhances memory. *Psychological Science*, *20*(8), 963–973. https://doi.org/10.1111/j.1467-9280.2009.02402.x

Kim, H. (2011). Neural activity that predicts subsequent memory and forgetting: A meta-analysis of 74 fMRI studies. *NeuroImage*, *54*(3), 2446–2461. https://doi.org/10.1016/j.neuroimage.2010.09.045

Knowlton, B. J., & Castel, A. D. (2022). Memory and Reward-Based Learning: A Value-Directed Remembering Perspective. *Annual Review of Psychology*, *37*, 41. https://doi.org/10.1146/annurev-psych-032921

Kumle, L., Võ, M. L.-H., & Draschkow, D. (2020). *mixedpower: Pilotdata based simulations for estimating power in linear mixed models*.

Kumle, L., Võ, M. L.-H., & Draschkow, D. (2021). Estimating power in (generalized) linear mixed models: An open introduction and tutorial in R. *Behavior Research Methods*, *53*(6), 2528–2543. https://doi.org/10.3758/s13428-021-01546-0

Lang, M., Bischl, B., & Surmann, D. (2023). *batchtools: Tools for Computation on Batch Systems* (Version 0.9.17) [Computer software]. https://cran.r-project.org/web/packages/batchtools/index.html

Lehner, R., Balsters, J. H., Herger, A., Hare, T. A., & Wenderoth, N. (2017). Monetary, Food, and Social Rewards Induce Similar Pavlovian-to-Instrumental Transfer Effects. *Frontiers in Behavioral Neuroscience*, *10*. https://doi.org/10.3389/fnbeh.2016.00247

Lenth, R. V. (2024). *emmeans: Estimated Marginal Means, aka Least-Squares Means*. https://CRAN.R-project.org/package=emmeans

Leung, S.-O. (2011). A Comparison of Psychometric Properties and Normality in 4-, 5-, 6-, and 11-Point Likert Scales. *Journal of Social Service Research*, *37*(4), 412–421. https://doi.org/10.1080/01488376.2011.580697

Ligneul, R., Mermillod, M., & Morisseau, T. (2018). From relief to surprise: Dual control of epistemic curiosity in the human brain. *NeuroImage*, *181*, 490–500. https://doi.org/10.1016/j.neuroimage.2018.07.038

Limesurvey GmbH. (n.d.). *LimeSurvey: An Open Source survey tool* [Computer software]. LimeSurvey GmbH. http://www.limesurvey.org

Lloyd, D. R., Medina, D. J., Hawk, L. W., Fosco, W. D., & Richards, J. B. (2014). Habituation of reinforcer effectiveness. *Frontiers in Integrative Neuroscience*, *7*. https://doi.org/10.3389/fnint.2013.00107

Loewenstein, G. (1994). The Psychology of Curiosity: A Review and Reinterpretation. *Psychological Bulletin*, *116*(1), 75–98.

Loh, E., Deacon, M., De Boer, L., Dolan, R. J., & Duzel, E. (2016). Sharing a Context with Other Rewarding Events Increases the Probability that Neutral Events will be Recollected. *Frontiers in Human Neuroscience*, *9*. https://doi.org/10.3389/fnhum.2015.00683

Loh, E., Kumaran, D., Koster, R., Berron, D., Dolan, R., & Duzel, E. (2016). Context-specific activation of hippocampus and SN/VTA by reward is related to enhanced long-term memory for embedded objects. *Neurobiology of Learning and Memory*, *134*, 65–77. https://doi.org/10.1016/j.nlm.2015.11.018

Long, J. A. (2022). *jtools: Analysis and Presentation of Social Scientific Data*. https://cran.r-project.org/package=jtools

Madan, C. R., & Spetch, M. L. (2012). Is the enhancement of memory due to reward driven by value or salience? *Acta Psychologica*, *139*(2), 343–349. https://doi.org/10.1016/j.actpsy.2011.12.010

Meliss, S., & Murayama, K. (2022). Curiosity-Motivated Incidental Learning With And Without Incentives: Early Consolidation And Midbrain-Hippocampal Resting-State Functional Connectivity. *bioRxiv*. https://doi.org/10.1101/2022.12.23.521819

Meliss, S., Tsuchiyagaito, A., Byrne, P., van Reekum, C., & Murayama, K. (2024). Broad brain networks support curiosity-motivated incidental learning of naturalistic dynamic stimuli with and without monetary incentives. *Imaging Neuroscience*, *2*, 1–27. https://doi.org/10.1162/imag_a_00134

Menon, V., & Uddin, L. Q. (2010). Saliency, switching, attention and control: A network model of insula function. *Brain Structure and Function*, *214*(5–6), 655–667. https://doi.org/10.1007/s00429-010-0262-0

Miendlarzewska, E. A., Bavelier, D., & Schwartz, S. (2016). Influence of reward motivation on human declarative memory. *Neuroscience and Biobehavioral Reviews*, *61*, 156–176. https://doi.org/10.1016/j.neubiorev.2015.11.015

Mikl, M., Mareček, R., Hluštík, P., Pavlicová, M., Drastich, A., Chlebus, P., Brázdil, M., & Krupa, P. (2008). Effects of spatial smoothing on fMRI group inferences. *Magnetic Resonance Imaging*, *26*(4), 490–503. https://doi.org/10.1016/j.mri.2007.08.006

Murayama, K., & Kitagami, S. (2014). Consolidation power of extrinsic rewards: Reward cues enhance long-term memory for irrelevant past events. *Journal of Experimental Psychology: General*, *143*(1), 15–20. https://doi.org/10.1037/a0031992

Murayama, K., & Kuhbandner, C. (2011). Money enhances memory consolidation—But only for boring material. *Cognition*, *119*(1), 120–124. https://doi.org/10.1016/j.cognition.2011.01.001

Murphy, C., Ranganath, C., & Gruber, M. J. (2021). Connectivity between the hippocampus and default mode network during the relief, but not elicitation, of curiosity supports curiosity-enhanced memory enhancements. *bioRxiv*. https://doi.org/10.1101/2021.07.26.453739

Numssen, O., Bzdok, D., & Hartwigsen, G. (2021). Functional specialization within the inferior parietal lobes across cognitive domains. *eLife*, *10*, e63591. https://doi.org/10.7554/eLife.63591

Palacio, N., & Cardenas, F. (2019). A systematic review of brain functional connectivity patterns involved in episodic and semantic memory. *Reviews in the Neurosciences*, *30*(8), 889–902. https://doi.org/10.1515/revneuro-2018-0117

Poh, J.-H., Vu, M.-A. T., Stanek, J. K., Hsiung, A., Egner, T., & Adcock, R. A. (2022a). Hippocampal convergence during anticipatory midbrain activation promotes subsequent memory formation. *Nature Communications*, *13*(1), 6729. https://doi.org/10.1038/s41467-022-34459-3

Poh, J.-H., Vu, M.-A. T., Stanek, J. K., Hsiung, A., Egner, T., & Adcock, R. A. (2022b). Hippocampal convergence during anticipatory midbrain activation promotes subsequent memory formation. *Nature Communications*, *13*(1), 6729. https://doi.org/10.1038/s41467-022-34459-3

Poldrack, R. A., Fletcher, P. C., Henson, R. N., Worsley, K. J., Brett, M., & Nichols, T. E. (2008). Guidelines for reporting an fMRI study. *NeuroImage*, *40*(2), 409–414. https://doi.org/10.1016/j.neuroimage.2007.11.048

Poli, F., O'Reilly, J. X., Mars, R. B., & Hunnius, S. (2024). Curiosity and the dynamics of optimal exploration. *Trends in Cognitive Sciences*, *28*(5), 441–453. https://doi.org/10.1016/j.tics.2024.02.001

R Core Team. (2023). *R: A Language and Environment for Statistical Computing*. R Foundation for Statistical Computing. https://www.R-project.org/

Reniers, K., Stikker, I., & Van Lieshout, L. (2025). *How do curiosity and reward contribute to memory formation?* https://doi.org/10.17605/OSF.IO/V35NF

Revelle, W. (2025). *psych: Procedures for Psychological, Psychometric, and Personality Research*. Northwestern University. https://CRAN.R-project.org/package=psych

Rolls, E. T. (2022). The hippocampus, ventromedial prefrontal cortex, and episodic and semantic memory. *Progress in Neurobiology*, *217*, 102334. https://doi.org/10.1016/j.pneurobio.2022.102334

Ryan, R. M., & Deci, E. L. (2020). Intrinsic and extrinsic motivation from a self-determination theory perspective: Definitions, theory, practices, and future directions. *Contemporary Educational Psychology*, *61*, 101860. https://doi.org/10.1016/j.cedpsych.2020.101860

Sarkar, D. (2008). *Lattice: Multivariate Data Visualization with R*. Springer. http://lmdvr.r-forge.r-project.org

Smith, D. V., Clithero, J. A., Boltuck, S. E., & Huettel, S. A. (2014). Functional connectivity with ventromedial prefrontal cortex reflects subjective value for social rewards. *Social Cognitive and Affective Neuroscience*, *9*(12), 2017–2025. https://doi.org/10.1093/scan/nsu005

Smith, S. M., Jenkinson, M., Woolrich, M. W., Beckmann, C. F., Behrens, T. E. J., Johansen-Berg, H., Bannister, P. R., De Luca, M., Drobnjak, I., Flitney, D. E., Niazy, R. K., Saunders, J., Vickers, J., Zhang, Y., De Stefano, N., Brady, J. M., & Matthews, P. M. (2004). Advances in functional and structural MR image analysis and implementation as FSL. *NeuroImage*, *23*, S208–S219. https://doi.org/10.1016/j.neuroimage.2004.07.051

Swirsky, L. T., Shulman, A., & Spaniol, J. (2021). The Interaction of Curiosity and Reward on Long-Term Memory in Younger and Older Adults. *Psychology and Aging*. https://doi.org/10.1037/pag0000623.supp

Temple, J. L., Giacomelli, A. M., Roemmich, J. N., & Epstein, L. H. (2008). Habituation and within-session changes in motivated responding for food in children. *Appetite*, *50*(2–3), 390–396. https://doi.org/10.1016/j.appet.2007.09.005

Ten, A., Kaushik, P., Oudeyer, P.-Y., & Gottlieb, J. (2021). Humans monitor learning progress in curiosity-driven exploration. *Nature Communications*, *12*(5972). https://doi.org/10.1038/s41467-021-26196-w

Uddin, L. Q., Nomi, J. S., Hébert-Seropian, B., Ghaziri, J., & Boucher, O. (2017). Structure and Function of the Human Insula. *Journal of Clinical Neurophysiology*, *34*(4), 300–306. https://doi.org/10.1097/WNP.0000000000000377

Uncapher, M. R., & Wagner, A. D. (2009). Posterior parietal cortex and episodic encoding: Insights from fMRI subsequent memory effects and dual-attention theory. *Neurobiology of Learning and Memory*, *91*(2), 139–154. https://doi.org/10.1016/j.nlm.2008.10.011

Uri, & Leif. (2014, September 17). [27] Thirty-somethings are Shrinking and Other U-Shaped Challenges. *Data Colada*. https://datacolada.org/27

Van Lieshout, L. L. F., De Lange, F. P., & Cools, R. (2021). Uncertainty increases curiosity, but decreases happiness. *Scientific Reports*, *11*(1), 14014. https://doi.org/10.1038/s41598-021-93464-6

Van Lieshout, L. L. F., Traast, I. J., De Lange, F. P., & Cools, R. (2021). *Curiosity or savouring? Information seeking is modulated by both uncertainty and valence*. https://doi.org/10.1371/journal.pone.0257011

Van Lieshout, L. L. F., Vandenbroucke, A. R. E., Müller, N. C. J., Cools, R., & De Lange, F. P. (2018). Induction and Relief of Curiosity Elicit Parietal and Frontal Activity. *The Journal of Neuroscience*, *38*(10), 2579–2588. https://doi.org/10.1523/JNEUROSCI.2816-17.2018

Van Lieshout, L. L. F., Vandenbroucke, A. R. E., Müller, N. C. J., Cools, R., & de Lange, F. P. (2018). Induction and relief of curiosity elicit parietal and frontal activity. *Journal of Neuroscience*, *38*(10), 2579–2588. https://doi.org/10.1523/JNEUROSCI.2816-17.2018

Vehtari, A., Gelman, A., & Gabry, J. (2017). Practical Bayesian model evaluation using leave-one-out cross-validation and WAIC. *Statistics and Computing*, *27*(5), 1413–1432. https://doi.org/10.1007/s11222-016-9696-4

Vickery, T. J., & Jiang, Y. V. (2009). Inferior Parietal Lobule Supports Decision Making under Uncertainty in Humans. *Cerebral Cortex*, *19*(4), 916–925. https://doi.org/10.1093/cercor/bhn140

Volz, K. G., Schubotz, R. I., & Cramon, D. Y. V. (2005). Variants of uncertainty in decision-making and their neural correlates. *Brain Research Bulletin*, *67*(5), 403–412. https://doi.org/10.1016/j.brainresbull.2005.06.011

Wickham, H. (2016). *ggplot2: Elegant Graphics for Data Analysis*. Springer-Verlag New York. https://ggplot2.tidyverse.org

Wickham, H., François, R., Henry, L., Müller, K., & Vaughan, D. (2023). *dplyr: A Grammar of Data Manipulation*. https://CRAN.R-project.org/package=dplyr

Wittmann, B. C., Schiltz, K., Boehler, C. N., & Düzel, E. (2008). Mesolimbic interaction of emotional valence and reward improves memory formation. *Neuropsychologia*, *46*(4), 1000–1008. https://doi.org/10.1016/j.neuropsychologia.2007.11.020

Wittmann, B. C., Schott, B. H., Guderian, S., Frey, J. U., Heinze, H.-J., & Düzel, E. (2005). Reward-Related fMRI Activation of Dopaminergic Midbrain Is Associated with Enhanced Hippocampus- Dependent Long-Term Memory Formation. *Neuron*, *45*(3), 459–467. https://doi.org/10.1016/j.neuron.2005.01.010

Woo, C.-W., Krishnan, A., & Wager, T. D. (2014). Cluster-extent based thresholding in fMRI analyses: Pitfalls and recommendations. *NeuroImage*, *91*, 412–419. https://doi.org/10.1016/j.neuroimage.2013.12.058

Zeidman, P., & Maguire, E. A. (2016). Anterior hippocampus: The anatomy of perception, imagination and episodic memory. *Nature Reviews. Neuroscience*, *17*(3), 173–182. https://doi.org/10.1038/nrn.2015.24

Appendix

Appendix A: Descriptives

Table 3

Descriptive statistics of the variables of interest including bivariate correlations with 95% confidence intervals (N=43, n=6024)

Variable	Mean [95%-CI]	SD	1	2	3	4	5
1. Curiosity	6.21 [6.14, 6.28]	2.70					
2. Confidence	3.01 [2.95, 3.07]	2.31	.337 [.314, .359]				
3. Surprise	5.48 [5.40, 5.56]	2.99	.030 [.005, .056]	-.230 [-.253, -.206]			
4. Immediate Recall (% correct)	74.04 [72.93, 75.14]	43.85	.152 [.128, .177]	.148 [.123, .173]	-.096 [-.121, -.070]		
5. Delayed Recall (% correct)	64.34 [63.13, 65.55]	47.90	.160 [.135, .184]	.160 [.135, .184]	-.139 [-.164, -.115]	.671 [.657, .685]	
6. Condition (NR (0) – R (1))	0.50 Count: 3000 (0), 3024 (1)	0.50	-.005 [-.031, .020]	-.003 [-.028, 0.023]	.003 [-.022, .028]	.027 [.001, .052]	.015 [-.010, .041]
7. Reward*	1.33 [1.29, 1.38]	1.25	.023 [-.012, .059]	.009 [-.026, .045]	.036 [.000, .072]	.023 [-.013, .058]	.039 [.004, .075]

Note: These descriptives are based on the selected trials after the prescreening, since only 144 trials were further selected for the MRI and test phases. Correlations are reported with 95%-CIs; SD = Standard Deviation, CI = Confidence Interval.
* Only for the Reward Condition trials (N=43, n=3024).

Appendix B: Power Analysis

Below is a description of how we estimated power in our preregistration with details that were not mentioned in the Method Sample size justification paragraph.

In our statistical analysis, we have aimed for the use of (near-) maximal model. For this analysis, in practice, it turned out that a power calculation using a maximal model was computationally too time-consuming and resource heavy. Hence, we have only used estimates of the random intercepts in our models to estimate power.
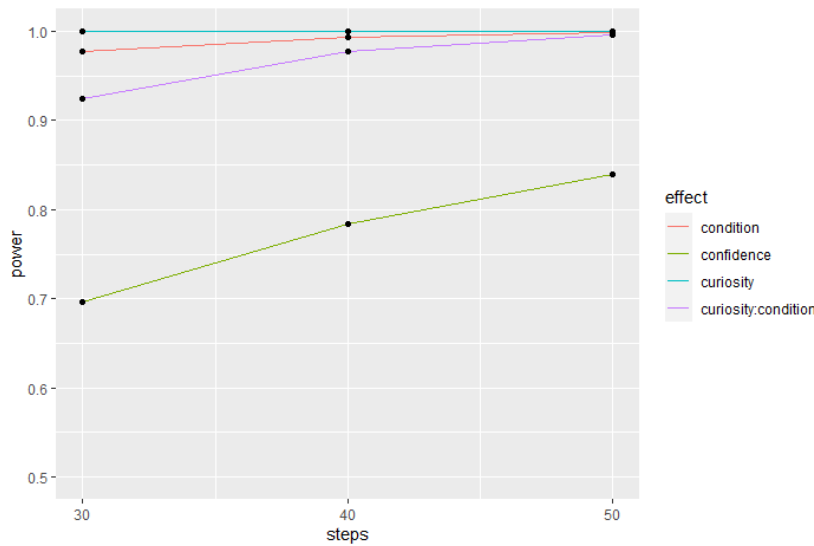
We aimed for a power of 80%, given an alpha of 5%. Within the models, this alpha of 5% is represented by a critical value of 2 (Kumle et al., 2021).

First, we create an artificial dataset of 40 participants times 144 trials - which is based on the practical number of participants we can sample given the costs of an fMRI experiment and the number of trials that fit in one continuous MRI session without taking too long (while staying divisible by six). We shuffle all question id's between participants and alternate the condition variable value (effect coded using -1 for a non-rewarded trial and +1 for a rewarded trial). Then, using the dataset from Fastrich et al. (2018) we calculate the standard deviation for the curiosity and confidence ratings and randomly assign ratings to all trials based on these standard deviations (the values are demeaned and hence their mean is 0). We now have an artificial dataset which we will use in the building of the artificial model. From Fastrich et al. (2018) we get the estimates of the fixed effect of confidence, and the estimates for the variances of the random intercepts for both the participant and question random intercepts. We base these estimates on the study from Fastrich et al. (2018) because Swirsky et al., (2021) don't report these. Swirsky et al., (2021) do have a reward incentive included in their paradigm which Fastrich et al. (2018) don't have, making their available effect sizes more exemplary of our study. Then, using the effect sizes from Swirsky et al. (2021) and the data-based estimates from Fastrich et al. (2018) we fit an artificial glmer model using the 'makeGlmer' function from the 'simr' package (Green & MacLeod, 2016; Version 1.0.7). Using this artificial model, and the artificial dataset, we estimate the power for a range of different participant sample sizes using the 'mixedpower' function of the 'mixedpower' package (Kumle et al., 2020; Version 0.1.0).

The results from this power analysis are shown in Figure 23 from the appendix. We conclude that 40 participants and 144 trials are enough to detect the required effect sizes (condition, curiosity and their interaction) reported in the literature with more than 80% power. We are not interested in the confidence estimate and only include it as a controlling variable; hence, its power is not of concern to us.

Figure 23

Estimated effects based on the power analysis

Note: The confidence effect is not of interest for us and only included as a covariate in the models. We will therefore not be bothered by its estimated power given a sample of 40.

Appendix C: Behavioural results

Model 1: Condition Model

Table 4

Condition Model: Bayesian mixed-effects model results

Effect	Estimate	Error	95% CI*	
			LL	*UL*
Fixed Effects				
Intercept	1.01	0.20	0.61	1.41
Curiosity^c	**0.08**	**0.03**	**0.03**	**0.14**
Condition (R)	0.06	0.11	-0.15	0.26
Test (Imm.)	**0.81**	**0.10**	**0.62**	**1.02**
Confidence^c	**0.13**	**0.02**	**0.08**	**0.18**
Curiosity^c x Condition (R)	0.02	0.03	-0.04	0.09
Curiosity^c x Test (Imm.)	0.00	0.03	-0.06	0.06
Condition (R) x Test (Imm.)	0.10	0.12	-0.13	0.33
Curiosity^c x Condition (R) x Test (Imm.)	0.01	0.04	-0.07	0.09

Note: N=43, n=6024 (number of observations in long format=12048). Effects with a credible interval not including zero are in bold (excl. intercept). Random effects were estimated for both participants and questions. CI = Credible Interval; ^{c} = centred variable; LL = Lower Limit; UL = Upper Limit; R = Reward Condition (with respect to the No Reward Condition); Imm. = Immediate Recall (with respect to the Delayed Recall test).
*Model formula: is_correct ~ 1 + curiosity * condition * test_type + confidence + (1 + curiosity * condition * test_type + confidence | participant_ID) + (1 + curiosity * condition * test_type + confidence | question_ID).*

Model 2: Reward Levels Model

Table 5

Reward Level Model: Bayesian mixed-effects model results

Effect	Estimate	Error	95% CI		OR	95% CI (OR)	
			LL	UL		LL	UL
Fixed Effects							
Intercept	1.78	0.20	1.38	2.19	5.96	3.99	8.94
Curiosity^c	**0.07**	**0.03**	**0.01**	**0.13**	**1.08**	**1.01**	**1.14**
Reward (0)	**0.31**	**0.16**	**0.01**	**0.62**	**1.36**	**1.01**	**1.85**
Reward (1)	0.27	0.17	-0.05	0.60	1.31	0.95	1.82
Reward (3)	**0.52**	**0.17**	**0.19**	**0.88**	**1.69**	**1.21**	**2.40**
Test (Del.)	**-0.74**	**0.09**	**-0.93**	**-0.55**	**0.48**	**0.40**	**0.57**
Confidence^c	**0.15**	**0.02**	**0.10**	**0.20**	**1.16**	**1.11**	**1.22**
Curiosity^c x Reward (0)	0.05	0.06	-0.06	0.16	1.05	0.94	1.18
Curiosity^c x Reward (1)	**0.12**	**0.06**	**0.01**	**0.23**	**1.13**	**1.01**	**1.26**
Curiosity^c x Reward (3)	0.02	0.06	-0.09	0.13	1.02	0.92	1.14
Curiosity^c x Test (Del.)	0.00	0.03	-0.05	0.06	1.00	0.95	1.06
Reward (0) x Test (Del.)	-0.21	0.16	-0.53	0.11	0.81	0.59	1.11
Reward (1) x Test (Del.)	-0.22	0.17	-0.54	0.11	0.81	0.58	1.12
Reward (3) x Test (Del.)	-0.08	0.17	-0.41	0.25	0.92	0.66	1.28
Curiosity^c x Reward (0) x Test (Del.)	0.04	0.06	-0.08	0.17	1.04	0.93	1.18
Curiosity^c x Reward (1) x Test (Del.)	-0.05	0.06	-0.17	0.07	0.95	0.84	1.08
Curiosity^c x Reward (3) x Test (Del.)	-0.01	0.06	-0.13	0.12	0.99	0.88	1.12

Note: N=43, n=6024 (number of observations in long format=12048). Effects with a credible interval not including zero are in bold (excl. intercept). Random effects were estimated for both participants and questions. CI = Credible Interval; ^{c} = centred variable; LL = Lower Limit; UL = Upper Limit; Del. = Delayed Recall (with respect to the Immediate Recall test). Rewards are compared to the NR condition.
Model formula: is_correct ~ 1 + curiosity * reward * test_type + confidence + (1 + curiosity * reward * test_type + confidence || participant_ID) + (1 + curiosity * reward * test_type + confidence || question_ID).

Model 3: Trial Model

Table 6

The effect of trial on recall within an adapted Reward Levels Model: Bayesian mixed-effects model results

Effect	Estimate	SE	95% CI*	
			LL	UL
Fixed Effects				
Intercept	1.9490	0.2280	1.5036	2.4015
Trial (main)	0.0021	0.0019	-0.0017	0.0059
Curiosity^c	**0.0764**	**0.0277**	**0.0217**	**0.1304**
Reward (0)	0.2279	0.1611	-0.0867	0.5535
Reward (1)	0.2735	0.1897	-0.0852	0.6676
Reward (3)	**0.6899**	**0.2071**	**0.3021**	**1.1169**
Confidence^c	**0.1627**	**0.0295**	**0.1060**	**0.2208**
Test (Del.)	**-0.9309**	**0.0943**	**-1.1196**	**-0.7488**
Trial^c x Curiosity^c	-0.0009	0.0006	-0.0020	0.0003
Trial^c x Reward (0)	-0.0042	0.0042	-0.0124	0.0041

Trial^c x Reward (1)	-0.0031	0.0048	-0.0126	0.0063
Trial^c x Reward (3)	**-0.0114**	**0.005**	**-0.0212**	**-0.0017**
Curiosity^c x Reward (0)	0.0754	0.0592	-0.0399	0.1913
Curiosity^c x Reward (1)	0.0793	0.0598	-0.0391	0.1957
Curiosity^c x Reward (3)	-0.0022	0.0613	-0.1256	0.1171
Trial^c x Curiosity^c x Reward (0)	**0.0031**	**0.0013**	**0.0005**	**0.0057**
Trial^c x Curiosity^c x Reward (1)	**0.0031**	**0.0015**	**0.0000**	**0.0061**
Trial^c x Curiosity^c x Reward (3)	**0.0039**	**0.0017**	**0.0007**	**0.0073**

Note: N=43, n=6024 (number of observations in long format=12048). Effects with a credible interval not including zero are in bold (excl. intercept). Random effects were estimated for both participants and questions. CI = Credible Interval; ^{c} = centred variable; LL = Lower Limit; UL = Upper Limit; Del. = Delayed Recall (with respect to the Immediate Recall test). Rewards are compared to the No Reward condition.
*Model formula: is_correct ~ 1 + trial * curiosity * reward + test_type + confidence + (1 + trial * curiosity * reward + test_type + confidence | participant_ID) + (1 + trial * curiosity * reward + test_type + confidence | question_ID).*

Appendix D: Additional Analyses

Additional analysis 1: The effect of 0-euro trials does not depend on past presentation of 3-euro trials

We found that 0-euro trials showed to have a significant impact on recall compared to trials in the non-rewarded context. Thus, even though the probability to receive rewards in the NR condition and 0-euro trials in the R condition was equal (i.e. zero), 0-euro trials still showed higher levels of recall. Some theories suggest that a long-lasting tonic dopaminergic firing might cause reward-motivating effects from non-zero rewards (i.e. 1 and 3 euro trials) to 'bleed' into temporally proximate non-rewarded trials (Loh, Kumaran, et al., 2016). To see if proximity to the highest (and only significant non-zero) reward level – 3 euro – is related to recall, we test whether recall is dependent on the number of trials since a 3-euro incentivised trial. We use a Bayesian mixed effects model including reward, the number of trials since the 3-euro reward and their interaction, including by-question and by-participant random slopes.

We found that recall performance was not based on the number of trials since the previous 3-euro trial (β=0.019, *Error*=0.050, 95% CI [-0.078, 0.121]), and this effect also did not interact with 1-euro (β=0.040, *Error*=0.089, 95% CI [-0.130, 0.226]) or 3-euro (β=-0.021, *Error*=0.074, 95% CI [-0.164, 0.125]) trials compared to 0-euro trials – i.e. there is no evidence that any effect of distance to 3-euro trials is different in 0-euro trials compared to 1- or 3-euro trials. We did find, as would be expected, that 3-euro trials had higher recall relative to 0-euro trials (β=0.340, *Error*=0.160, 95% CI [-0.031, 0.661]), although 1-euro trials did not (β=0.114, *Error*=0.146, 95% CI [-0.167, 0.409]).

Table 7

Effect of distance to past 3-euro trials on recall

Effect	Estimate	SE	95% CI*	
			LL	UL
Fixed Effects				
Intercept	1.360	0.209	0.953	1.782
Reward (1)	0.114	0.146	-0.167	0.409
Reward (3)	**0.340**	**0.160**	**0.031**	**0.661**
Trials since 3 euro	0.019	0.050	-0.078	0.121
Reward (1) x Trials since 3 euro	0.040	0.089	-0.130	0.226
Reward (3) x Trials since 3 euro	-0.021	0.074	-0.164	0.125

Note: N=43, n=3024 (number of observations in long format=6048). Only rewarded trials were included. Effects with a credible interval not including zero are in bold (excl. intercept). Random effects were estimated for both participants and questions. CI = Credible Interval; LL = Lower Limit; UL = Upper Limit. Rewards are compared to the No Reward condition.
*Model formula: is_correct ~ 1 + trials_since_3euro * reward + (1 + trials_since_3euro * reward | participant_ID) + (1 + trials_since_3euro * reward + | question_ID).*
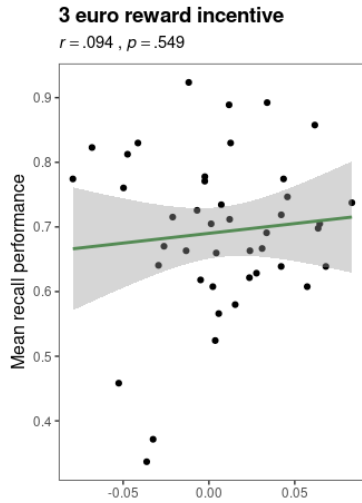
Additional analysis 2: Ceiling effects

In our second behavioural model (see Model 2: Reward Levels Model), we found that the interaction effect between curiosity and reward in the reward levels model was only statistically significantly different from zero for the 1-euro level, and not for the 3-euro level. There might be reason to suspect a ceiling effect in recall, limiting the ability for the curiosity estimate to interact with higher levels of reward given that performance is already at or close to maximum. To explore the possibility of this ceiling effect, we correlate the random slope estimates of the different reward levels with people's mean recall performance proportion. We find that there is no significant correlation between the *mean recall performance* and the *curiosity and 3-euro reward level interaction by-participant random slope* estimates (r=.094, p=.55). Hence, we find no evidence for a ceiling effect that might drive the fixed effect estimate for the curiosity and 3-euro reward level interaction effect from these data. See **Figure 24** for a graphical representation of these effects.

Additionally, there is no significant correlation between the individual random effect estimates for the *interaction between curiosity and the 3-euro reward* and the *main effect of curiosity* (r=.011, p=.52). Thus, there is no evidence that for people who were already influenced by curiosity to a higher degree, that there was no more 'room' for an extra curiosity-recall boost by the 3-euro reward.

Figure 24

Ceiling effect
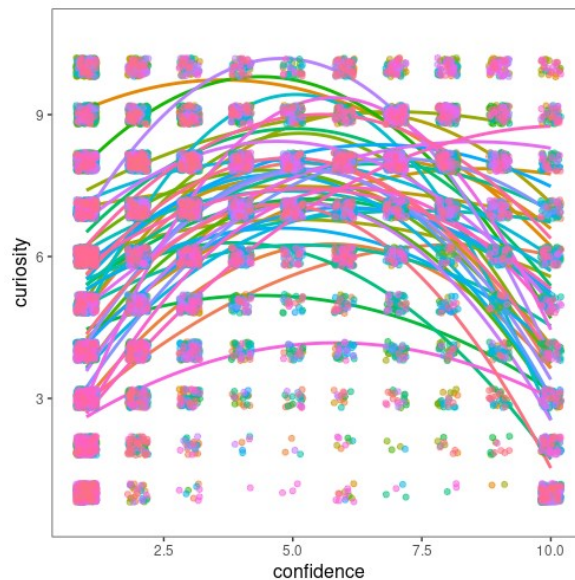
Note: The Reward level effect is with respect to the NR (No Reward) condition. Random slope estimates are from the by-participant random structure.

Additional analysis 3: Confirming the inverted-U shape between curiosity and confidence

The level of curiosity one has to get to know an answer to a trivia question and the confidence they feel for already knowing the answer are known to correlate strongly (e.g. Kang et al., 2009). This relation is known to be of an inverted-U type. To confirm this relation and provide a rationale for including confidence as a covariate in our models estimating the effects of curiosity on recall, we ran a Bayesian mixed-effects model using a Gaussian link function. Curiosity was predicted using the quadratic formula with a centred and squared transformation of confidence whilst including random intercepts and random slopes for confidence for both participants and question items.

Model results (N=45, n=11131; see Table 8) indicate a statistically significant negative term for the squared confidence term (β=-0.11, *Error*=0.01, 95% CI [-0.13, -0.09]). However, the significance of this negative square term does not imply a significant inverse-U relation (Uri & Leif, 2014). We use their proposed two-line method to explicitly test for an inverse-U shape in the relation between confidence and curiosity.

We estimate two linear regression lines, one left of the maximal confidence value (confidence$_{max}$ = 5.57) and one right of the maximal confidence value. If the left line is positive, and the right is negative, and both are statistically significant, we may conclude that there is an inverse U shape in the relation between curiosity and confidence. The results (see Table 9) indicate that the left regression line is indeed positive (β=0.57, *Error*=0.06, 95% CI [0.46, 0.68]) and the right line is negative (β=-0.43, *Error*=0.09, 95% CI [-0.61, -0.25]). Thus, we conclude that the relation between curiosity and confidence is of an inverse-U shape type.

Figure 25

Inverse-U relationship between curiosity and confidence

Note: Each line represents the relationship for one participant.

Table 8

Curiosity as a function of confidence: Bayesian mixed-effects model results

Effect	Estimate	Error	95% CI	
			LL	UL
Fixed Effects				
Intercept	7.10	0.19	6.72	7.47
Confidence	**0.41**	**0.04**	**0.32**	**0.49**
Confidence^{sq}	**-0.11**	**0.01**	**-0.13**	**-0.09**

Note: Sample size was N=45 (not 43 as in the main behavioural analyses) for this model. Total number of trials was n=11131. Effects with a credible interval not including zero are in bold (excl. intercept). Random effects were estimated for both participants and questions. ^{sq} = square transformation; CI = Credible Interval.
Model formula is based on the quadratic formula: curiosity ~ confidence + confidence^{sq} + (1 + confidence + confidence^{sq} | participant_ID) + (1 + confidence + confidence^{sq} | question_ID).

Table 9

Two-line interrupted regression for the inverted-U model: Bayesian mixed-effects model results

Effect	Estimate	Error	95% CI	
			LL	UL
Fixed Effects				
Intercept	8.02	0.19	7.65	8.41
Confidence (Left of Max)	**0.57**	**0.06**	**0.46**	**0.68**
Confidence (Right of Max)	**-0.43**	**0.09**	**-0.61**	**-0.25**

Line (Right)	-0.29	0.15	-0.58	0.00
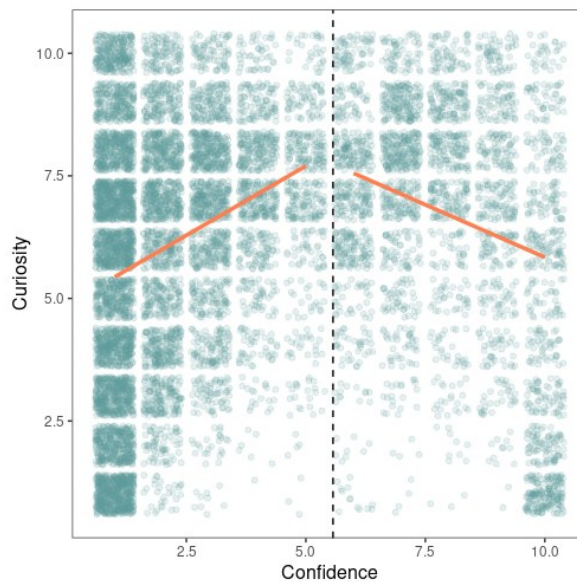
Note: Sample size was N=45 (not 43 as in the main behavioural analyses) for this model. Total number of trials was n=11131. Effects with a credible interval not including zero are in bold (excl. intercept). Random effects were estimated for both participants and questions. CI = Credible Interval.
Model formula: curiosity ~ confidence$_{left}$ + confidence$_{right}$ + line$_{right}$ + (1 + confidence$_{left}$ + confidence$_{right}$ + line$_{right}$ | participant_ID) + (1 + confidence$_{left}$ + confidence$_{right}$ + line$_{right}$ | question_ID).
Line is a dummy code with 1 for the right line and 0 for the left line.

Figure 26

The two-line method interrupted regression results for the inverted-U effect of curiosity and

confidence

Discussion additional analysis 3: Curiosity and uncertainty, an odd relationship

We took the liberty to investigate how curiosity and the confidence in knowing the answer to a trivia questions are related to each other. Previous findings had shown that they were related according to an inverse-u shape, where an optimal intermediate level of confidence would predict the highest level of curiosity (Kang et al., 2009). We indeed found and confirmed this earlier finding by using an interrupted two-line linear model (Uri & Leif, 2014) which can robustly test for inverse-u shapes, but is not typically used. These results imply that curiosity is related to uncertainty (the inverse of confidence), as has been reported before for curiosity for lottery outcomes (Van Lieshout, De Lange, et al., 2021; Van Lieshout, Traast, et al., 2021; Van Lieshout, Vandenbroucke, Müller, Cools, & De Lange, 2018) and for perceptual curiosity (Cohanpour et al., 2024). However, these previous findings showed a linear or mere polynomial relationship between curiosity and uncertainty and no (inverse-)u shape. Poli et al. (2024) discuss how there exist three potential antecedents of curiosity: uncertainty, information gain and learning progress and these three can be differently

combined to enforce optimal exploratory behaviour. Perhaps differences between optimal exploring demands for perceptual, stochastic lottery and epistemic tasks require different recruitment of uncertainty which results in these differing confidence/uncertainty-curiosity relationships.
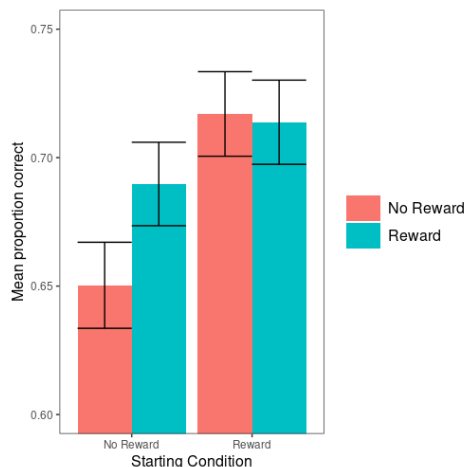
Additional analysis 4: Order effects

We were also interested in whether there are any order effects within the data. Therefore, we plotted the mean recall performance (both immediate and delayed) as a function of the starting condition and the condition itself (see Figure 27 and Table 10). Visually, mean proportion correct is lower for people who started in the No Reward compared to the Reward condition. Their performance is especially low during the No Reward condition itself (*M*=65.03, 95% CI [63.36, 66.71]) and gets boosted in the Reward condition (*M*=68.97, 95% CI [67.35, 70.60]). To formally test if we can speak of order effects, we ran a Bayesian Mixed Effects model to predict recall with starting condition, condition and their interaction. We found no statistically significant estimates (see

Table *11*) for any of the effects (i.e. no 95% credible interval excluded 0). Hence, we conclude there is no evidence for reward condition order effects.

Figure 27

Order effects for the mean proportion of correct answers between reward conditions

Note: Take note of the scale of the graphs when interpreting the magnitude of these effects.

Table 10

Mean percentage of correct answers between starting reward conditions and reward conditions

Starting Condition	Reward Condition	Mean percentage correct (%)	95% CI

No Reward	NR	65.03	[63.36, 66.71]
	R	68.97	[67.35, 70.60]
Reward	NR	71.70	[70.06, 73.35]
	R	71.38	[69.74, 73.02]

Note: CI = Confidence Interval; NR = No Reward; R = Reward

Table 11

Order effects for the Reward variable: Bayesian Mixed-Effects Model

Effect	Estimate	*Error*	95% CI	
			LL	UL
Fixed Effects				
Intercept	1.35	0.18	0.99	1.71
Start Condition (NR)	-0.13	0.15	-0.43	0.16
Condition (NR)	-0.05	0.05	-0.14	0.05
Start Condition (NR) : Condition (NR)	-0.02	0.05	-0.11	0.07

*Note: Effects with a credible interval not including zero are in bold (excl. intercept). Random effects were estimated for both participants and questions. For all variables and their interaction, sum-to-zero contrasts were used. CI = Credible Interval. Model formula: is_correct ~ 1 + start_condition * condition + (1 + start_condition * condition | participant_ID) + (1 + start_condition * condition | question_ID).*

Appendix E: Whole brain results

fMRI model 1: Condition Model

Table 12

Whole brain Condition Model significant clusters

Peak Structure	Hemisphere	z – value (peak)	Cluster size	p – value	Coordinates		
					x	y	z
Reward effect (answer screen)							
Reward > No Reward							
Occipital Pole	Left	4.35	191	0.00146	-30	-92	-6
Middle Frontal Gyrus	Left	4.3	112	0.0256	-44	12	30
No Reward > Reward							
Subsequent-memory effect (answer screen)							
Remembered > Forgotten							
Superior Frontal Gyrus	Left	6.89	17449	0	-4	42	58
Lateral Occipital Cortex, superior division	Left	6.66	2878	7.61e-23	-40	-70	32
Cerebellum	Right	6.32	546	2.98e-07	14	-82	-28
Lateral Occipital Cortex, superior division	Right	5.01	480	1.25e-06	48	-66	32
Cerebellum	Left	4.76	310	7.42e-05	-16	-82	-28

Temporal Fusiform Cortex, posterior division	Left	5.28	171	0.00392	-34	-42	-10

Forgotten > Remembered

Precentral Gyrus, medial	Right	6.33	15289	0	4	-24	48
Precentral Gyrus, lateral	Left	5.83	2744	4.06e-22	-60	0	20
Lateral Occipital Cortex, inferior division	Left	5.88	2381	4.38e-20	-50	-78	-2
Lateral Occipital Cortex, inferior division	Right	5.97	2096	2.05e-18	48	-70	2
Insular Cortex	Right	6.06	1709	5.09e-16	34	18	6
Frontal Pole	Right	6.17	1184	1.87e-12	38	44	28
Precentral Gyrus, lateral	Right	4.87	312	7.05e-05	56	8	42
Superior Frontal Gyrus	Left	4.47	304	8.68e-05	-20	2	68
Middle Frontal Gyrus	Left	4.34	120	0.0216	-28	30	36
Frontal Pole	Right	4.3	102	0.0414	-34	46	24

Curiosity effect*

Curiosity-motivated subsequent-memory effect (Remembered only; answer screen)

High Curiosity > Low Curiosity (Remembered items)

Superior Frontal Gyrus	Right	5.12	1195	2.52e-12	4	20	66
Lateral Occipital Cortex, superior division	Right	4.7	739	8.1e-09	54	-60	36
Frontal Pole	Left	4.53	336	5.06e-05	-34	52	-2
Frontal Pole	Right	4.26	324	6.85e-05	42	50	-8
Frontal Orbital Cortex	Right	4.82	294	0.000149	30	20	-12
Frontal Orbital Cortex	Left	4.66	193	0.00252	-30	20	-10
Middle Temporal Gyrus, posterior division	Left	4.15	187	0.00302	64	-26	-4
Frontal Pole	Left	4.25	179	0.00386	-24	52	34
Paracingulate Gyrus	Left	4.47	177	0.0041	-2	46	14
Lateral Occipital Cortex, superior division	Left	3.94	161	0.00679	-54	-64	38
Cerebellum	Right	4.2	109	0.0393	36	-52	-30

Low Curiosity > High Curiosity (Remembered items)

Lateral Occipital Cortex, superior division	Right	4.99	3821	2.66e-27	28	-60	54
Occipital Pole	Left	5.6	1826	1.66e-16	-36	-90	10
Central Opercular Cortex	Right	4.71	682	2.47e-08	56	-8	6
Lateral Occipital Cortex, inferior	Right	4.23	520	7.15e-07	48	-66	-12
Inferior Frontal Gyrus, pars opercularis	Left	4.55	447	3.58e-06	-48	10	30
Precentral Gyrus	Right	4.65	360	2.79e-05	58	12	38
Lateral Occipital Cortex, superior division	Left	4.29	261	0.000359	-24	-74	36
Superior Temporal Gyrus, posterior division	Left	4.32	183	0.00341	-70	-30	2

Reward-motivated subsequent-memory effect (answer screen)

Remembered > Forgotten and No Reward > Reward							
Paracingulate Gyrus	Right	3.74	119	0.0233	6	30	32
Forgotten > Remembered and Reward > No Reward							
Paracingulate Gyrus	Right	3.74	119	0.0233	6	30	32

Note: Anatomical labels were obtained from the Harvard-Oxford Cortical (and Subcortical) Structural Atlas in FSLeyes, Version 1.5.0 and FSL Version 6.0.6; Cluster significance was determined using a primary z-threshold of 2.3 (p<.01) and a secondary cluster threshold of p<.05.
* There were no clusters for the High > Low and Low > High curiosity (during the question screen) contrast due to an inability for FSL to estimate the variance of the High Curiosity COPE. We look more closely at the curiosity effect in the Reward Levels Only model.

fMRI model 2: Reward Levels Only Model

Table 13

Whole Brain Reward Levels Only Model significant clusters

Peak Structure	Hemisphere	z – value (peak)	Cluster size	p – value	Coordinates		
					x	y	z
Curiosity effect (question screen)							
High Curiosity > Low Curiosity							
Paracingulate Gyrus	Left	5.17	1265	8.77e-14	-6	32	40
Precuneous Cortex	Bilateral	5.17	1019	7.61e-12	0	-74	32
Frontal Pole	Left	4.94	991	1.29e-11	-44	44	-2
Middle Frontal Gyrus	Left	4.32	435	1.97e-06	-48	24	42
Superior Parietal Lobule	Left	4.81	352	1.69e-05	-34	-58	40
Middle Temporal Gyrus, posterior division	Left	4.76	336	2.6e-05	-58	-40	-14
Insular Cortex	Left	4.96	294	8.37e-05	-28	24	-2
Frontal Orbital Cortex	Right	4.73	240	0.000411	30	26	-4
Inferior Frontal Gyrus, pars opercularis	Left	4.3	134	0.014	-50	20	10
Frontal Pole	Right	5	129	0.0168	38	40	-10
Low Curiosity > High Curiosity							
Lateral Occipital Cortex, inferior division	Left	5.61	2630	7.28e-23	-42	-68	-14
Lateral Occipital Cortex, inferior division	Right	5.67	2391	2.04e-21	44	-74	-8
Postcentral Gyrus	Right	4.97	1660	1.19e-16	46	-26	40
Lateral Occipital Cortex, superior division	Right	5.08	1021	7.33e-12	26	-66	46
Postcentral Gyrus	Left	5.4	675	7.63e-09	-56	-20	24
Insular Cortex	Right	4.36	375	9.18e-06	40	-2	-16
Frontal Pole	Right	4.61	324	3.61e-05	34	42	22
Cingulate Gyrus, posterior division	Right	4.05	235	0.000479	10	-26	38
Precentral Gyrus	Right	4.25	156	0.00634	46	2	32
Supramarginal Gyrus, posterior division	Right	4.75	119	0.0245	44	-36	12
Thalamus	Right	4.57	114	0.0296	18	-26	4
Cluster peak on the border of white matter, but overlap with hippocampus and amygdala	Left	4.02	101	0.0493	-22	-18	-8
Reward effect (parametric modulation; answer screen)							
Positive modulation							
Occipital Pole	Left	6.45	7791	0	-26	-92	14
Precentral Gyrus	Left	4.75	630	2.55e-10	-50	-8	50
Inferior Frontal Gyrus, pars triangularis	Left	4.6	525	4.76e-09	-58	28	-4

Middle Temporal Gyrus, posterior division	Left	4.26	144	0.00229	-50	-24	-10
Amygdala	Left	4.44	98	0.0198	-18	-4	-20
Negative modulation							
Precuneous Cortex	Right	5.43	2012	2.68e-23	8	-36	46
Precuneous Cortex	Right	5.12	440	5.96e-08	10	-72	36
Superior Parietal Lobule	Left	5.15	358	7.75e-07	-24	-46	74
Superior Frontal Gyrus	Right	4.61	287	8.64e-06	26	14	66
Frontal Pole	Right	4.29	225	8.36e-05	28	40	42
Supramarginal Gyrus, anterior division	Left	4.4	210	0.000149	-62	-32	44
Paracingulate Gyrus	Right	4.33	118	0.0075	12	46	2
Lateral Occipital Cortex, superior division	Left	3.85	106	0.0133	-38	-82	34
Precentral Gyrus	Right	4.72	94	0.0242	22	-12	74
Supramarginal Gyrus, anterior division	Right	4.08	91	0.0281	54	-28	32
Subcallosal Cortex	Right	3.9	86	0.0363	2	20	-2
Subsequent-memory effect (answer screen)							
Remembered > Forgotten							
Occipital Pole	Right	9.72	16561	0	12	-96	16
Precentral Gyrus	Left	7.14	5005	1.29e-43	-48	4	42
Superior Frontal Gyrus, medial	Left	5.57	729	1.67e-11	-8	18	50
Putamen	Left	5	290	7.33e-06	-20	8	0
Superior Temporal Gyrus, posterior division	Right	6.39	278	1.13e-05	48	-32	0
Lateral Occipital Cortex, superior division	Right	6.04	254	2.68e-05	30	-76	26
Thalamus	Left	6.49	180	0.000475	-20	-28	-4
Insular Cortex	Right	4.78	138	0.0029	32	22	-4
White matter, cluster overlapping the thalamus and hippocampus	Right	6.02	126	0.00501	24	-26	-4
Temporal Pole	Right	5	100	0.0174	54	10	-18
Forgotten > Remembered							
Superior Parietal Lobule	Left	8.73	17748	0	-36	-42	70
Heschl's Gyrus	Left	5.94	2009	2.25e-23	-54	-20	8
Ventricle, cluster overlapping thalamus	Right	5.06	474	1.95e-08	20	-34	16
Ventricle (Type 1 error)	Left	5.06	418	1.19e-07	-30	-46	2
Lateral Occipital Cortex, inferior division	Right	5.6	353	8.34e-07	56	-62	4
Precuneous Cortex	Right	4.58	345	1.13e-06	12	-64	28
Middle Frontal Gyrus	Left	5.41	321	2.5e-06	-28	36	44
Cerebellum	Right	4.52	166	0.000853	2	-40	-18
Lateral Occipital Cortex, inferior division	Left	4.81	84	0.0394	-56	-68	12
Curiosity-motivated Subsequent-memory effect (answer screen; Remembered items only)							
High Curiosity > Low Curiosity (Remembered items)							
Occipital Pole	Right	8.07	7075	0	28	-96	12
Inferior Frontal Gyrus, pars opercularis	Left	4.94	487	1.78e-08	-50	18	26
Lateral Occipital Cortex, superior division	Left	4.74	328	2.5e-06	-28	-60	52
Frontal Pole	Left	4.51	299	6.62e-06	-52	34	-12
Low Curiosity > High Curiosity (Remembered items)							
Postcentral Gyrus	Right	5.61	5549	0	30	-36	68
Planum Temporale	Right	4.69	880	5.97e-13	62	-10	6
Insular Cortex	Left	5.08	334	2.03e-06	-38	-20	0
Frontal Pole, medial	Right	4.41	316	3.7e-06	4	60	12

Middle Temporal Gyrus, temporooccipital part	Right	4.04	241	5.19e-05	42	-50	10
Parietal Operculum Cortex	Right	4.4	188	0.000397	34	-28	18
Planum Temporale	Left	4.31	163	0.00111	-52	-24	8
Ventricle (Type 1 error)	Left	4.66	152	0.00177	-22	-46	10
Lateral Occipital Cortex, inferior division	Left	5.44	124	0.00611	-48	-66	14
White matter, cluster overlapping the thalamus	Right	4.25	111	0.0112	6	-24	18
Reward-motivated Subsequent-memory effect (answer screen; Reward x Subsequent-Memory Effect))							
Reward x (Remembered > Forgotten)							
Occipital Pole	Left	6.27	4732	1.32e-41	-8	-94	-8
Precentral Gyrus	Left	4.26	238	5.41e-05	-46	4	46
Inferior Frontal Gyrus, pars triangularis	Right	4.21	237	5.62e-05	48	22	12
Temporal Fusiform Cortex, posterior division	Right	4.69	146	0.00218	36	-38	-26
Lateral Occipital Cortex, superior division	Right	4.4	114	0.00936	40	-74	52
Reward x (Forgotten > Remembered)							
Postcentral Gyrus	Left	5.28	1551	2.28e-19	-4	-40	78
Planum Temporale	Right	4.89	470	2.62e-08	64	-24	14
Parietal Operculum Cortex	Left	4.66	256	2.79e-05	-60	-30	22
Frontal Pole	Right	4.1	139	0.00297	8	62	10
Frontal Medial Cortex	Right	3.95	109	0.0119	8	52	-8
Lateral Occipital Cortex, superior division	Right	3.85	99	0.0193	16	-60	62
Reward x Curiosity-motivated Subsequent-memory effect (answer screen; Reward x (High Curiosity > Low Curiosity with Remembered items only))							
Reward x (High Curiosity > Low Curiosity (Remembered items))							
Lingual Gyrus		4.05	186	0.00156	6	-86	-8

Note: Anatomical labels were obtained from the Harvard-Oxford Cortical (and Subcortical) Structural Atlas in FSLeyes, Version 1.5.0 and FSL Version 6.0.6; Cluster significance was determined using a primary z-threshold of 2.3 (p<.01) and a secondary cluster threshold of p<.05.

Appendix F: Additional discussion of exploratory findings in the whole brain analysis

Processing in the superior parietal lobule

Within both the curiosity- and reward-motivated SME's we see significant clusters in the superior parietal lobule with decreased activity for high curiosity or high reward trials. During the question presentation, we see no large overlaps of clusters in the SPL related to curiosity. During the answer presentation, the main effect of reward does show to be negatively modulating activity in the SPL too.

Murphy et al. (2021) found the superior parietal lobule and default-mode network connectivity to predict curiosity-motivated memory and Meliss et al. (2024) found a negative effect of curiosity-motivated SME in the superior parietal lobule using inter-subject representational similarity analysis – with very similar activity in default-mode and frontal-parietal network areas. Uncapher & Wagner (2009) explain how the superior parietal lobule is part of a dorsal attention network that is related to top-down modulation of attention, whereas the ventral network, including the inferior parietal lobule, is

associated with more bottom-up attention. Their review shows that the superior parietal lobule generally tends to be positively associate with the subsequent-memory effect, in contrast to our findings.

Our negatively extending clusters for both motivated-SME effects extend from the mid-posterior parietal cortex into the precuneus and post- and central gyrus, as it did for Duan et al. (2020), who attribute this effect to attentional resources needing to be diverted from irrelevant stimuli, like the reward. Similarly, Daselaar et al. (2004) found that deactivation in relation to the subsequent-memory effect can be beneficial. Since our main reward effect, and the two motivated subsequent-memory effects were estimated during answer presentation, when the task demands were mostly related to remembering the answer and not the task-unrelated motivational aspects of curiosity and reward, it might have been necessary for the brain to deactivate this regions in support of correct encoding for later recall.

The anterior insula: a potential intrinsic motivation hub

Within the reward only model, respectively during curiosity-induction and curiosity-relief, clusters of BOLD activity in the posterior insula showed a downmodulation for high curiosity and the high curiosity-motivated SME. Contrarily, we saw bilateral clusters within the anterior insula that showed increased activity for high curiosity levels during curiosity induction and for remembered high curiosity items (i.e. the curiosity-motivated SME) during curiosity relief within the condition model – similar to previous findings related to the curiosity-motivated SME (Duan et al., 2020; Meliss et al., 2024; Van Lieshout, Vandenbroucke, Müller, Cools, & De Lange, 2018). Slightly differently, Jepma et al. (2012) found anterior insular activity to increase for high perceptual uncertainty states during curiosity induction and the posterior insula to be related to uncertainty relief.

As Meliss et al. (2024) discuss, the anterior insula has been related to uncertainty processing during decision-making (e.g. Volz et al., 2005). Ligneul et al. (2018) found that nonspecific curiosity is related to a reduction in BOLD response in the anterior insula. Another account specifies that the posterior part of the insula is generally associated with bodily processes. The more anteriorly one goes, the more that activity in the insula represents abstract, integrated states (Uddin et al., 2017) such as curiosity related processes.

Di Domenico & Ryan (2017) hypothesize that the anterior insula, as a main constituent of the salience network (Menon & Uddin 2010), integrates information on what is motivationally valuable and

will then deploy the central executive network to enact control on behaviour based on this motivational salience. According to their idea, the anterior insula would be an intrinsic motivation hub. This hypothesis is in line with our curiosity-related findings and could provide one piece of the puzzle of motivated memory.

A role for cognitive control in motivated memory formation

We also saw two distinct clusters in the left middle frontal gyrus – a region that encompasses the dorsolateral prefrontal cortex (dlPFC) – and in the left frontal pole – a region overlapping the rostral lateral prefrontal cortex (rlPFC) – for high curiosity questions during curiosity induction and high curiosity remembered questions during curiosity relief (curiosity-motivated SME). Multiple earlier studies have found the curiosity-motivated SME (Duan et al., 2020; Meliss et al., 2024) or curiosity induction-related outcome uncertainty (Van Lieshout, Vandenbroucke, Müller, Cools, & de Lange, 2018) to be related to left or bilateral middle frontal gyrus activity. Gruber & Ranganath (2019) discuss how their PACE framework predicts that the lateral prefrontal cortex appraises incoming information gaps and/or prediction errors which would result in either curious, exploratory behaviour or anxiety.

Additionally, within our reward only model, activity in the dlPFC (left MFG) was positively parametrically modulated by reward magnitude and the reward-motivated SME during answer presentation. The left rlPFC was also positively modulated by reward magnitude during answer presentation.

Ballard et al. (2011) showed using dynamic causal modelling that the dlPFC was the primary input in a dlPFC, nucleus accumbens (NAcc) and ventral tegmental (VTA) network for reward-motivated initiation of behaviour. They conclude that the dlPFC sends information about what is valuable towards the NAcc and VTA in support of goal-directed behaviour. Similarly, both regions have been attributed to hierarchical control (Badre & Nee, 2018). The rlPFC is thought to contain schematic information and this information is sent to the dlPFC. The dlPFC is then thought to function as a contextual controller on the top of the control hierarchy. In other words, based on the context behaviour or thoughts are controlled.

Combining these converging findings in our experiment and those of the reward and curiosity literature, we can interpret the consistent activation of the dlPFC (part of the MFG) and the rlPFC (part of the frontal pole) in response to the reward, curiosity and motivated SME effects as the prefrontal system organising the motivational incentives into its control system. Based on the motivational

incentives (information incentives for curiosity or reward incentives for the euro rewards), the dlPFC controls what is deemed important enough to remember, and what not. Functional connectivity analysis of our data could in the future show if there is input into the dlPFC, from the (left) inferior parietal lobule and insular cortex and output towards the midbrain, NAcc and subsequently the hippocampus for curiosity and/or reward-motivated memory.

Appendix G: fMRIprep boilerplates

Below are exact copies of the automatically generated boilerplate from the fMRIprep HTML report.

Version 24.1.1

Results included in this manuscript come from preprocessing performed using *fMRIPrep* 24.1.1 (Esteban et al. (2019); Esteban et al. (2018); RRID:SCR_016216), which is based on *Nipype* 1.8.6 (K. Gorgolewski et al. (2011); K. J. Gorgolewski et al. (2018); RRID:SCR_002502).

Preprocessing of B_0 inhomogeneity mappings

A total of 2 fieldmaps were found available within the input BIDS structure for this particular subject. A B_0 nonuniformity map (or *fieldmap*) was estimated from the phase-drift map(s) measure with two consecutive GRE (gradient-recalled echo) acquisitions. The corresponding phase-map(s) were phase-unwrapped with prelude (FSL None).

Anatomical data preprocessing

A total of 1 T1-weighted (T1w) images were found within the input BIDS dataset. The T1w image was corrected for intensity non-uniformity (INU) with N4BiasFieldCorrection (Tustison et al. 2010), distributed with ANTs 2.5.3 (Avants et al. 2008, RRID:SCR_004757), and used as T1w-reference throughout the workflow. The T1w-reference was then skull-stripped with a *Nipype* implementation of the antsBrainExtraction.sh workflow (from ANTs), using OASIS30ANTs as target template. Brain tissue segmentation of cerebrospinal fluid (CSF), white-matter (WM) and gray-matter (GM) was performed on the brain-extracted T1w using fast (FSL (version unknown), RRID:SCR_002823, Zhang, Brady, and Smith 2001). Brain surfaces were reconstructed using recon-all (FreeSurfer 7.3.2, RRID:SCR_001847, Dale, Fischl, and Sereno 1999), and the brain mask estimated previously was refined with a custom variation of the method to reconcile ANTs-derived and FreeSurfer-derived segmentations of the cortical gray-matter of Mindboggle (RRID:SCR_002438, Klein et al. 2017). Volume-based spatial normalization to two standard spaces (MNI152NLin6Asym, MNI152NLin2009cAsym) was performed through nonlinear registration with antsRegistration (ANTs

2.5.3), using brain-extracted versions of both T1w reference and the T1w template. The following templates were were selected for spatial normalization and accessed with *TemplateFlow* (24.2.0, Ciric et al. 2022): *FSL's MNI ICBM 152 non-linear 6th Generation Asymmetric Average Brain Stereotaxic Registration Model* [Evans et al. (2012), RRID:SCR_002823; TemplateFlow ID: MNI152NLin6Asym], *ICBM 152 Nonlinear Asymmetrical template version 2009c* [Fonov et al. (2009), RRID:SCR_008796; TemplateFlow ID: MNI152NLin2009cAsym].

Functional data preprocessing

For each of the 6 BOLD runs found per subject (across all tasks and sessions), the following preprocessing was performed. First, a reference volume was generated from the shortest echo of the BOLD run, using a custom methodology of *fMRIPrep*, for use in head motion correction. Head-motion parameters with respect to the BOLD reference (transformation matrices, and six corresponding rotation and translation parameters) are estimated before any spatiotemporal filtering using mcflirt (FSL , Jenkinson et al. 2002). The estimated *fieldmap* was then aligned with rigid-registration to the target EPI (echo-planar imaging) reference run. The field coefficients were mapped on to the reference EPI using the transform. The BOLD reference was then co-registered to the T1w reference using bbregister (FreeSurfer) which implements boundary-based registration (Greve and Fischl 2009). Co-registration was configured with six degrees of freedom. Several confounding time-series were calculated based on the *preprocessed BOLD*: framewise displacement (FD), DVARS and three region-wise global signals. FD was computed using two formulations following Power (absolute sum of relative motions, Power et al. (2014)) and Jenkinson (relative root mean square displacement between affines, Jenkinson et al. (2002)). FD and DVARS are calculated for each functional run, both using their implementations in *Nipype* (following the definitions by Power et al. 2014). The three global signals are extracted within the CSF, the WM, and the whole-brain masks. Additionally, a set of physiological regressors were extracted to allow for component-based noise correction (*CompCor*, Behzadi et al. 2007). Principal components are estimated after high-pass filtering the *preprocessed BOLD* time-series (using a discrete cosine filter with 128s cut-off) for the two *CompCor* variants: temporal (tCompCor) and anatomical (aCompCor). tCompCor components are then calculated from the top 2% variable voxels within the brain mask. For aCompCor, three probabilistic masks (CSF, WM and combined CSF+WM) are generated in anatomical space. The implementation differs from that of Behzadi et al. in that instead of eroding the masks by 2 pixels on BOLD space, a mask of pixels that

likely contain a volume fraction of GM is subtracted from the aCompCor masks. This mask is obtained by dilating a GM mask extracted from the FreeSurfer's *aseg* segmentation, and it ensures components are not extracted from voxels containing a minimal fraction of GM. Finally, these masks are resampled into BOLD space and binarized by thresholding at 0.99 (as in the original implementation). Components are also calculated separately within the WM and CSF masks. For each CompCor decomposition, the *k* components with the largest singular values are retained, such that the retained components' time series are sufficient to explain 50 percent of variance across the nuisance mask (CSF, WM, combined, or temporal). The remaining components are dropped from consideration. The head-motion estimates calculated in the correction step were also placed within the corresponding confounds file. The confound time series derived from head motion estimates and global signals were expanded with the inclusion of temporal derivatives and quadratic terms for each (Satterthwaite et al. 2013). Frames that exceeded a threshold of 0.5 mm FD or 1.5 standardized DVARS were annotated as motion outliers. Additional nuisance timeseries are calculated by means of principal components analysis of the signal found within a thin band (*crown*) of voxels around the edge of the brain, as proposed by (Patriat, Reynolds, and Birn 2017). All resamplings can be performed with *a single interpolation step* by composing all the pertinent transformations (i.e. head-motion transform matrices, susceptibility distortion correction when available, and co-registrations to anatomical and output spaces). Gridded (volumetric) resamplings were performed using nitransforms, configured with cubic B-spline interpolation.

Many internal operations of *fMRIPrep* use *Nilearn* 0.10.4 (Abraham et al. 2014, RRID:SCR_001362), mostly within the functional processing workflow. For more details of the pipeline, see the section corresponding to workflows in *fMRIPrep*'s documentation.

Copyright Waiver

References

Abraham, Alexandre, Fabian Pedregosa, Michael Eickenberg, Philippe Gervais, Andreas Mueller, Jean Kossaifi, Alexandre Gramfort, Bertrand Thirion, and Gael Varoquaux. 2014. "Machine Learning

for Neuroimaging with Scikit-Learn." *Frontiers in Neuroinformatics* 8.

https://doi.org/10.3389/fninf.2014.00014.

Avants, B. B., C. L. Epstein, M. Grossman, and J. C. Gee. 2008. "Symmetric Diffeomorphic Image Registration with Cross-Correlation: Evaluating Automated Labeling of Elderly and Neurodegenerative Brain." *Medical Image Analysis* 12 (1): 26–41. https://doi.org/10.1016/j.media.2007.06.004.

Behzadi, Yashar, Khaled Restom, Joy Liau, and Thomas T. Liu. 2007. "A Component Based Noise Correction Method (CompCor) for BOLD and Perfusion Based fMRI." *NeuroImage* 37 (1): 90–101.

https://doi.org/10.1016/j.neuroimage.2007.04.042.

Ciric, R., William H. Thompson, R. Lorenz, M. Goncalves, E. MacNicol, C. J. Markiewicz, Y. O. Halchenko, et al. 2022. "TemplateFlow: FAIR-Sharing of Multi-Scale, Multi-Species Brain Models." *Nature Methods* 19: 1568–71. https://doi.org/10.1038/s41592-022-01681-2.

Dale, Anders M., Bruce Fischl, and Martin I. Sereno. 1999. "Cortical Surface-Based Analysis: I. Segmentation and Surface Reconstruction." *NeuroImage* 9 (2): 179–94.

https://doi.org/10.1006/nimg.1998.0395.

Esteban, Oscar, Ross Blair, Christopher J. Markiewicz, Shoshana L. Berleant, Craig Moodie, Feilong Ma, Ayse Ilkay Isik, et al. 2018. "fMRIPrep 24.1.1." *Software*. https://doi.org/10.5281/zenodo.852659.

Esteban, Oscar, Christopher Markiewicz, Ross W Blair, Craig Moodie, Ayse Ilkay Isik, Asier Erramuzpe Aliaga, James Kent, et al. 2019. "fMRIPrep: A Robust Preprocessing Pipeline for Functional MRI." *Nature Methods* 16: 111–16. https://doi.org/10.1038/s41592-018-0235-4.

Evans, AC, AL Janke, DL Collins, and S Baillet. 2012. "Brain Templates and Atlases." *NeuroImage* 62 (2): 911–22. https://doi.org/10.1016/j.neuroimage.2012.01.024.

Fonov, VS, AC Evans, RC McKinstry, CR Almli, and DL Collins. 2009. "Unbiased Nonlinear Average Age-Appropriate Brain Templates from Birth to Adulthood." *NeuroImage* 47, Supplement 1: S102.

https://doi.org/10.1016/S1053-8119(09)70884-5.

Gorgolewski, K., C. D. Burns, C. Madison, D. Clark, Y. O. Halchenko, M. L. Waskom, and S. Ghosh. 2011. "Nipype: A Flexible, Lightweight and Extensible Neuroimaging Data Processing Framework in Python." *Frontiers in Neuroinformatics* 5: 13. https://doi.org/10.3389/fninf.2011.00013.

Gorgolewski, Krzysztof J., Oscar Esteban, Christopher J. Markiewicz, Erik Ziegler, David Gage Ellis, Michael Philipp Notter, Dorota Jarecka, et al. 2018. "Nipype." *Software*.

https://doi.org/10.5281/zenodo.596855.

Greve, Douglas N, and Bruce Fischl. 2009. "Accurate and Robust Brain Image Alignment Using Boundary-Based Registration." *NeuroImage* 48 (1): 63–72. https://doi.org/10.1016/j.neuroimage.2009.06.060.

Jenkinson, Mark, Peter Bannister, Michael Brady, and Stephen Smith. 2002. "Improved Optimization for the Robust and Accurate Linear Registration and Motion Correction of Brain Images." *NeuroImage* 17 (2): 825–41. https://doi.org/10.1006/nimg.2002.1132.

Klein, Arno, Satrajit S. Ghosh, Forrest S. Bao, Joachim Giard, Yrjö Häme, Eliezer Stavsky, Noah Lee, et al. 2017. "Mindboggling Morphometry of Human Brains." *PLOS Computational Biology* 13 (2): e1005350. https://doi.org/10.1371/journal.pcbi.1005350.

Patriat, Rémi, Richard C. Reynolds, and Rasmus M. Birn. 2017. "An Improved Model of Motion-Related Signal Changes in fMRI." *NeuroImage* 144, Part A (January): 74–82. https://doi.org/10.1016/j.neuroimage.2016.08.051.

Power, Jonathan D., Anish Mitra, Timothy O. Laumann, Abraham Z. Snyder, Bradley L. Schlaggar, and Steven E. Petersen. 2014. "Methods to Detect, Characterize, and Remove Motion Artifact in Resting State fMRI." *NeuroImage* 84 (Supplement C): 320–41. https://doi.org/10.1016/j.neuroimage.2013.08.048.

Satterthwaite, Theodore D., Mark A. Elliott, Raphael T. Gerraty, Kosha Ruparel, James Loughead, Monica E. Calkins, Simon B. Eickhoff, et al. 2013. "An improved framework for confound regression and filtering for control of motion artifact in the preprocessing of resting-state functional connectivity data." *NeuroImage* 64 (1): 240–56. https://doi.org/10.1016/j.neuroimage.2012.08.052.

Tustison, N. J., B. B. Avants, P. A. Cook, Y. Zheng, A. Egan, P. A. Yushkevich, and J. C. Gee. 2010. "N4ITK: Improved N3 Bias Correction." *IEEE Transactions on Medical Imaging* 29 (6): 1310–20. https://doi.org/10.1109/TMI.2010.2046908.

Zhang, Y., M. Brady, and S. Smith. 2001. "Segmentation of Brain MR Images Through a Hidden Markov Random Field Model and the Expectation-Maximization Algorithm." *IEEE Transactions on Medical Imaging* 20 (1): 45–57. https://doi.org/10.1109/42.906424.

Version 25.1.2

Results included in this manuscript come from preprocessing performed using *fMRIPrep* 25.1.2 (Esteban et al. (2019); Esteban et al. (2018); RRID:SCR_016216), which is based on *Nipype* 1.10.0 (K. Gorgolewski et al. (2011); K. J. Gorgolewski et al. (2018); RRID:SCR_002502).

Preprocessing of B_0 inhomogeneity mappings

A total of 2 fieldmaps were found available within the input BIDS structure for this particular subject. A B_0 nonuniformity map (or *fieldmap*) was estimated from the phase-drift map(s) measure with two consecutive GRE (gradient-recalled echo) acquisitions. The corresponding phase-map(s) were phase-unwrapped with prelude (FSL None).

Anatomical data preprocessing

A total of 1 T1-weighted (T1w) images were found within the input BIDS dataset. The T1w image was corrected for intensity non-uniformity (INU) with N4BiasFieldCorrection (Tustison et al. 2010), distributed with ANTs 2.6.0 (Avants et al. 2008, RRID:SCR_004757), and used as T1w-reference throughout the workflow. The T1w-reference was then skull-stripped with a *Nipype* implementation of the antsBrainExtraction.sh workflow (from ANTs), using OASIS30ANTs as target template. Brain tissue segmentation of cerebrospinal fluid (CSF), white-matter (WM) and gray-matter (GM) was performed on the brain-extracted T1w using fast (FSL (version unknown), RRID:SCR_002823, Zhang, Brady, and Smith 2001). Brain surfaces were reconstructed using recon-all (FreeSurfer 7.3.2, RRID:SCR_001847, Dale, Fischl, and Sereno 1999), and the brain mask estimated previously was refined with a custom variation of the method to reconcile ANTs-derived and FreeSurfer-derived segmentations of the cortical gray-matter of Mindboggle (RRID:SCR_002438, Klein et al. 2017). Volume-based spatial normalization to two standard spaces (MNI152NLin6Asym, MNI152NLin2009cAsym) was performed through nonlinear registration with antsRegistration (ANTs 2.6.0), using brain-extracted versions of both T1w reference and the T1w template. The following templates were were selected for spatial normalization and accessed with *TemplateFlow* (24.2.2, Ciric et al. 2022): *FSL's MNI ICBM 152 non-linear 6th Generation Asymmetric Average Brain Stereotaxic Registration Model* [Evans et al. (2012), RRID:SCR_002823; TemplateFlow ID: MNI152NLin6Asym], *ICBM 152 Nonlinear Asymmetrical template version 2009c* [Fonov et al. (2009), RRID:SCR_008796; TemplateFlow ID: MNI152NLin2009cAsym].

Functional data preprocessing

For each of the 6 BOLD runs found per subject (across all tasks and sessions), the following preprocessing was performed. First, a reference volume was generated from the shortest echo of the BOLD run, using a custom methodology of *fMRIPrep*, for use in head motion correction. Head-motion parameters with respect to the BOLD reference (transformation matrices, and six corresponding rotation and translation parameters) are estimated before any spatiotemporal filtering using mcflirt (FSL , Jenkinson et al. 2002). The estimated *fieldmap* was then aligned with rigid-registration to the target EPI (echo-planar imaging) reference run. The field coefficients were mapped on to the reference EPI using the transform. The BOLD reference was then co-registered to the T1w reference using bbregister (FreeSurfer) which implements boundary-based registration (Greve and Fischl 2009). Co-registration was configured with six degrees of freedom. Several confounding time-series were calculated based on the *preprocessed BOLD*: framewise displacement (FD), DVARS and three region-wise global signals. FD was computed using two formulations following Power (absolute sum of relative motions, Power et al. (2014)) and Jenkinson (relative root mean square displacement between affines, Jenkinson et al. (2002)). FD and DVARS are calculated for each functional run, both using their implementations in *Nipype* (following the definitions by Power et al. 2014). The three global signals are extracted within the CSF, the WM, and the whole-brain masks. Additionally, a set of physiological regressors were extracted to allow for component-based noise correction (*CompCor*, Behzadi et al. 2007). Principal components are estimated after high-pass filtering the *preprocessed BOLD* time-series (using a discrete cosine filter with 128s cut-off) for the two *CompCor* variants: temporal (tCompCor) and anatomical (aCompCor). tCompCor components are then calculated from the top 2% variable voxels within the brain mask. For aCompCor, three probabilistic masks (CSF, WM and combined CSF+WM) are generated in anatomical space. The implementation differs from that of Behzadi et al. in that instead of eroding the masks by 2 pixels on BOLD space, a mask of pixels that likely contain a volume fraction of GM is subtracted from the aCompCor masks. This mask is obtained by dilating a GM mask extracted from the FreeSurfer's *aseg* segmentation, and it ensures components are not extracted from voxels containing a minimal fraction of GM. Finally, these masks are resampled into BOLD space and binarized by thresholding at 0.99 (as in the original implementation). Components are also calculated separately within the WM and CSF masks. For each CompCor decomposition, the *k* components with the largest singular values are retained, such that the retained components' time series are sufficient to explain 50 percent of variance across the

nuisance mask (CSF, WM, combined, or temporal). The remaining components are dropped from consideration. The head-motion estimates calculated in the correction step were also placed within the corresponding confounds file. The confound time series derived from head motion estimates and global signals were expanded with the inclusion of temporal derivatives and quadratic terms for each (Satterthwaite et al. 2013). Frames that exceeded a threshold of 0.5 mm FD or 1.5 standardized DVARS were annotated as motion outliers. Additional nuisance timeseries are calculated by means of principal components analysis of the signal found within a thin band (*crown*) of voxels around the edge of the brain, as proposed by (Patriat, Reynolds, and Birn 2017). All resamplings can be performed with *a single interpolation step* by composing all the pertinent transformations (i.e. head-motion transform matrices, susceptibility distortion correction when available, and co-registrations to anatomical and output spaces). Gridded (volumetric) resamplings were performed using nitransforms, configured with cubic B-spline interpolation.

Many internal operations of *fMRIPrep* use *Nilearn* 0.11.1 (Abraham et al. 2014, RRID:SCR_001362), mostly within the functional processing workflow. For more details of the pipeline, see the section corresponding to workflows in *fMRIPrep*'s documentation.

Copyright Waiver

References

Abraham, Alexandre, Fabian Pedregosa, Michael Eickenberg, Philippe Gervais, Andreas Mueller, Jean Kossaifi, Alexandre Gramfort, Bertrand Thirion, and Gael Varoquaux. 2014. "Machine Learning for Neuroimaging with Scikit-Learn." *Frontiers in Neuroinformatics* 8. https://doi.org/10.3389/fninf.2014.00014.

Avants, B. B., C. L. Epstein, M. Grossman, and J. C. Gee. 2008. "Symmetric Diffeomorphic Image Registration with Cross-Correlation: Evaluating Automated Labeling of Elderly and Neurodegenerative Brain." *Medical Image Analysis* 12 (1): 26–41. https://doi.org/10.1016/j.media.2007.06.004.

Behzadi, Yashar, Khaled Restom, Joy Liau, and Thomas T. Liu. 2007. "A Component Based Noise Correction Method (CompCor) for BOLD and Perfusion Based fMRI." *NeuroImage* 37 (1): 90–101. https://doi.org/10.1016/j.neuroimage.2007.04.042.

Ciric, R., William H. Thompson, R. Lorenz, M. Goncalves, E. MacNicol, C. J. Markiewicz, Y. O. Halchenko, et al. 2022. "TemplateFlow: FAIR-Sharing of Multi-Scale, Multi-Species Brain Models." *Nature Methods* 19: 1568–71. https://doi.org/10.1038/s41592-022-01681-2.

Dale, Anders M., Bruce Fischl, and Martin I. Sereno. 1999. "Cortical Surface-Based Analysis: I. Segmentation and Surface Reconstruction." *NeuroImage* 9 (2): 179–94. https://doi.org/10.1006/nimg.1998.0395.

Esteban, Oscar, Ross Blair, Christopher J. Markiewicz, Shoshana L. Berleant, Craig Moodie, Feilong Ma, Ayse Ilkay Isik, et al. 2018. "fMRIPrep 25.1.2." *Software*. https://doi.org/10.5281/zenodo.852659.

Esteban, Oscar, Christopher Markiewicz, Ross W Blair, Craig Moodie, Ayse Ilkay Isik, Asier Erramuzpe Aliaga, James Kent, et al. 2019. "fMRIPrep: A Robust Preprocessing Pipeline for Functional MRI." *Nature Methods* 16: 111–16. https://doi.org/10.1038/s41592-018-0235-4.

Evans, AC, AL Janke, DL Collins, and S Baillet. 2012. "Brain Templates and Atlases." *NeuroImage* 62 (2): 911–22. https://doi.org/10.1016/j.neuroimage.2012.01.024.

Fonov, VS, AC Evans, RC McKinstry, CR Almli, and DL Collins. 2009. "Unbiased Nonlinear Average Age-Appropriate Brain Templates from Birth to Adulthood." *NeuroImage* 47, Supplement 1: S102. https://doi.org/10.1016/S1053-8119(09)70884-5.

Gorgolewski, K., C. D. Burns, C. Madison, D. Clark, Y. O. Halchenko, M. L. Waskom, and S. Ghosh. 2011. "Nipype: A Flexible, Lightweight and Extensible Neuroimaging Data Processing Framework in Python." *Frontiers in Neuroinformatics* 5: 13. https://doi.org/10.3389/fninf.2011.00013.

Gorgolewski, Krzysztof J., Oscar Esteban, Christopher J. Markiewicz, Erik Ziegler, David Gage Ellis, Michael Philipp Notter, Dorota Jarecka, et al. 2018. "Nipype." *Software*. https://doi.org/10.5281/zenodo.596855.

Greve, Douglas N, and Bruce Fischl. 2009. "Accurate and Robust Brain Image Alignment Using Boundary-Based Registration." *NeuroImage* 48 (1): 63–72. https://doi.org/10.1016/j.neuroimage.2009.06.060.

Jenkinson, Mark, Peter Bannister, Michael Brady, and Stephen Smith. 2002. "Improved Optimization for the Robust and Accurate Linear Registration and Motion Correction of Brain Images." *NeuroImage* 17 (2): 825–41. https://doi.org/10.1006/nimg.2002.1132.

Klein, Arno, Satrajit S. Ghosh, Forrest S. Bao, Joachim Giard, Yrjö Häme, Eliezer Stavsky, Noah Lee, et al. 2017. "Mindboggling Morphometry of Human Brains." *PLOS Computational Biology* 13 (2): e1005350. https://doi.org/10.1371/journal.pcbi.1005350.

Patriat, Rémi, Richard C. Reynolds, and Rasmus M. Birn. 2017. "An Improved Model of Motion-Related Signal Changes in fMRI." *NeuroImage* 144, Part A (January): 74–82. https://doi.org/10.1016/j.neuroimage.2016.08.051.

Power, Jonathan D., Anish Mitra, Timothy O. Laumann, Abraham Z. Snyder, Bradley L. Schlaggar, and Steven E. Petersen. 2014. "Methods to Detect, Characterize, and Remove Motion Artifact in Resting State fMRI." *NeuroImage* 84 (Supplement C): 320–41. https://doi.org/10.1016/j.neuroimage.2013.08.048.

Satterthwaite, Theodore D., Mark A. Elliott, Raphael T. Gerraty, Kosha Ruparel, James Loughead, Monica E. Calkins, Simon B. Eickhoff, et al. 2013. "An improved framework for confound regression and filtering for control of motion artifact in the preprocessing of resting-state functional connectivity data." *NeuroImage* 64 (1): 240–56. https://doi.org/10.1016/j.neuroimage.2012.08.052.

Tustison, N. J., B. B. Avants, P. A. Cook, Y. Zheng, A. Egan, P. A. Yushkevich, and J. C. Gee. 2010. "N4ITK: Improved N3 Bias Correction." *IEEE Transactions on Medical Imaging* 29 (6): 1310–20. https://doi.org/10.1109/TMI.2010.2046908.

Zhang, Y., M. Brady, and S. Smith. 2001. "Segmentation of Brain MR Images Through a Hidden Markov Random Field Model and the Expectation-Maximization Algorithm." *IEEE Transactions on Medical Imaging* 20 (1): 45–57. https://doi.org/10.1109/42.906424.